Deubiquitinating enzyme A20 and its role in NF-κB regulation: Implications for treatment of Duchenne muscular dystrophy

by

Rakshita A. Charan

B.Sc., Mumbai University, Mumbai, India, 2002

M.S., Biology, Tata Institute of Fundamental Research, Mumbai, India, 2006

Submitted to the Graduate Faculty of

School of Medicine in partial fulfillment

of the requirements for the degree of

Doctor of Philosophy

University of Pittsburgh

December 2011

UNIVERSITY OF PITTSBURGH

SCHOOL OF MEDICINE

This dissertation was presented

by

Rakshita A. Charan

It was defended on

December 15, 2011

and approved by

Paul D. Robbins, PhD, Department of Microbiology and Molecular Genetics

Johnny Huard, PhD, Department of Orthopedic Surgery

Neal A. DeLuca, PhD, Department of Microbiology and Molecular Genetics

Gutian Xiao, PhD, Department of Microbiology and Molecular Genetics

Dissertation Advisor: Paula R. Clemens, MD, Department of Neurology

Deubiquitinating enzyme A20 and its role in NF-κB regulation: Implications for treatment of Duchenne muscular dystrophy

Rakshita Charan, PhD

University of Pittsburgh, 2011

Duchenne muscular dystrophy (DMD) is one of the most common muscle disorders affecting about 1 in 3500 male births worldwide. It is caused by mutations in the gene dystrophin, the protein product of which is required for muscle structure and stability. Studies suggest that lack of dystrophin protein leads to dystrophic pathology in skeletal muscle; an important pathologic mediator is nuclear factor kappa B (NF-κB), a transcription factor that regulates several genes responsible for stress responses, cell survival and various inflammatory conditions. NF-κB is pathologically activated in dystrophic muscle in DMD patients and in the *mdx* mouse model for DMD. NF-κB activation in *mdx* mice is thought to activate protein degradation and cause chronic inflammation in skeletal muscle. Furthermore, pathological activation of NF-κB downregulates myogenic regulatory factors and interferes with muscle regeneration. Attenuation of NF-κB activation in *mdx* mice has been shown to improve muscle stability and strength. Thus, strategies to inhibit NF-κB activation are being actively pursued as a therapeutic option for DMD.

In this thesis, I have characterized the role of A20, a deubiquitinating enzyme known to attenuate NF-κB activation, in skeletal muscle and examined its potential as a therapeutic target to attenuate NF-κB activation in DMD. I investigated the effect of A20 on NF-κB activation in cultured *mdx* and control C57BL/10 myotubes *in vitro* and observed its role in muscle

regeneration and differentiation. Characterization of A20 localization in *mdx* muscle demonstrated expression predominantly in regenerating fibers; interestingly, most were fast-twitch muscle fibers. This correlation between expression of an NF-κB inhibitor attenuating NF-κB activation and pathology of DMD was a promising observation to further explore the efficacy of A20 as a therapeutic target. To this effect, I developed adeno-associated viral vectors carrying A20 expression cassettes to test the therapeutic benefit of A20 over-expression in the *mdx* model of DMD. Over-expression of A20 caused a significant decrease in NF-κB activation, an overall reduction in regeneration and number of inflammatory cells in skeletal muscle. These studies show that A20 could be pursued further as a therapeutic agent for inhibition of NF-κB activation, not only in DMD, but also in other disorders.

TABLE OF CONTENTS

LIST OF TABLES

LIST OF FIGURES

ACKNOWLEDGEMENTS

First and foremost, I would like to acknowledge my advisor Dr. Paula Clemens, for being such a great mentor and helping me with my project in every single way. I am truly grateful to her for giving me an opportunity to work in her lab. She showed me how to think like an independent researcher and always gently guided me towards the right direction every time I felt lost or frustrated with my project. I will forever be indebted to her for making me a better researcher and thank her for everything she has taught me, science and beyond.

I would like to thank my thesis committee members, Dr. Paul Robbins, Dr. Johnny Huard, Dr. Gutian Xiao, Dr. Hiroyuki Nakai and Dr. Neal DeLuca for all their helpful suggestions and discussions. They have been excellent critics of my project and have always guided me in the right direction that helped me understand my project from an unbiased point of view. I would specifically like to thank Dr. Hiroyuki Nakai for all the discussions and suggestions he has provided over the years. I am grateful to him for giving me an opportunity to work in his lab and for teaching me everything I know about viruses.

I am thankful for my labmates Daniel Reay and Gabriela Niizawa for being great friends and for always being there. The discussions I have had with them regarding my project have been invaluable and I could not have done it without them. I would like to thank Dan for teaching me various techniques in the lab and helping me out with mice and other experiments. Thank you Gabi, for taking care of me and being more than a friend to me. I will definitely miss

our lunches together. I would also like to thank past lab members, Saman, Munil, Heng, Kae for all the fun times in the lab. I would like to thank Ryan and Aditee, for being excellent mentees, and for helping me with my project.

I would like to thank my husband Ashwin, who has been like a rock in my life; my PhD or my life would not be complete without him. My discussions with him regarding my project every evening helped me with my work and his comments and advice have truly been invaluable. I feel lucky to have him in my life and hope to continue having scientific discussions with him for a long time.

My parents, who have always encouraged me to aspire, aim higher and taught me that education is the best gift one could receive. They have always been patient and kind through the years and I hope after all these years, I have done them proud. I am truly thankful to them for believing in me.

I would like to thank the administrative staff, Cindy Duffy and Kristin DiGiacomo, and the staff at Office of International Services, for their constant support throughout my graduate studies. Their timely reminders and response to all my emails made my graduate life much easier.

The work presented here would not be possible without the help and support of my many colleagues, friends and family and I would like to thank all of them for supporting me through my graduate studies.

1.0 INTRODUCTION

1.1 SKELETAL MUSCLE

Skeletal muscles in the human body make up about 40-50% of our body weight. Different types of skeletal muscles are connected to the skeleton, and their primary function is to move in co-ordination enabling complex movements. The movement of these muscles is voluntary and is controlled by the central nervous system (CNS). An individual skeletal muscle may be made up of hundreds, or even thousands, of muscle fibers bundled together and wrapped in a connective tissue covering [1]. The perimysium, a layer of connective tissue, surrounds each bundle of muscle fibers forming a fascicle [2]. A sheath of connective tissue called the epimysium surrounds the fascicles of muscle. The connective tissue outside the epimysium surrounds and separates the muscles. Sections of the epimysium project inward to divide the muscle into compartments, and these compartments make up the bundle of muscle fibers that are surrounded by the perimysium (Figure 1).

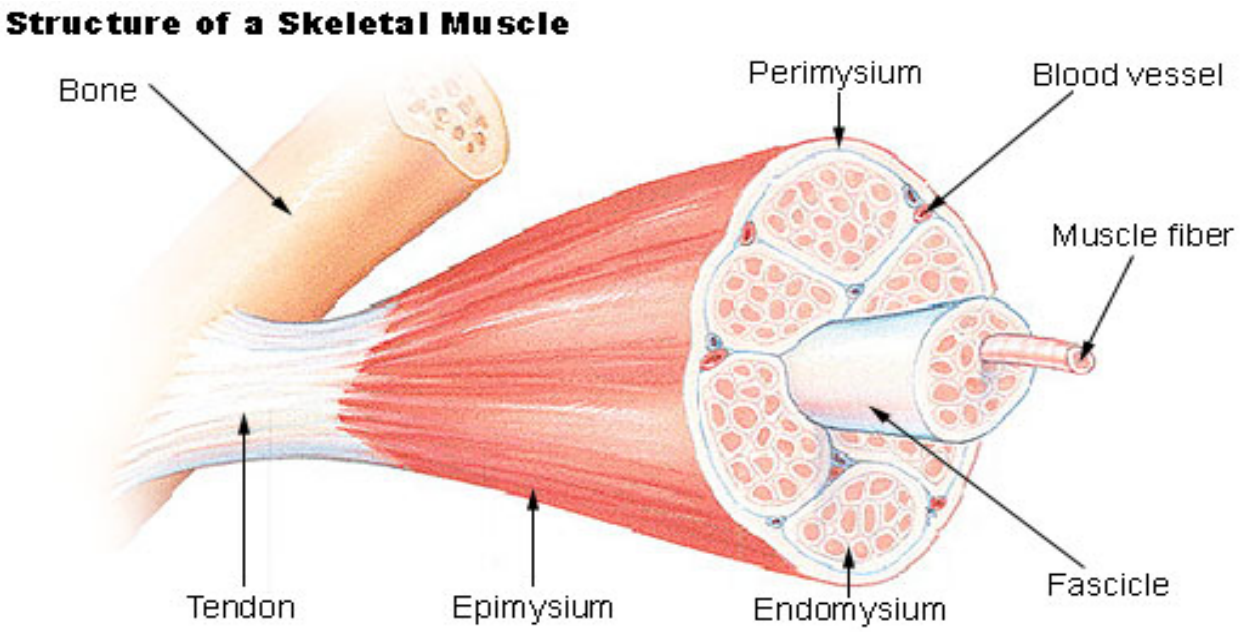

Figure 1: Schematic of the structure of a skeletal muscle [3].

Muscle consists of several individual muscle fibers. Each compartmentalized bundle of muscle fiber is surrounded by connective tissue called perimysium, and the whole muscle is surrounded by protective epimysium.

Each skeletal muscle fiber is a single cylindrical muscle cell. Muscle fibers are made up of multi-nucleated cells called myotubes. The myotubes are in turn made up of several muscle cells called myoblasts that fuse together in a process called differentiation. Upon any form of injury to the muscle fibers, satellite cells residing between the cell-membrane of the muscle-cell known as sarcolemma, and the endomysium are stimulated to differentiate into myoblasts, and undergo differentiation, forming myotubes [4, 5]; these myotubes would ultimately replace the injured myotubes or fuse with the injured myotubes. During the maturation of the myotube, the centrally localized nuclei move to the periphery (Figure 2) [2]. Thus, the maturity of a muscle fiber can be determined by the localization of the nucleus in the fiber.

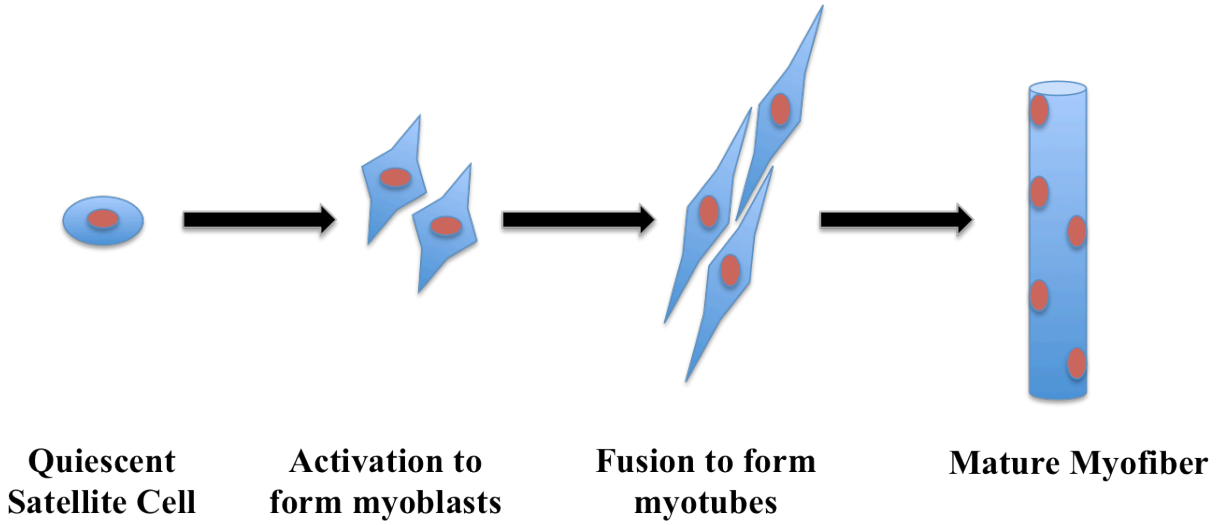

Figure 2: Schematic of formation of a myofiber.

Quiescent satellite cells are activated upon muscle injury to form myoblasts. Induced expression of differentiation factors initiates the fusion of myoblasts to form multi-nucleated myotubes. Several myotubes come together to form a functional mature myofiber.

Muscles consist of two types of muscle fibers: Type I (slow) and Type II (fast) [6], here after referred to as fast and slow fibers. The fast fibers are further classified into Type IIa and Type IIb fibers. Each fiber type has different properties as stated in Table 1, and perform different functions in the muscle. For example, slow fibers are mostly used for energy inexpensive activities such as standing, whereas fast fibers are utilized during strenuous activities like running or sprinting [6].

Table 1: Properties of Type I and Type II fibers.

Properties	*Type I*	*Type II*
Contraction	Fast	Slow
Glycolytic capacity	Low	High
Respiration	Aerobic	Anaerobic
Blood supply	High	Low
Fatigue resistance	High	Low

The hind limb skeletal muscles of mice such as quadriceps, gastrocnemius, tibialis anterior (TA) and the extensor digitorum longus (EDL) consist of about 90% of fast fiber type and about 10% of slow fiber type (Figure 3). The soleus muscle is the only exception and has a majority of slow type fibers [7]. This difference in number of fiber type in each muscle indicates their specific function and the role they play in movement.

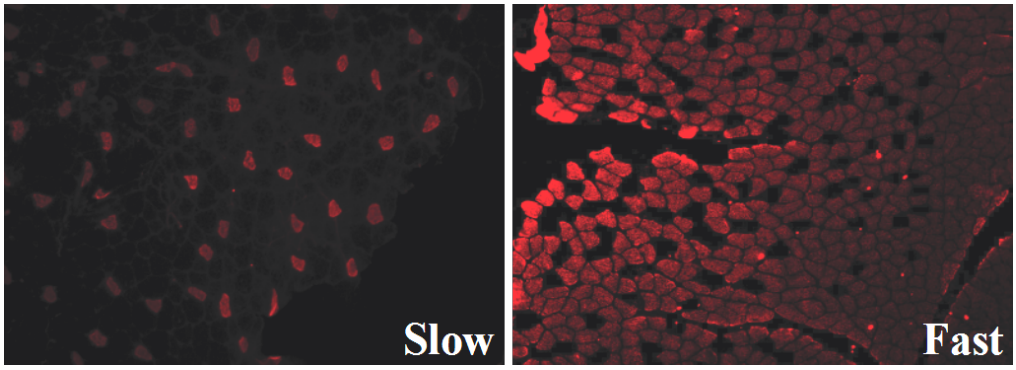

Figure 3: Visualization of slow fibers and fast fibers in skeletal muscle.

Quadriceps of 8wk old C57 mice was immunostained using slow myosin heavy chain (Slow) and fast myosin heavy chain (Fast) to visualize slow and fast fibers respectively.

1.2 DUCHENNE MUSCULAR DYSTROPHY

Muscular dystrophy is a group of genetic disorders and is characterized by progressive muscle weakness and atrophy among other symptoms. Of this group, Duchenne Muscular Dystrophy (DMD) is one of the most common of dystrophies [8]. Guillaume Benjamin Amand Duchenne, a French neurologist first characterized the disorder by providing some of the first clinical descriptions of DMD patients. DMD affects about 1 in 3500 liveborn males [8] and individuals suffering from this disease require a wheelchair for ambulation by their early teens and die due to respiratory or cardiac failure in their twenties. The disease is characterized by chronic muscle inflammation and muscle degeneration beginning as early as 6 months of age and progresses with age. This degeneration is followed by a brief burst of regeneration due to the presence of satellite cells [9]. However, this reserve of satellite cells is exhausted and the muscle fibers are replaced by fat and connective tissue. DMD is primarily caused by a mutation in the gene encoding for dystrophin resulting in a defective protein product [10]. Dystrophin is one of the cytoskeletal components of the Dystrophin-Glycoprotein Complex (DGC) (Figure 4) and is located on the cytoplasmic face of the sarcolemma [11]. Dystrophin is a 2.4 Mb gene present on the X-chromosome containing 79 exons, encoding for a 427 kDa protein [10]. Absence of this protein leads to the disruption of the DGC [12], causing membrane instability leading to a loss of muscle integrity and an increase in progressive muscle degeneration [13]. Due to muscle damage, high serum levels of creatine kinase, an intracellular muscle protein are also observed [14]. There is increased necrosis and accumulation of fibrotic tissue in muscle that leads to infiltration of inflammatory cells and subsequently causes muscle atrophy.

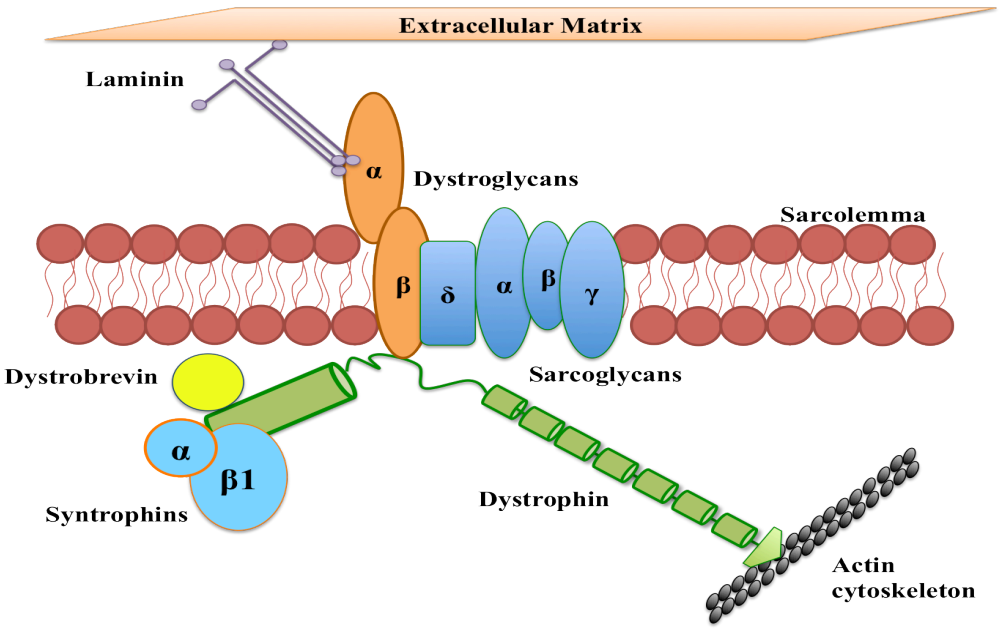

Figure 4: Schematic of the DGC complex.

Dystrophin connects the actin filaments to the sarcolemma surrounding the muscle. Lack of dystrophin disrupts the dystrophin-glycoprotein complex and causes muscle instability.

In DMD patients, fast fibers are selectively affected. They are the first fibers to degenerate and also the first set of fibers to regenerate before the slow fibers are affected [15]. Since the contraction rates of fast fibers are higher than slow fibers, absence of dystrophin might cause the fast fibers to become unstable faster and ultimately undergo degeneration.

There has been immense amount of research to find a cure for the disease, which, to date, have not resulted in treatments that significantly alter the morbidity and mortality rates. Currently, available therapies only ameliorate symptoms temporarily and support declining function levels. Administration of corticosteroids reduces inflammation in muscle [16]. However, this treatment only slows the progression rate of the muscle degeneration and partially improves muscle function [17]. Thus, despite characterization of the clinical phenotype over a century ago, there is yet a cure to be found. A mouse model with a spontaneous mutation in the dystrophin gene, known as *mdx*, was discovered to have a mutation on the X-chromosome,

similar to that in human patients [18]. *Mdx* mice have been extensively studied to understand the molecular mechanisms underlying the pathology of DMD, and to develop therapies to treat DMD. Similar to patients with DMD, *mdx* mice display chronic inflammation in muscle, progressive muscle degeneration and subsequent atrophy (Figure 5) [18].

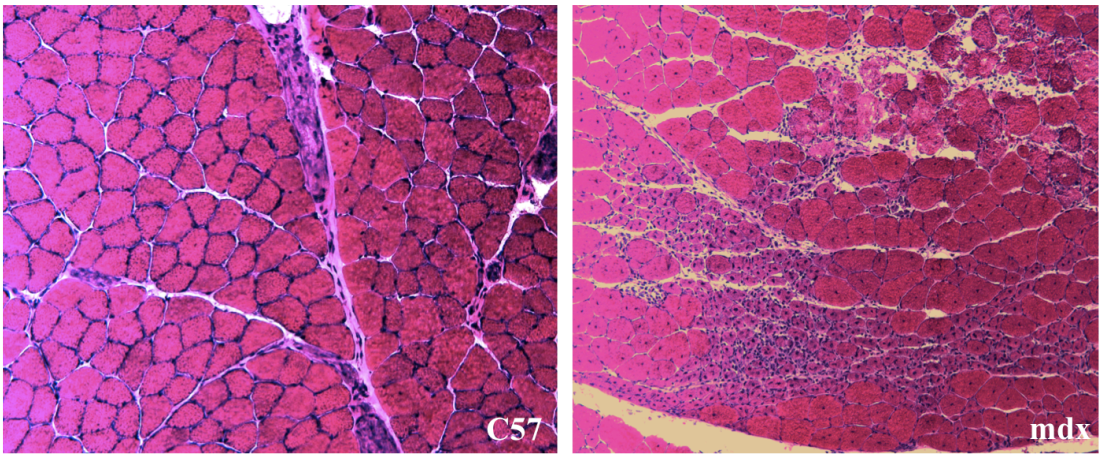

Figure 5: H&E stained sections of quadriceps of 8 wk old C57 and *mdx* mice.
Quadriceps from *mdx* mice show increased regeneration as observed by muscle fibers with centralized nuclei, accumulation of fibrotic tissue replacing muscle and infiltration of inflammatory molecules in muscle.

1.3 NUCLEAR FACTOR OF KAPPA B (NF-κB)

Absence of dystrophin causes instability of the muscle membrane, making it highly susceptible to muscle damage. This leads to inflammatory cytokines such as TNF-α and other molecules infiltrating the muscle increasing inflammation within the muscle, activating downstream inflammatory pathways. One of the transcription factors known to be up-regulated in muscle of DMD patients as well as in *mdx* mice is the transcription factor Nuclear factor-kappa B (NF-κB) [19, 20]. NF-κB was named so because it was first discovered in 1986 as a nuclear factor

involved in the transcription of the immunoglobulin κ light chains in B cells [21]. It is a family of transcription factors known as Rel/NF-κB and has since been shown to play a role in many important biological processes such as apoptosis, cell proliferation, stress and injury, mounting an innate as well as adaptive immune response [22]. The mammalian family of NF-κB consists of five members: p50, p52, p65 (RelA), RelB and c-Rel, and these subunits can exist as homodimers or heterodimers in different cell types. These 5 members of the family have a common Rel homology domain (RHD), which is highly conserved. The RHD plays a role in protein-protein interactions such as dimerization and also facilitates DNA binding at target sites called the κB site to initiate transcription [23]. The most commonly occurring dimers that are also key regulators of gene expression are the p50-p65 heterodimers [24]. Activation of the pathway leads to the activation of its downstream targets, including genes involved in the immune and inflammatory response.

The NF-κB signaling pathway is activated by multiple mechanisms. The two main mechanisms known are the classical (canonical pathway) and the alternate (non-canonical) pathway [25]. In the classical pathway, NF-κB is sequestered in the cytoplasm by its inhibitor IκB, rendering it inactive. Upon stimulation, IκB is phosphorylated by components of the IκB kinase (IKK) complex, then ubiquitinated by βTrCP, an E3 ubiquitin ligase [26]. IκB binds to the NF-κB p50/p65 dimers such that the Nuclear Localization Sequence (NLS) is masked [27, 28]. IκB is subsequently degraded by the ubiquitin-proteasome system, freeing NF-κB [29]. Upon degradation of IκB, the NLS is now exposed, causing nuclear translocation of NF-κB. IκB also has nuclear export sequences (NES), and has been shown to shuttle in and out of the nucleus [30]. The alternate pathway, on the other hand depends on the NF-κB inducing kinase (NIK)

induced activation of the IKKα subunit [31, 32] and leads to the phosphorylation and processing of p100, generating p52/RelB heterodimers [32, 33].

1.3.1 Factors that trigger pathway activation

The classical and the alternate pathways of NF-κB activation play distinct roles in different cell types, and are activated by different molecular cues. The classical pathway is typically activated by binding of TNF-α to the tumor necrosis factor type 1/2 receptors (TNFR1/2) (Figure 6). Lipoploysaccharide (LPS) binding to Toll-like receptor 4 (TLR4) also robustly activates the classical pathway [34]. T-cell receptors (TCR), B-cell receptors (BCR), or the, interleukin-1 receptor (IL-1R) superfamily members are all implicated to play a role in triggering classical pathway activation [35]. Activation of the pathway in turn causes increased transcription of target genes encoding chemokines, cytokines, and molecules playing a role in the immune response. The alternative pathway, however is triggered by the activation of certain TNF receptor family members, including lymphotoxin β receptor (LTβR), B-cell-activating factor belonging to the TNF family receptor (BAFF-R), CD40, and receptor activator of NF-κB (RANK) [35, 36]. It is also known that some oncogenic viruses such as the Epstein-Barr virus (EBV) also activate the alternate pathway [37]. Stimuli that activate the alternate pathway are also capable of activating the classical pathway [38].

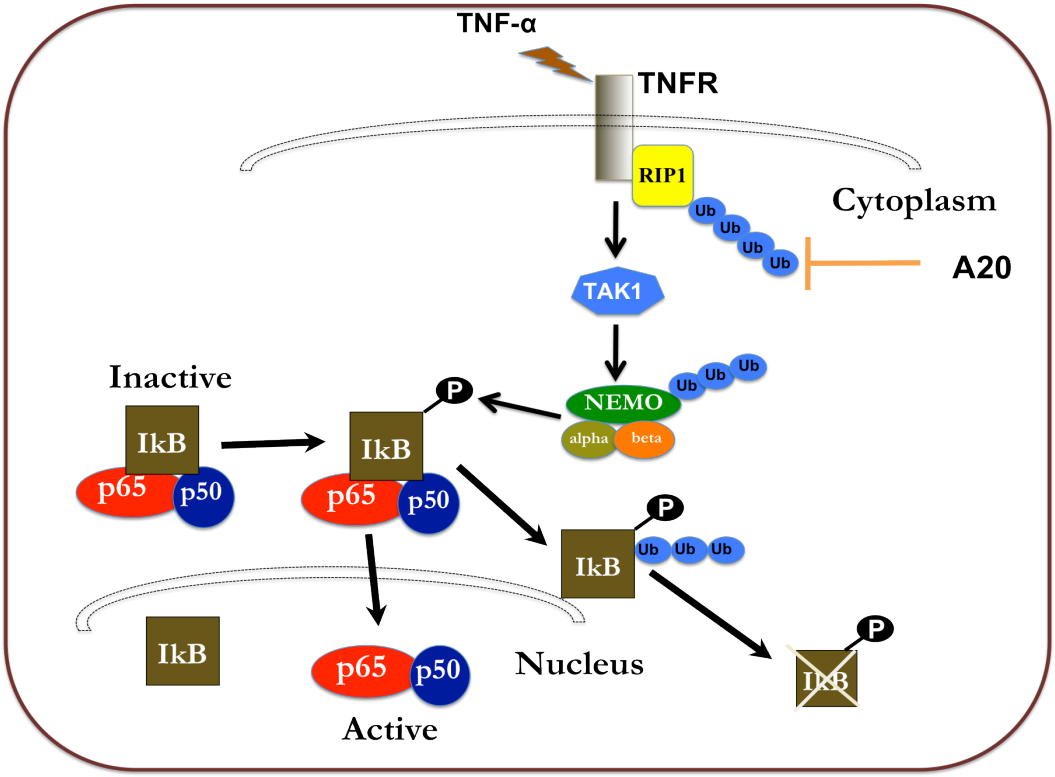

Figure 6: Schematic of classical NF-κB pathway activation.

Binding of TNF-α to the TNF receptor triggers activation of the pathway. Adaptor protein RIP1 binds to the receptor and gets ubiquitinated to initiate the activation of the pathway. This process then leads to the activation of the IKK complex consisting of IKKα, IKKβ and IKKγ. The IKK complex phosphorylates IκB which targets it for degradation. The p50-p65 heterodimer is free to enter the nucleus and initiate transcription of downstream targets.

1.3.2 Regulation of the pathway

The role of NF-κB in various pathways warrants its need to be highly regulated. Upon stimulation by TNF-α or IL-1β, adaptor molecules such as TAK1[39], RIP1 [40] and TRAF6 [41] are recruited and associated with the receptor and molecules downstream of it. This leads to activation of ubiquitin ligase activity of TRAF6 leading to ubiquitination of IKKγ (NEMO) and TRAF6 itself [23]. In order for the pathway to be activated, RIP1 is also ubiquitinated [42]. The ubiquitinated TRAF6 then binds to TAK1, activating it, resulting in the phosphorylation of

IKKβ, activating it [43]. Another form of regulation in order to translocate to the nucleus is the phosphorylation of the p65 subunit. p65 can be phosphorylated by different kinases [44], but the p50-p65 heterodimer is acetylated by p300/CBP after its phosphorylation and after nuclear import [45]. Also, NF-κB has several feedback loops that ensure that the pathway is held in check. For instance, one of the downstream targets of NF-κB is its inhibitor IκBα that then helps sequester NF-κB by transporting it back to the cytoplasm and rendering it inactive [46].

A major field of research is to explore the different natural and synthetic inhibitors of NF-κB, in order to attenuate its activation [47, 48]. Various approaches attempted for this are inhibition of downstream as well as upstream effector molecules, like proteosome inhibitors such as MG-132 to prevent IκB degradation [49], inhibitors of IκB kinase to prevent phosphorylation of IκB [50], and using acetylation inhibitors to prevent acetylation of the NF-κB subunit and to prevent its DNA binding capacity [45]. Despite the many approaches to inhibit NF-κB developed to date, a greater understanding about the mechanism of NF-κB activation and subsequent inhibition is required.

1.4 ROLE OF NF-κB IN DUCHENNE MUSCULAR DYSTROPHY

Chronic activation of NF-κB is related to several disease states including cancer, cachexia, rheumatoid arthritis, asthma, sepsis and DMD [38, 51]. In DMD, due to muscle degeneration, there is a high level of inflammatory cells infiltrating muscle [52]. This leads to higher levels of TNF-α in muscle, increasing activation of NF-κB [19, 52]. This over expression of NF-κB leads to the up-regulation of the ubiquitin-proteosome pathway by up-regulation of molecules such as MuRF1 [53], resulting in increased protein degradation and atrophy of muscle [54]. Moreover,

many cytokines such as TNF-α and chemokines are downstream targets of NF-κB, promoting chronic muscle inflammation [55]. Also, NF-κB was found to suppress MyoD, a transcription factor that is required for muscle regeneration and differentiation [56]. Studies have also shown that blocking the NF-κB pathway improved muscle strength and regeneration capacity [57]. Thus, it is important to dissect out the mechanism of this pathway to identify potential drug targets.

1.5 CURRENT THERAPIES TO AMELIORATE NF-κB IN DMD

A lot of ongoing research that studies muscular dystrophy, DMD in particular, target various pathways affecting muscle integrity [58-61]. One of the molecules that affect the DGC complex is neuronal nitric oxide synthase (nNOS), and has been studied in *mdx* mice as a potential target for therapy. Proper localization of nNOS enables the components of the DGC complex to properly localize to the membrane, thus providing stability to the muscle membrane [62, 63]. Many studies target the dystrophin gene itself and correct the mutations in the gene by several mechanisms, including exon skipping using antisense oligonucleotides (AON) [64] or introducing the dystrophin gene into mice [65, 66] to enable restoration of the DGC complex and thus improve stability of the muscle.

However, a significant research direction toward therapy targets the NF-κB pathway to decrease the severity of the pathological symptoms of DMD. There have been several approaches to suppress NF-κB activation in *mdx* mouse muscle that improve muscle health and stability and reduce muscle degeneration. The targets for reduction range from blockade of the

activation of the IKK complex to reduction of inflammation in muscle by introduction of pharmaceuticals. These different approaches are summarized below:

1.5.1 Pharmaceutical drugs (Anti-inflammation and fibrosis)

There are many drugs that are used to ameliorate symptoms in DMD patients. One of the most common corticosteroid medications prescribed for DMD patients is prednisone [67, 68]. Prednisone has a glucocorticoid effect and has potent anti-inflammatory properties. Due to ongoing necrosis and cycles of chronic muscle degeneration and repair, there is an accumulation of collagen and fibrotic tissue in the muscle. Drugs such as pirfenidone [69] and losartan [70] have been tested in *mdx* mice and shown to attenuate fibrosis in skeletal muscle. A plant-based drug curcumin was shown to be a potent inhibitor of NF-κB pathway activation and alleviated dystrophic pathology in mdx mice [71].

1.5.2 Peptide based inhibition (Targeting the IKK complex)

Activation of the IKK complex is one of the key steps for the activation of the NF-κB pathway and initiation of transcription of its downstream targets. The IKK complex consists of three subunits: IKKα, IKKβ and the regulatory subunit IKKγ, also known as NEMO (NF-κB essential modulator). In 2000, May and colleagues designed a peptide that would inhibit the interaction of IKKβ and NEMO, known as the NEMO binding domain (NBD) peptide, thus disrupting the formation of the IKK complex [72]. Delivery of the NBD peptide covalently attached to a protein transduction domain (PTD), which facilitates entry of the peptide into cells showed a significant reduction in the activation of the NF-κB pathway and improvement of dystrophic

pathology in *mdx* mice [73, 74]. Treatment with the NBD peptide was also effective in the dystrophin-utrophin double-knockout mice [75] that display severe muscular dystrophy symptoms due to the absence of both the compensatory protein utrophin and dystrophin.

1.5.3 Proteosome inhibitors (Targeting IκB)

The phosphorylation and subsequent proteosomal degradation of the cytoplasmic inhibitor IκB activates the NF-κB dimer to enter the nucleus. Proteosome inhibitors block the 26S subunit of the proteasome preventing the degradation of IκB, leaving the inhibitor bound to the NF-κB dimer, thus preventing entry of the NF-κB dimer into the nucleus. MG-132 is one of the most common and well-characterized proteasome inhibitors used for the treatment of dystrophy in the *mdx* mouse model. MG-132 was shown to rescue expression levels of α-sarcoglycan, β-dystroglycan, and dystrophin, components of the DGC complex and also to restore their localization to the plasma membrane [76]. Treatment with MG-132 also improved muscle histopathology and reduced muscle membrane damage. Velcade (Bortezomib or PS-341) and MLN273 (PS-273) that selectively block the ubiquitin-proteosome pathway were also shown to reduce activation of NF-κB in skeletal muscle of *mdx* mice [77]. They also restored localization of the components of the DGC complex to the membrane.

1.5.4 Antioxidants (Targeting ROS)

Several studies have implicated reactive oxygen species (ROS) as a factor in increased inflammation in the muscle that ultimately leads to muscle atrophy. Elevated levels of oxidative stress have been implicated to play a role in muscle damage, weakness and possibly fibrosis [78].

Oxidative stress is also thought to exacerbate the disruption of the DGC complex, and cause increased activation of the NF-κB pathway, and thus impair muscle health. Antioxidants such as coenzyme Q10 [79], genistein [80] and melatonin [81] have been shown to ameliorate DMD symptoms by causing reduction of the NF-κB pathway activation. Melatonin was also shown to reduce inflammation in erythrocytes of DMD patients [82]. Treatment of *mdx* mice with protandim, a drug that induces anti-oxidant enzymes showed a reduction in the levels of profibrotic factor, osteopontin [83]. Overall, oxidative stress may play a role in the pathology of DMD, and antioxidants could attenuate some of the symptoms [78].

1.5.5 Gene therapy

One of the newer approaches to treating DMD is the use of gene therapy to introduce molecules of interest that would help ameliorate the symptoms and pathogenesis of DMD. Many studies involve introduction of molecules that would inhibit NF-κB pathway activation using vehicles such as viral vectors. Delivery of dominant-negative IKKα and IKKβ using an AAV vector was shown to decrease activation of the NF-κB pathway in 11 month-old *mdx* mice [84]. The authors also observed decreased necrosis and increased muscle regeneration. This suggests that inhibition of NF-κB activation in muscle was capable of ameliorating dystrophic symptoms in skeletal muscle of *mdx* mice.

1.6 TUMOR NECROSIS FACTOR α-INDUCED PROTEIN 3 (A20)

Ubiquitination plays a very important role in NF-κB pathway activation [51, 85, 86]. Ubiquitin is a small 76-aa protein that is covalently attached to various substrate proteins on their lysine residues that either marks them for degradation via the proteasome system or modifies the function of the protein. This process is known as ubiquitination and requires three enzymes. The first enzyme is the ubiquitin-activating enzyme E1 activating free-floating ubiquitin and passes it on to the second enzyme, ubiquitin-conjugating enzyme E2, the main function of which is to recognize substrate, which then activates ubiquitin-ligase E3, the third enzyme, that transfers the ubiquitin molecule to the protein substrate [87]. Substrates can undergo either mono- or polyubiquitination, defining the protein for either functional modification or degradation. Poly-ubiquitination through lysine 63, in general, leads to a modification of function of the substrate, and mono- and poly-ubiquitination of the substrate may lead to proteosomal degradation. Ubiquitination of upstream molecules of the NF-κB pathway such as RIP1, IKKγ, TRAF6 and IκB are critical for its activation and regulation. Since the NF-κB pathway plays a role in critical pathways such as inflammation and the immune response, the presence of several negative regulators keep it in check. Deubiquitinating enzymes (DUBs) such as A20 and CYLD have been shown to inhibit pathway activation (Figure 6).

A20, also known as tumor necrosis factor α-induced protein 3, was first described to be rapidly induced by TNF-α and protect cells from cytotoxicity that could be induced by increased TNF-α levels [88]. This was the first evidence of A20 playing a role in the regulation of the NF-κB pathway. A20 also plays a role in inhibiting TNF-induced apoptosis in Jurkat T cells [89]. A20 contains an N-terminal OTU domain and 7 C-terminal zinc-finger domains (Figure 7) [90,

91]. A20 deubiquitinates the adaptor protein RIP1, that binds to the TNF receptor and gets polyubiquitinated through lysine 63 of ubiquitin after binding of TNF-α to the receptor. A20 then reubiquitinates RIP1 through Lysine 48 of ubiquitin marking it for degradation, thus inhibiting activation [42]. Recent studies have shown that A20 also interacts with TRAF1, TRAF2 [92] and TRAF6 [93], regulating NF- κB activation. The zinc-finger domains play a role in facilitating the deubiquitination and reubiquitination properties of the enzyme [42].

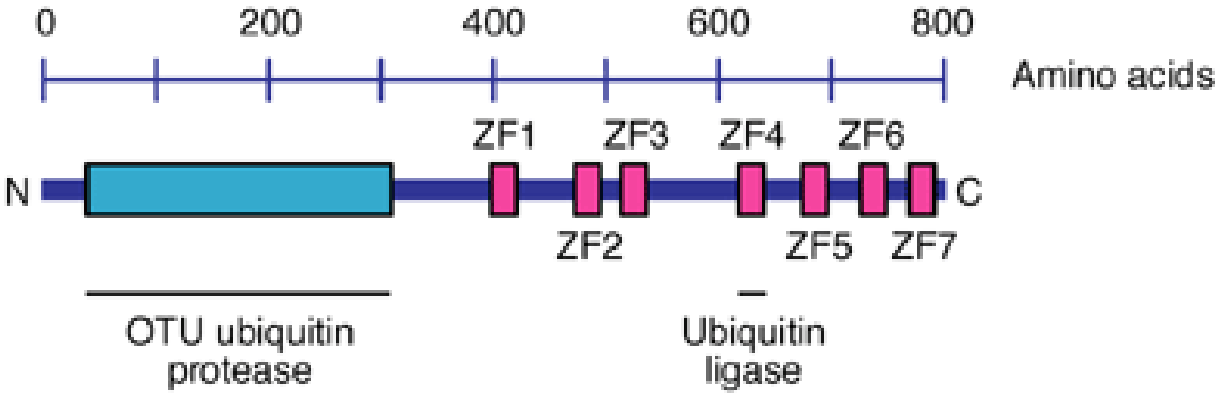

Figure 7: Domain structure of A20 [94].

The N-terminal half carries an OTU-type ubiquitin protease domain. The C-terminal portion contains seven zinc fingers (ZFs). The OTU domain of A20 inactivates RIP by removing Lys63-linked polyubiquitin. The E3 ligase domain then coordinates the addition of Lys48-linked polyubiquitin, which is known to target RIP to the proteasome, where it is destroyed. Abbreviations: OTU - ovarian tumor.

A20 plays a critical role in regulating the NF-κB pathway in many different tissues, such as liver, spleen and cell types such as epithelial cells and cancer cells [87, 95, 96]. Mice deficient in A20 die shortly after birth (6-8 weeks) and display severe inflammation in multiple tissues, including the liver, spleen, muscle and hypersensitivity to TNF-α [97]. A20-deficient mice have chronic activation of the NF-κB pathway. Recently, A20 has been associated with several diseases including arthritis, Crohn's disease, Type-1 diabetes and B-cell lymphoma [96].

Specifically, studies showed mutations in the A20 gene leading to a non-functional protein in lymphoma cell lines [98], and was proposed to play a role as a tumor suppressor gene [99]. However, the precise mechanism of action and molecular function of A20 are now just beginning to get dissected out, and further studies are needed to shed light on the role of A20 in inflammatory diseases and cancers.

1.7 ADENO-ASSOCIATED VIRAL VECTORS IN GENE THERAPY

Adeno-associated virus (AAV) is a non-enveloped particle, about 22nm in diameter with icosahedral symmetry [100, 101]. The AAV genome is single-stranded, approximately 4.7kb in length [102], and consists of two open reading frames, the *rep* and *cap* gene. The *rep* gene codes for several Rep proteins that are required for replication of the virus and the *cap* gene codes for capsid proteins that are responsible for the formation of the capsid [103]. In addition, the AAV genome also contains an inverted terminal repeat (ITR) sequence, that flanks the AAV genome [104]. The ITR sequences are essential for the rescue, packaging and integration of AAV. These ITRs are also required to convert the single-stranded genome into double-stranded DNA [105].

Recombinant AAV (rAAV) vectors are replication-deficient viruses belonging to the family of Parvoviruses. They typically require the presence of a helper virus such as Adenovirus or Herpes simplex virus in order to cause infection [106, 107]. In the absence of a helper virus, however, wild-type AAV is able to integrate into the host genome, and remain in a quiescent state [108, 109]. The helper virus provides proteins that are required for the AAV genome to enter a lytic cycle and cause infection [107]. Several serotypes of AAV have been identified to date; the AAV serotype 2 has been most extensively studied. Different AAV serotypes display

differential tissue tropism due to the varied capsid-host interactions [110]. For example, heparin sulphate proteoglycan (HSPG) acts as a cell surface receptor for AAV2 [111], but the laminin receptor was identified as the receptor for AAV2, 3, 8 and 9 [112]. This differential tissue tropism can be exploited to express a specific gene of interest in certain tissues, but not others.

Thus, AAV vectors are currently being studied as promising gene delivery vehicles. AAV is non-pathogenic and has not been associated with any diseases in humans, even though a majority of humans were found to be sero-positive for AAV [113]. Moreover, these viruses are replication-deficient and need a helper virus to replicate. Also, upon infection in mouse and large animal models, AAV viral vectors did not elicit a significant host immune response [105], which is very beneficial for gene transfer.

1.8 A20 IN SKELETAL MUSCLE – POTENTIAL THERAPEUTIC

As mentioned earlier, several molecules are known to inhibit the activation of the NF-κB pathway and have been proven effective to regulate pathway activation in muscle and achieve muscle health and stability. Chronic NF-κB activation leads to increased inflammation in muscle, which in turn leads to muscle weakness and ultimately, muscle atrophy. Several studies have shown that inhibiting NF-κB in the muscle results in improved regenerative capacity of muscle and improved muscle strength in *mdx* mice.

In this thesis, I characterize A20 and its role in skeletal muscle and assess its role in NF-κB activation and muscle regeneration. A20 is an intrinsic negative regulator of the classical pathway of NF-κB activation. I hypothesized that A20 can regulate the NF-κB pathway in muscle, and lead to improvement of muscle health. I also analyzed the overexpression of A20 in

muscle and asked if it could inhibit NF-κB pathway activation in muscle. These studies provided the potential to understand the role of A20 in muscle and to further explore a potential novel therapeutic to treat DMD.

In order to achieve these goals, I did a step-by-step analysis to understand the role of A20 in skeletal muscle. To this end, I designed three aims and discuss each aim in detail in this thesis.

1. Characterization of A20 in skeletal muscle to understand its role in NF-κB pathway activation.

This study encompasses the protein expression, mRNA levels and localization of A20 in skeletal muscle of normal C57 and *mdx* mice. I also assessed the role of A20 with respect to the NF-κB pathway, and its affect on muscle regeneration.

2. Study the effect of over-expression of A20 in *mdx* mice, and assess its potential as a therapeutic target.

This study tests the potential of A20 as a therapeutic target for DMD in skeletal muscle by over-expression of A20 in muscle using an AAV8 vector. I observed changes in protein levels and histopathology in muscle caused by over-expression of A20.

3. Study the expression patterns of A20 in mice with heterozygous deletion of the p65 subunit of the NF-κB pathway.

This study assesses A20 protein levels in *mdx* mice deficient in the p65 subunit of the NF-κB pathway. I assessed localization and expression of A20 in the *mdx*;$p65^{+/-}$ mice over a range of ages compared to *mdx*;$p65^{+/+}$ mice.

2.0 CHARACTERIZATION OF A20 IN SKELETAL MUSCLE IN *MDX* MICE

2.1 RATIONALE

Chronic activation of the NF-κB pathway is one of the manifestations of the lack of dystrophin in skeletal muscle. Some negative regulators of the NF-κB pathway such as the IκBSR [114], NBD peptides [74] and pharmaceuticals such as curcumin [71] have been used to inhibit the pathway in muscle. However, these drugs have been shown to have long-term side effects, thus rendering the therapy insufficient and ineffective in the long run.

I chose to explore the naturally occurring negative regulators of the NF-κB pathway in the body, enhancing the likelihood and feasibility that this approach could be therapeutic. Hence, in this study, I focused on A20, a critical negative regulator of the pathway, known to inhibit pathway activation in spleen, lymph nodes and the liver [96]. Since the role of A20 was unknown in skeletal muscle, I first characterized A20 in skeletal muscle and determined its role in NF-κB pathway activation. This study was done to determine the expression, localization and role of A20 in skeletal muscle in *mdx* mice.

2.2 INTRODUCTION

The NF-κB signaling pathway plays a crucial role in dystrophic pathology caused by dystrophin deficiency [19, 38, 51, 52, 54-56] and chronic activation of NF-κB is one of the secondary manifestations of the lack of dystrophin protein in muscle [19, 115]. As stated earlier, A20 is one of the critical negative regulators of TNF-α induced activation of the NF-κB pathway [96, 116] and exploring its role in muscle would help understand its molecular function and help assess its role in the pathology of DMD.

Even though the function of A20 in the NF-κB pathway has been studied in many different tissues and cell types, the role of A20 in skeletal muscle has not been reported yet. It is not known if A20 negatively regulates NF-κB in muscle and what role it plays in muscle regeneration. Ladner and colleagues in 2003 observed that overexpression of A20 in C2C12 myotubes led to a reduction in the NF-κB pathway activation [117]. This suggested that A20 might play its regulatory role in muscle cells too. I hypothesized that A20 would negatively regulate NF-κB in skeletal muscle of *mdx* mice. Since C2C12 is a cell line, I decided to characterize the functional role of A20 in primary muscle cells isolated from *mdx* mice and study its localization in *mdx* mice. I focused on A20 protein and mRNA expression and localization in hind-limb muscles of *mdx* mice. I also assessed the role of A20 in the modulation of the NF-κB pathway in the isolated muscle cells. Since NF-κB has been shown to negatively affect muscle regeneration, I evaluated the role of A20 in muscle regeneration.

I characterized the A20 localization in normal and *mdx* mice at different ages of normal and *mdx* mice to understand the expression patterns of A20 as pathological symptoms of DMD begin to manifest in the *mdx* mouse. The classical NF-κB pathway has been shown to inhibit

muscle regeneration, however, the alternate pathway is thought to be required for the maintenance of myofibers. Therefore, I characterized the time profile of the activation of both the pathways over a broad range of ages in *mdx* mice and assessed how activation of each pathway affects the dystrophic pathology. I further explored the role of A20 in relation to the activation of each pathway and assessed how this affected regeneration of muscle.

2.3 MATERIALS AND METHODS

Animals and reagents: C57BL/10/J (C57) and C57BL/10ScSn-*Dmd*^{mdx}/J (*mdx*) mice were purchased from The Jackson Laboratory (Bar Harbor, ME) and were housed at the University of Pittsburgh Animal Housing Facility and used under approval by the University of Pittsburgh Institutional Animal Care and Use Committee (IACUC).

Antibodies used for western blotting and immunohistochemical analyses were A20 (sc-22834), p65 (sc-109), p-IκB (sc-7977), p-p65 (sc-101748), RelB (sc-28689), GAPDH (sc-25778), MyoD (sc-760), Myf-5 (sc-302), secondary antibody for Western blotting goat anti-rabbit HRP (sc-2030) (Santa Cruz Biotechnology, Inc, Santa Cruz, CA). Monoclonal antibodies were used to detect myosin heavy chain (MHC, Fast and Slow) (Vector Laboratories, Burlingame, CA). Monoclonal antibodies to embryonic MHC (eMyHC) (F1.652), used to detect regenerating fibers, obtained from the Developmental Studies Hybridoma Bank, developed by Helen Blau (University of Iowa, Department of Biological Sciences, Iowa City, IA).

Primary myoblast cell isolation, propagation and differentiation: Primary myoblasts were isolated from hind limb muscles of 4-6 week old C57 and *mdx* mice as previously described [114]. Briefly, muscle tissue samples were processed by mechanical and enzymatic (1%

collagenase for 2 hrs at 37°C) digestion. The slurry was filtered through an 85mm Nytex filter and plated on collagen-coated plates to obtain primary myoblasts. Growth media used for primary myoblasts consisted of F-12 nutrient mixture (Gibco, Invitrogen, Carlsbad, CA) supplemented with 20% FBS, 1% penicillin/streptomycin and 2.5ng/ml bFGF (Invitrogen, Carlsbad, CA). Myogenic cell lineage was confirmed by demonstrating capability to fuse to form myotubes when cultured with differentiation media as described previously [114].

Muscle tissue processing: Hind limb muscles obtained from *mdx* and C57 mice were snap-frozen using 2-methylbutane pre-cooled on dry ice and stored at -80°C. For immunohistochemical analysis, tissue samples were sectioned at a thickness of 10μm and transferred onto slides. For biochemical and genetic analysis, tissues samples were extracted as described in each relevant section.

RT-PCR analysis: Total cellular RNA was extracted from myoblasts and differentiated myotubes from C57 and *mdx* mice using TRIzol reagent (Invitrogen, Carlsbad, CA). Single-stranded cDNA was generated using Superscript III First-strand Synthesis Supermix (Invitrogen, Carlsbad, CA) at 50°C for 50min; the reaction was terminated at 85°C for 5 min. Primer sequences for GAPDH and the GAPDH probe (VIC) were obtained from TaqMan Rodent GAPDH Control Reagents (Applied Biosystems, USA). Primer sequences and probe for A20 (FAM) were designed using the Primer Express software (Applied Biosystems, USA). Amplification was carried out as follows: 50°C for 2 min, 95°C for 10 min, followed by 40 cycles of 95°C for 15s and 60°C for 1 min. PCR products were analyzed and quantified on the Applied Biosystems 7300 Real-time PCR System.

siRNA assays: Myoblasts from C57 and *mdx* mice cultured to 80-90% confluence on collagen-coated plates were transfected with control (sc-37007) or A20 (sc-37655) siRNA using

siRNA transfection reagent and transfection medium according to the manufacturer's protocol (Santa Cruz Biotechnology, Inc, Santa Cruz, CA). The cells were incubated with 6-8μg of A20 or control siRNA for 5 hrs at 37°C followed by a media change to differentiation media containing twice the normal amount of serum (DMEM with 4% horse serum, 1% penicillin/streptomycin) for 24 hours. Cells were then induced to differentiate using differentiation media containing 2% serum for 4 days.

Muscle differentiation assay: Differentiated myotubes were fixed using 2% paraformaldehyde and then blocked with 10% goat serum in 1X PBS for 1 hour. The fixed myotubes were incubated with rabbit anti-skeletal myosin (Sigma-Aldrich, St. Louis, MO) for 1 hr followed by goat anti-rabbit Alexa 594 (Sigma-Aldrich, St. Louis, MO) for 1 hr, mounted with Dapi Fluoromount-G (SouthernBiotech, Birmingham, AL), imaged and quantified. The differentiation index, which reflects the degree of differentiation, is the number of nuclei present within myotubes divided by the total number of nuclei per field. All quantifications were performed using MCID software (InterFocus Imaging Ltd, Cambridge, England).

Electrophoretic mobility shift assay (EMSA): Nuclear extracts were obtained using NE-PER nuclear and cytoplasmic extraction reagent (ThermoFisher Scientific, Rockford, IL) from C57 and *mdx* myoblasts treated at specific time-points with 10 ng/μl TNF-α. Protein concentrations of the extracts were measured using the BCA assay (ThermoFisher Scientific, Rockford, IL). In order to study NF-κB activity the nuclear extracts was pre-incubated with 5X gel shift binding buffer (Promega, Madison, WI) and nuclease-free distilled water. This was followed by incubation with an α-^{32}P-deooxycytidine triphosphate (CTP)-labeled, double-stranded DNA probe containing the NF-κB binding domain (Perkin Elmer, Waltham, MA). The probe was added at a count per minute (cpm) of ~100,000/μl to bring the final volume to 10μl.

The NF-κB probe was designed as described previously [118]. Briefly, 15bp annealing nucleotides were annealed to a 31bp oligonucleotide template at the 3' end of the template strand. The overhang was filled in with dNTPs in conjunction with ^{32}P dCTP using Polymerase I, Large (Klenow) fragment (Invitrogen, Carlsbad, CA). Labeled reactions were purified using MicroSpin G50 columns (GE Healthcare, Piscataway, NJ). Oligonucleotide sequences were as follows – NF-κB template: 5' – cagggctggggattccccatctccacagtttcacttc – 3'; NF-κB annealing: 5' – gaagtgaaactgtgg – 3' (Integrated DNA Technologies, Inc, Coralville, IA). DNA-protein complexes were separated on 6% polyacrylamide gels and resolved by electrophoresis in 1X TBE buffer at 100V for 1 hr. The gel was then dried at 80°C for 1 hr and autoradiographed at -80°C for 24-48 hrs.

Western blot analysis: Total lysates from myoblasts and myotubes were obtained by using M-PER Mammalian Extraction reagent (ThermoFisher Scientific, Rockford, IL) for cultured cells and T-PER Tissue Extraction Reagent (ThermoFisher Scientific, Rockford, IL) for muscle tissues. Nuclear and cytoplasmic extracts were obtained using NE-PER nuclear and cytoplasmic extraction reagent (ThermoFisher Scientific, Rockford, IL). Lysates were run on 10% SDS-PAGE gel for 1 hr and transferred onto a Hybond nitrocellulose membrane at 100V for 90 min. Membranes were blocked using blocking buffer (1X PBS with 10% goat serum) for 1 hr, followed by incubation with specific primary antibodies and HRP-conjugated secondary antibodies. The blot was then incubated with electrochemiluminescence reagents (GE Healthcare, Piscataway, NJ) and autoradiographed to visualize protein bands. Standard protein markers were run with proteins to determine protein size. All quantifications were performed using MCID software (InterFocus Imaging Ltd, Cambridge, England).

Immunohistochemical analysis: Muscle sections were thawed at room temperature for 5 min and hydrated using 1X PBS. The sections were then blocked using blocking buffer (10% goat serum in 1X PBS) for 1 hr and probed with specific primary and secondary antibodies diluted in DAKO antibody diluent (Invitrogen, Carlsbad, CA). Sections were then washed and mounted using Dapi FluoromountG mounting medium in the dark. Sections that were incubated with anti-mouse antibodies were treated with an additional blocking step using MOM Mouse IgG blocking reagent (Vector Laboratories, Burlingame, CA) in 1X PBS for 1 hr.

Statistical Analysis: All values are presented as mean ± standard deviation (SD) from independent experiments. Significance was determined using the 2-tailed and unpaired Student's t test. p-values < 0.05 were considered significant.

2.4 RESULTS

2.4.1 Protein and mRNA expression of A20 in myoblasts and myotubes

The biological role of A20 has been studied in several tissues, including lymph node and spleen [96], but has not been studied in skeletal muscle. Since A20 is activated by TNF-α, I induced myoblasts derived from hind limbs of C57 and *mdx* mice and differentiated myotubes using TNF-α and measured A20 protein expression. Since A20 is a relatively large protein (~90kd), protein translation takes approximately 2 hrs [119]. Hence, I assessed protein levels of A20 in myoblasts and myotubes treated with 10ng/μl of TNF-α at 1 hr intervals up to 5 hrs. I observed significantly decreased A20 protein levels in *mdx* myoblasts as compared to C57 myoblasts (Figure 7A, C). TNF-α treatment for 5 hrs did not alter A20 protein expression level in *mdx*

myoblasts. Interestingly, when I performed a similar experiment in differentiated myotubes, A20 protein levels were low in both *mdx* and C57, and did not change with TNF-α treatment (Figure 7B, C).

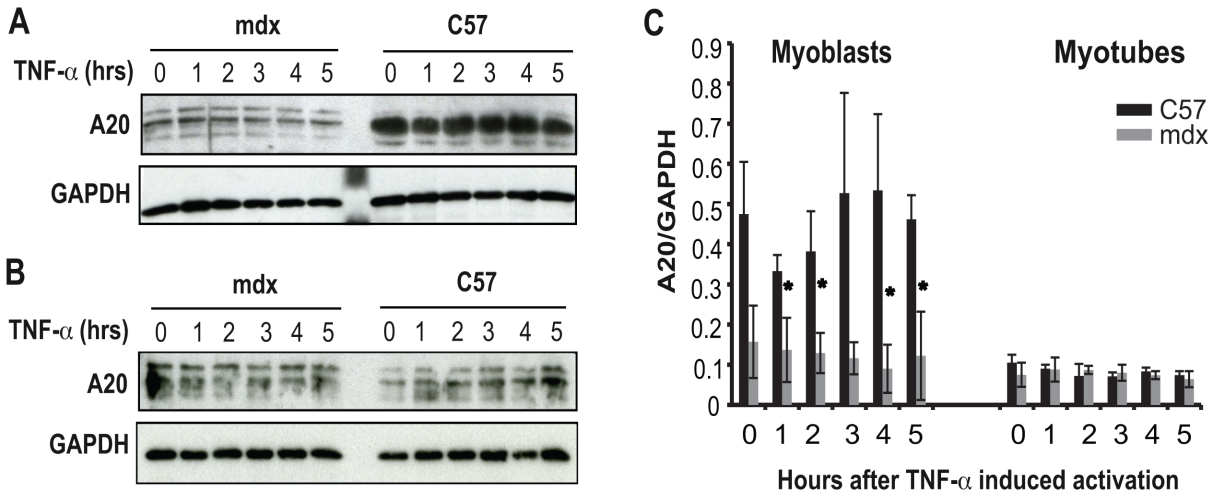

Figure 8: Reduction in A20 expression in myoblasts, but not in myotubes from *mdx* mouse muscle.

A) Myoblasts isolated from *mdx* and C57 mouse muscle were treated with TNF-α (10ng/μl) for 1-5 hours. Total lysates were extracted and analyzed for A20 protein levels by Western blotting. B) Myoblasts were induced to differentiate to form myotubes by changing growth media to differentiation media, followed by treatment with TNF-α (10ng/ml) for 1-5 hrs. C) Quantification of A20 levels normalized to GAPDH for myoblast and myotube extracts. Asterisks indicate significant difference between C57 and *mdx* (p-values for 0, 1, 2, 3, 4 and 5 hrs in myoblasts are 0.05, 0.04, 0.04, 0.07, 0.02 and 0.03, respectively; n=3 for each time point). GAPDH expression was used as a loading control.

To analyze whether the reduced A20 expression level in *mdx* myoblasts was reflected in decreased transcription, I analyzed A20 mRNA levels by RT-PCR. Consistent with the A20 protein expression results, levels of A20 mRNA in C57 myoblasts increased with TNF-α treatment of 1 hr and in C57 myotubes with TNF-α treatment of approximately 3-4 hrs (Figure 8A, B). In *mdx* myoblasts and myotubes, however, I observed no increase in A20 mRNA with 5

hours of TNF-α treatment suggesting that the low protein expression in *mdx* myogenic cells is due to decreased transcription.

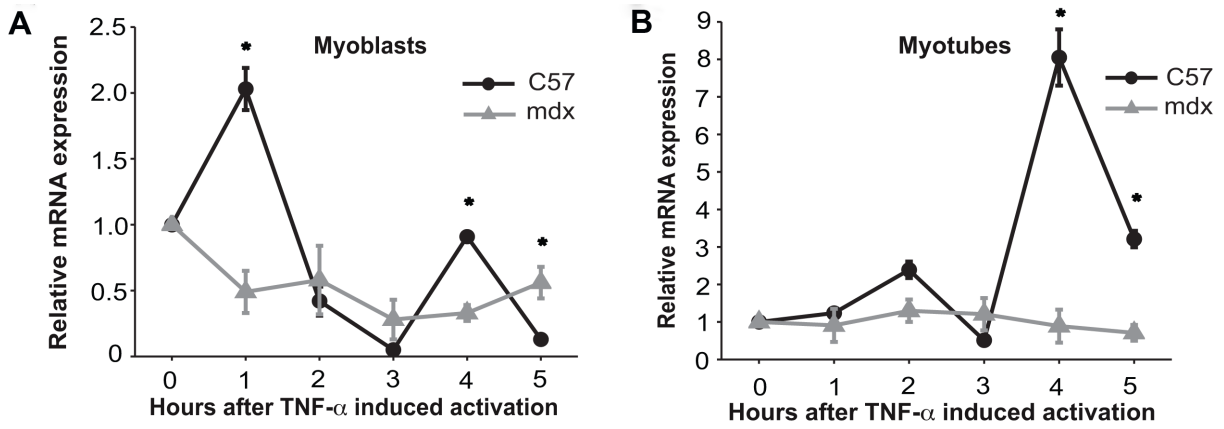

Figure 9: Analysis of A20 mRNA levels in C57 and *mdx* myoblasts and myotubes.

Relative expression of A20 mRNA levels compared to GAPDH mRNA assessed by RT-PCR in myoblasts (A) and myotubes (B). Asterisks indicate significant differences between C57 and *mdx* (p-values for 1, 2, 3, 4 and 5 hrs in myoblasts are 0.01, 0.53, 0.16, 0.01 and 0.04, respectively; p-values for 1, 2, 3, 4 and 5 hrs in myotubes are 0.4, 0.05, 0.15, 0.01 and 0.01, respectively; n=3 for each time point).

2.4.2 A20 silencing in myotubes in vitro

A20 is a known modulator of NF-κB activation triggered by TNF-α in several cell types including macrophages and Jurkat T-cells [89, 120]. In order to study the effect of lowering A20 expression in skeletal myotubes *in vitro*, I used siRNA to specifically knock down A20 expression. Myoblasts from C57 and *mdx* mice were treated with control or A20 siRNA for 5 hours and then induced to differentiate into myotubes. After 4 days, the differentiated myotubes were treated with TNF-α for 15, 30 and 60 minutes and nuclear and cytoplasmic lysates were collected. The efficacy of the A20 siRNA was shown by the demonstration of knock down of A20 protein levels with A20 siRNA but not control siRNA when treated with TNF-α for 30 and

60 mins (Fig 9A). Electrophoretic mobility shift assay (EMSA) was performed on nuclear extracts to assess NF-κB activation in the presence of A20 siRNA. I confirmed the specificity and efficacy of the NF-κB probe binding by competing the radioactive probe with cold wild-type or mutated probe at different time-points of TNF-α treatment. In nuclear extracts untreated with any siRNA or with control siRNA, NF-κB activation was observed within 15-30 minutes of TNF-□ addition and decreased around 60 minutes (Fig 9B). In myoblasts treated with A20 siRNA, however, increase in NF-κB activation was observed within 15 minutes and this activation persisted for 60 minutes (Fig 9B). NF-κB activation was greater and more prolonged for *mdx* as compared to C57 cells.

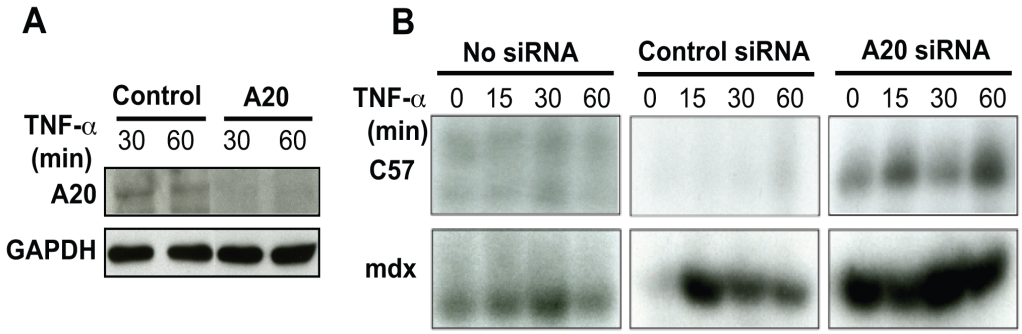

Figure 10: Knockdown of A20 causes increased NF-κB activation in C57 and *mdx* myotubes.
C57 and *mdx* myoblasts were transfected with control and A20 siRNA and induced to differentiate into myotubes. A) Western blot analysis to detect A20 protein levels in *mdx* myotubes after treatment with control and A20 siRNA after treatment with TNF-α for 30 and 60 minutes. GAPDH expression was used as a loading control. B) NF-κB activation as determined by electrophoretic mobility shift assay was assayed in untreated myotubes and myotubes transfected with control or A20 siRNA and activated with TNF-α (10ng/μl) for 15, 30, 60 min.

In order to confirm these results, I assessed the levels of phosphorylated IκB (p-IκB) as an indication of NF-κB pathway activation. I observed an increase in p-IκB levels in cytoplasmic extracts of both C57 and *mdx* myoblasts treated with A20 siRNA as compared to control siRNA

(Figure 10). Thus, this confirmed that knockdown of A20 led to chronic activation of the NF-κB pathway.

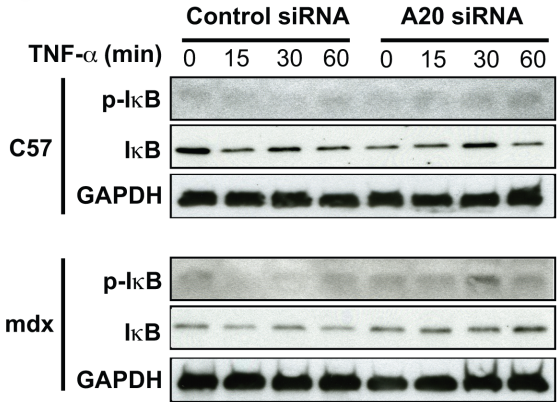

Figure 11: Increase in Phosphorylated IκB levels upon knockdown of A20 in myotubes.
Phosphorylated IκB levels in myotubes treated with control or A20 siRNA. Total IκB and GAPDH protein levels were used as a loading control.

Earlier reports demonstrated that an increase in NF-κB activation in skeletal muscle resulted in a decrease in muscle differentiation due to down-regulation of the transcription factor MyoD that is required for the regeneration and differentiation of muscle [56, 114]. Since A20 knockdown increased NF-κB activation in myotubes (Figure 9, 10), I wanted to study its effect on the differentiation capacity of myoblasts derived from *mdx* muscles. Therefore, *mdx* myoblasts were transfected with either A20 siRNA or control siRNA for 5 hrs and subsequently induced to differentiate into myotubes. After 4 days, myotubes were identified by expression of skeletal myosin heavy chain, a marker of myogenic differentiation. The differentiation index in myotubes treated with control siRNA was not significantly different from that of untreated myotubes. However, myoblasts treated with A20 siRNA show a significant delay or reduction in

myotube formation, which was reflected in a lower differentiation index, as compared to myoblasts treated with either control siRNA or no siRNA (Figure 11A, B).

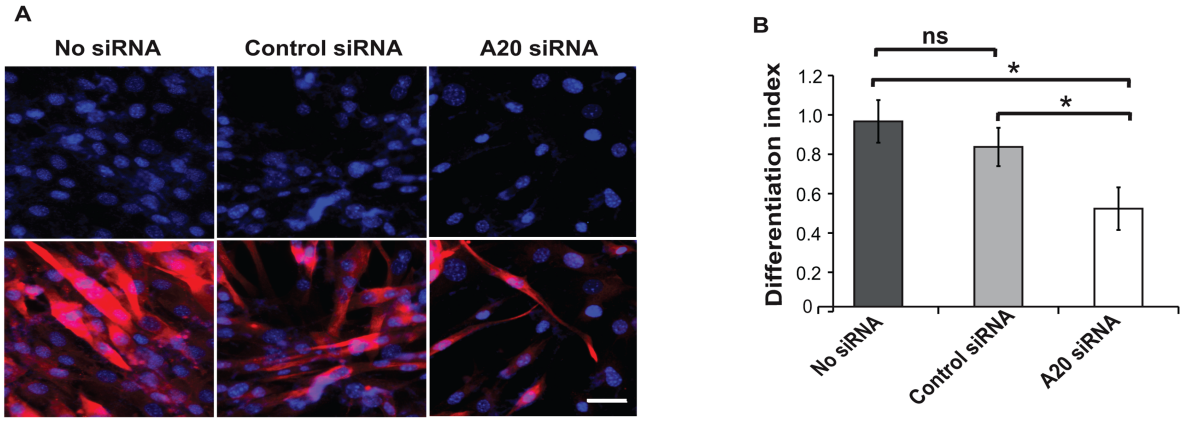

Figure 12: A20 siRNA causes impaired differentiation capacity of C57 myoblasts.

A) C57 myoblasts that were either untreated or transfected with control or A20 siRNA were induced to differentiate into myotubes by growth in differentiation media for 4 days. Myotubes were identified by expression of skeletal myosin heavy chain (MyHC) (red) by immunohistochemistry. Nuclei were stained using Dapi (blue). Scale bar - 30μm. B) Quantification of differentiation was determined by the ratio of the number of nuclei within myotubes to the total number of nuclei (differentiation index). Approximately 6-8 fields were counted and averaged to obtain a standard mean. A significant delay in differentiation was observed in A20 siRNA-treated myotubes as compared to control siRNA (p=0.00013) and untreated myotubes (p= 0.000016), and is indicated by asterisks. ns – not significant.

Since chronic NF-κB activation is known to inhibit muscle regeneration by suppressing MyoD, a transcription factor required for muscle differentiation, I speculated this impairment of myotube formation is due to suppression of MyoD and other myogenic factors by chronic NF-κB activation, caused by A20 knock down. In order to confirm this, I looked for MyoD and Myf-5 protein levels after induction of myoblast differentiation. I observe a decrease in both MyoD and

Myf-5 levels after A20 knockdown (Figure 12), supporting the hypothesis that lack of A20 impairs normal muscle differentiation.

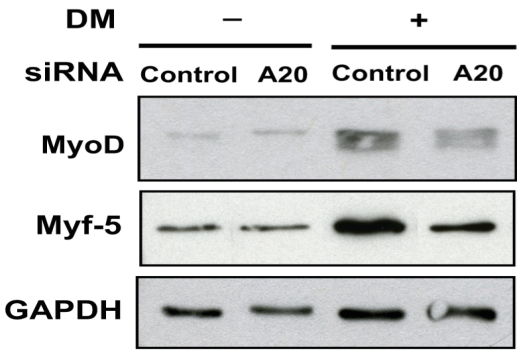

Figure 13: Differentiation factors MyoD and Myf-5 are down-regulated with A20 knockdown.
Protein levels of muscle differentiation markers, MyoD, Myf-5 in muscle cells, treated with A20 or control siRNA, before and after induction of muscle differentiation. DM - Differentiation media.

2.4.3 A20 expression and localization in gastrocnemius muscle of *mdx* mice

To study A20 expression in skeletal muscle *in vivo*, I analyzed the expression levels of A20 in gastrocnemius muscles at weekly intervals from 3 weeks to 20 weeks of age in *mdx* and C57 mice. However, only representative time-points across this age span are shown. Western blotting analysis revealed an up-regulation of A20 protein levels in muscle at 8-12 weeks of age in *mdx* mice represented by an increase observed at 10 weeks of age, an increase that was not observed in C57 mice (Figure 13A, B). A20 levels were significantly higher in *mdx* muscle at 10 weeks of age, and subsequently decreased to levels comparable to levels in C57 muscle by 14 weeks of age (Figure 13B). Localization of A20 by immunohistochemistry of muscle sections revealed an increase in the number of A20-expressing fibers between 8 and 12 weeks of age and a gradual decrease by 14 weeks of age (Figure 13C). To determine the fiber type of the A20-expressing

fibers, I performed co-localization assays. Co-localization studies in *mdx* mice revealed that A20 is expressed at higher levels by those fibers that express eMyHC, a marker of muscle fiber regeneration; all regenerating fibers demonstrated high expression of A20. In *mdx* mice, the numbers of degenerating and regenerating fibers began to increase after 3 weeks of age, reached a peak at 10-11 weeks and gradually decreased by 14 weeks of age [121]. This temporal pattern of muscle regeneration in *mdx* mice correlated with the temporal pattern of A20 protein level increases between 8 and 12 weeks of age (Figure 13B,C).

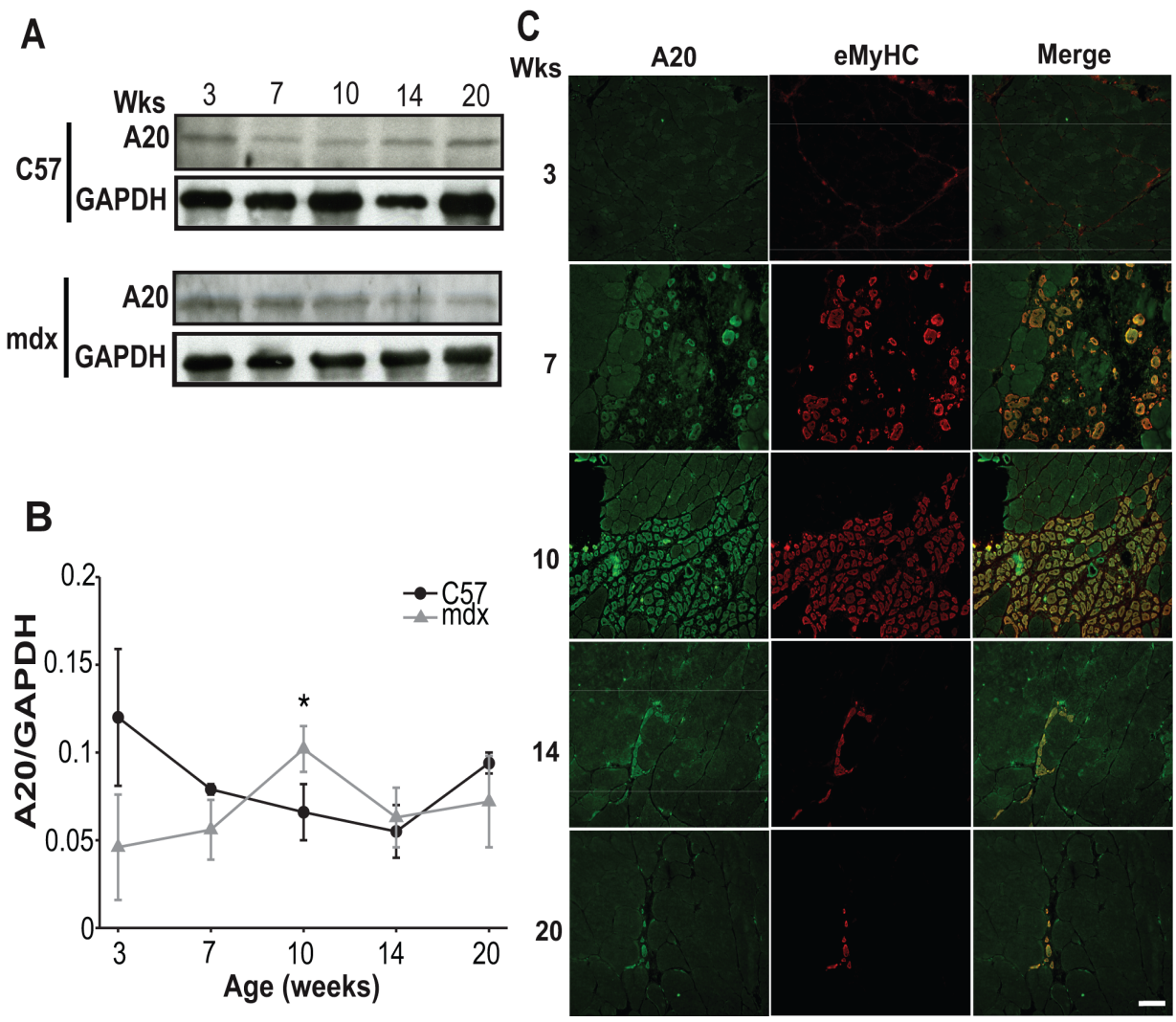

Figure 14: Skeletal muscle A20 expression is higher during regeneration-degeneration cycles in *mdx* mice.

Gastrocnemius muscles were collected from C57 and *mdx* mice from 3 weeks through 20 weeks of age (n=3). A20 expression levels were measured in total muscle lysates. A) A20 protein levels were measured by Western blot. Representative blots of C57 and *mdx* muscle at 3, 7, 10, 14 and 20 weeks are shown. GAPDH expression was used as a loading control. B) Quantification of A20 protein levels normalized to loading control GAPDH in skeletal muscle of *mdx* compared to C57. An asterisk indicates a significant difference (p-values for 3, 7, 10, 14 and 20 weeks are 0.05, 0.08, 0.04, 0.59 and 0.87 respectively). C) A20 localization (green) was determined by immunohistochemistry analysis of gastrocnemius muscle of *mdx* mice and co-localized with regenerating fibers, as determined by embryonic Myosin Heavy Chain (eMyHC) expression (red). Scale bar – 150μm.

Type II (glycolytic, fast) muscle fibers are preferentially involved in muscular dystrophy as compared to Type 1 (oxidative, slow) muscle fibers [15]. Because of our observation that higher levels of A20 expression were seen in regenerating fibers and knowledge that regenerating fibers in muscular dystrophy are largely type II, I studied the co-localization of A20 expression and fiber type. Muscle fibers expressing high levels of A20 co-localized exclusively with fast myosin heavy chain (fast MyHC), a marker for type II fibers, but not with slow myosin heavy chain (slow MyHC), a marker for type I fibers, in both C57 and *mdx* mice gastrocnemius muscle (Figure 14). It was also shown that down-regulation of A20 expression had an effect on angiogenesis [122], leading to the speculation that A20 expression might lead to better repair in fast fibers as compared to slow fibers.

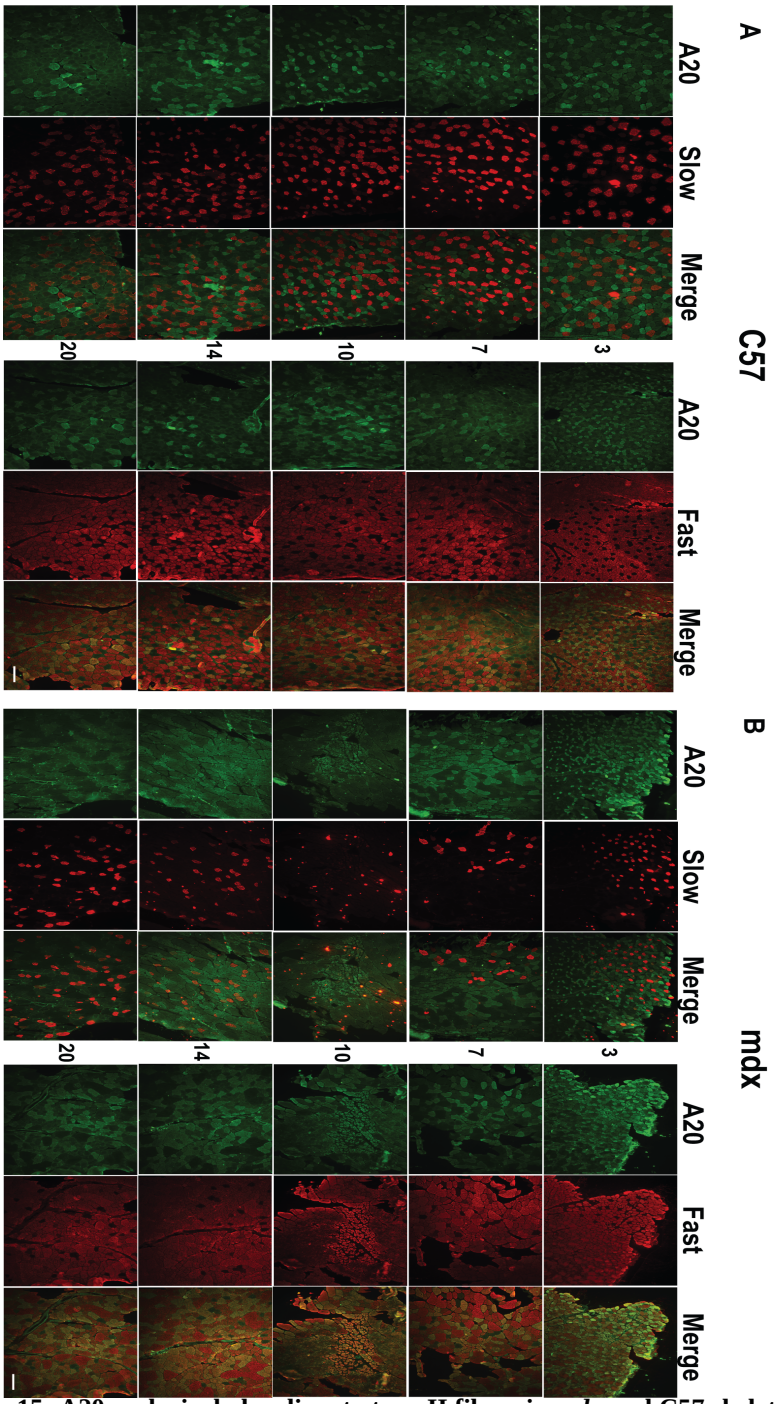

Figure 15: A20 exclusively localizes to type II fibers in *mdx* and C57 skeletal muscle.

Immunohistochemistry analysis on gastrocnemius muscle of C57 (A) and *mdx* (B) mice to study co-localization of A20 (green) with Type II (Fast) fibers (red), immunostained with fast myosin heavy chain (Fast MyHC), and with Type I (Slow) fibers (red), immunostained with slow myosin heavy chain (Slow MyHC). Merge shows co-localization (yellow). Representative images from the complete time-profile are shown. Scale bar – 150μm.

2.4.4 NF-κB subunits p65 and RelB expression and localization in muscle fibers of *mdx* mice

The NF-κB signaling pathway is activated by multiple mechanisms. The two main mechanisms known are the classical pathway involving subunits p50 and p65 and IκB as its cytoplasmic inhibitor, and the alternate pathway consisting of activation of subunits p50 and RelB. I investigated the levels of NF-κB subunits p65 and RelB in muscle samples across the age span of 3-20 weeks to assess the contributions of the classical and alternate pathways, respectively, of NF-κB activation in *mdx* and C57 mice. I observed that RelB protein levels in muscle were significantly increased in *mdx* mice at all time-points between 3 and 20 weeks of age as compared to wild-type C57 mice (Figure 15A, B). Phosphorylated p65 (p-p65) protein levels peaked in *mdx* muscle at time-points between 7 and 12 weeks of age and decreased to protein levels comparable to 14 and 20 weeks in C57 muscle (Figure 15C, D).

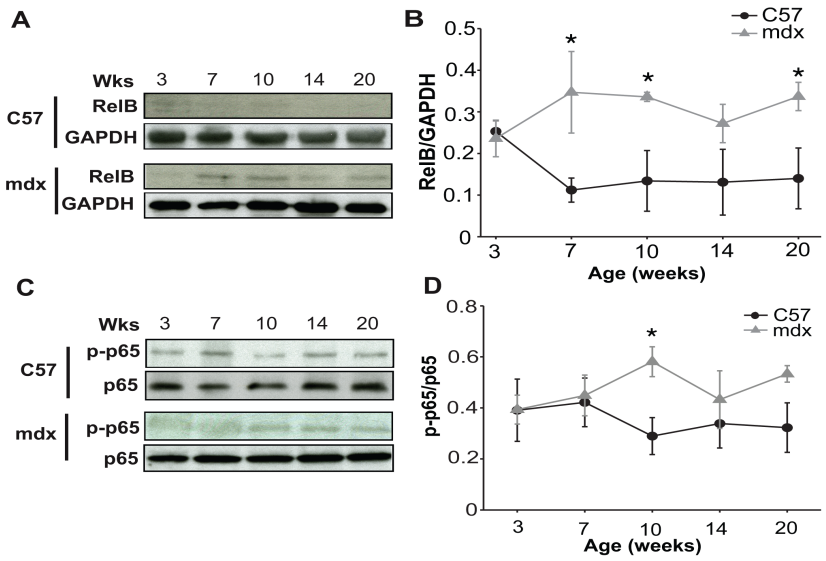

Figure 16: Increased expression of NF-κB subunits in skeletal muscle from *mdx* mice.

Gastrocnemius muscles were collected from C57 and *mdx* mice from 3 weeks through 20 weeks of age (n=3). Western blot analysis of total muscle lysates determined protein levels of RelB (A) and p-p65 (C). GAPDH and total p65 were used as loading controls. B) Quantification of the RelB levels. An asterisk indicates a significant difference between C57 and *mdx* (p-values for 3, 7, 10, 14 and 20 weeks are 0.58, 0.01, 0.01, 0.05 and 0.01, respectively). D) Quantification of p-p65 levels. An asterisk indicates a significant difference between C57 and *mdx* (p-values for 3, 7, 10, 14 and 20 weeks are 0.54, 0.28, 0.01, 0.9 and 0.24, respectively).

Because of the co-localization of high A20 expression and muscle fiber regeneration and our data showing that A20 down-regulates NF-κB activation in muscle cells *in vitro*, I hypothesized that NF-κB activation would be decreased in fibers that are regenerating. Therefore, I studied the localization patterns of p65 and RelB in muscle of *mdx* mice from 3-20 weeks of age. Representative images of the entire time-profile are shown here. I observed reduction in levels of p65 expression in fibers that were shown to be regenerating by expression of eMyHC at 7 and 10 weeks of age (Figure 16A). However, I observed an increase in RelB expression in these regenerating fibers (Figure 16B).

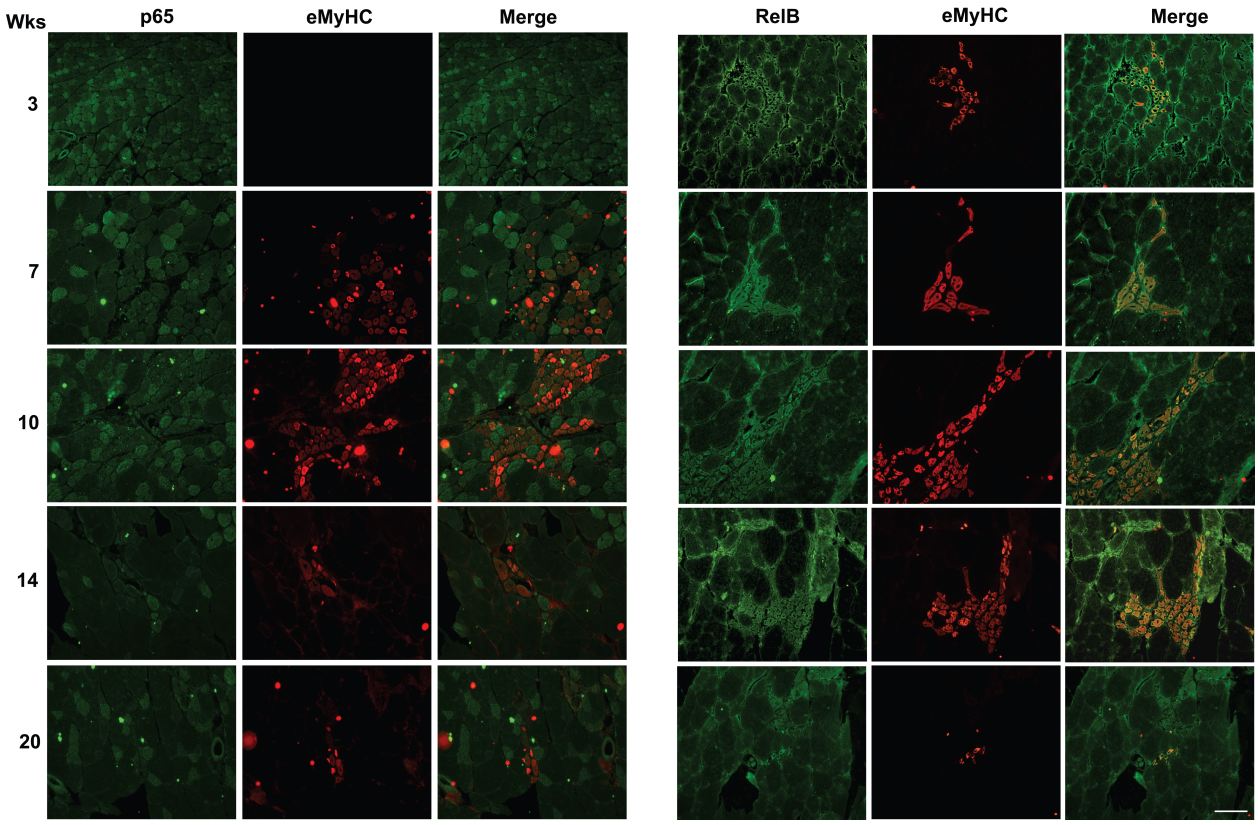

Figure 17: Regenerating muscle fibers in *mdx* mice demonstrate decreased p65 and increased RelB expression.

NF-κB subunit p65 (green) (A) and RelB (green) (B) were co-localized with regenerating fibers (red) immunostained for embryonic myosin heavy chain (eMyHC) expression in gastrocnemius muscles of *mdx* mice from 3 weeks through 20 weeks. Asterisks indicate fibers with increased p65 expression surrounding the regenerating fibers. Representative images from complete time-profile are shown. Scale bar – 100μm.

2.5 DISCUSSION

This is the first demonstration of a role for A20 in skeletal muscle. Alteration in A20 expression by the pathological process of muscular dystrophy in skeletal muscle of the *mdx* mouse model supports a pivotal role of A20 in skeletal muscle homeostasis maintained through the NF-κB signaling pathway. The largest increase in muscle A20 expression level was observed during the time of maximal muscle degeneration and regeneration of the *mdx* mouse. A20, but not p65,

expression co-localized with regenerating, type II fibers, suggesting that high expression of A20 suppresses NF-κB activation and promotes muscle fiber regeneration. Studies of cultured primary muscle cells suggest that this process is, at least in part, cell-autonomous since knock down of A20 expression in primary muscle cells resulted in higher levels of NF-κB activation triggered by TNF-α and failure of differentiation of myoblasts to myotubes.

My results show, for the first time, a correlation between expression of A20 in skeletal muscle and dystrophic pathology. A20 is expressed in skeletal muscle and plays a role in NF-κB regulation in muscles of *mdx* mice both *in vitro* in primary myoblasts obtained from hind limb muscles of mice and *in vivo*, in skeletal muscle. In primary myoblasts *in vitro*, I saw a reduction in differentiation capacity to myotubes and reductions of MyoD and Myf-5 protein levels in the absence of A20, suggesting its role in muscle differentiation. I also characterized A20 localization in murine hind limb muscles and observed over-expression of A20 exclusively in regenerating fibers. These fibers showed a lower level of p65 expression suggesting negative regulation of the NF-κB pathway intracellularly due to A20 expression, and thus, promoting regeneration of the fiber. Taken together, I have established that A20 is a negative regulator of NF-κB signaling in skeletal muscle, and has a role in muscle differentiation and regeneration.

Expression of A20 has been studied in several different cell types, including carcinoma cell lines, epithelial cells, lymphoid tissues and myotubes [96]. Ladner and colleagues showed that over-expression of A20 driven by the cytomegalovirus promoter in C2C12 myotubes effectively inhibited NF-κB activation [117]. Similar to our results in primary myogenic cells, they showed that A20 expression is induced in C2C12 myotubes within 1 hr of TNF-α activation. I observed similar activation in C57 primary myoblasts and differentiated myotubes; the folds of expression were higher in myoblasts than in myotubes. In contrast, I observed a

much lower level of expression of A20 in *mdx* primary myoblasts and myotubes. This was a very interesting and unexpected observation, since A20 is activated by TNF-α □and TNF-α □is known to be up-regulated in *mdx* mice [123]. I observed differences in A20 mRNA levels between normal and *mdx* myoblasts and myotubes. A20 mRNA levels increase in wild-type C57 myoblasts (1 hr) and myotubes (3 hr) with TNF-α stimulation; however this upregulation is not observed in either *mdx* myoblasts or *mdx* myotubes. One possible explanation for the reduction of A20 expression in myogenic cells from *mdx* mice could be a negative self-regulation by A20 due to its down-regulation of NF-κB activity [124]. Also, mRNA expression of A20 that is stimulated by TNF-α□is transient [125]; this may also contribute to the reduction of A20 expression in *mdx* muscle cells.

The critical role of A20 in the regulation of the immune response was proven in mice deficient in A20. A20 knockout mice display severe inflammation, multi-organ tissue damage and die within days of birth [97]. Chronic NF-κB activation was observed in mouse embryonic fibroblasts obtained from these knockout mice. In tissues other than muscle, there have been several studies showing A20 as a critical negative regulator of NF-κB activation. A20 is also shown to have an anti-apoptotic function in some cell types [97], mediated by protection of cells from the cytotoxic effects of TNF-α [126]. In *mdx* and C57 myotubes, I observed an increase in NF-κB activation upon siRNA-mediated knock down of A20. Therefore, I demonstrated a direct effect of A20 on regulation of NF-κB activation in myogenic cells. Studies have shown that chronic activation of NF-κB in dystrophic mice contributes to chronic muscle inflammation, muscle damage and subsequent muscle atrophy [52, 55]. NF-κB is also known to inhibit differentiation in skeletal muscle as well as regeneration of muscle by inhibiting MyoD [114, 127]. NF-κB activation is also known to inhibit myogenesis by regulation of cyclin D1 [118].

Also, there are numerous other muscle-specific transcription factors such as MRF4, myogenin and Myf-5 that play a role in the complicated process of skeletal muscle differentiation. Knockdown of A20 in myoblasts impaired their capacity for differentiation [128]. I also observed a reduction in protein levels of two of the factors, MyoD and Myf-5, in these differentiating muscle cells treated with knock down of A20. This supports the hypothesis that A20 plays a significant role in muscle regeneration through regulation of factors required for differentiation.

Skeletal muscle consists of different fiber types and very little is known about their role in muscular dystrophy. Webster and colleagues performed fiber typing in DMD patient skeletal muscle and concluded that a fast fiber subtype, type IIb fibers were preferentially involved in the process of muscle degeneration [15]. They also observed that regeneration occurred almost exclusively in type II fibers. Our observations in *mdx* mice are in line with these conclusions, since all regenerating fibers in *mdx* muscle were type II fibers. Also, higher levels of A20 expression localized to type II fibers and the level of expression correlated with the phase of cyclical muscle fiber degeneration and regeneration in *mdx* mice (7-12 weeks) [121]. Taken together, I hypothesize that A20 expression in regenerating type II fibers might confer cytoprotection by the inhibition of NF-κB activation and thus promote regeneration. This hypothesis was confirmed by our observation of reduction of p65 expression in regenerating fibers. Another study also showed a reduction in p65 expression in type II fibers [129]. This protective mechanism by A20 is ultimately lost, as more and more fibers undergo degeneration due to chronic activation of the NF-κB pathway, chronic inflammation in these fibers and exhaustion of satellite cells ultimately resulting in loss of muscle fibers in the later stages of the disease. I postulate that other muscle fibers in *mdx* muscle that had increased p65 expression are

in the initial stages of undergoing degeneration. Thus, one mechanism of the role that A20 plays in muscle regeneration is by inhibition of activation of muscle fiber NF-κB. This is a novel observation and establishes the regulatory role of A20 required for muscle regeneration in *mdx* mice.

Studies suggest that the two primary mechanisms of NF-κB activation, the classical and the alternate pathways, may each play a different role in myogenesis. The classical pathway, activated by the nuclear localization of NF-κB subunits p50 and p65, participates in the regulation of muscle differentiation, whereas the alternate pathway, which is activated by the nuclear localization of subunits p52 and RelB, participate in myofiber mitochondrial biogenesis [20]. Reduction in p65 expression in regenerating fibers is consistent with an inhibitory role of A20 on the classical pathway of NF-κB activation. In contrast, I observed an increase in RelB expression in regenerating muscle fibers, which is consistent with activation of the alternate pathway of NF-κB activation in these fibers. $RelB^{-/-}$ mice have been reported to display multi-organ inflammation, and a marked increase of immune cell infiltrate in skeletal muscles [130], whereas $p65^{-/-}$ mice are embryonic lethal [127]. $p65^{-/-}$ mice can be rescued with an additional deletion of TNF-α, and these mice display accelerated and increased myogenesis, and decreased NF-κB activation [127]. $p65^{+/-}$ mice were also shown to rescue dystrophic pathology by displaying reduction in necrotic fibers and muscle inflammation [20]. Recent studies indicate that the alternate pathway of NF-κB activation promotes the contractile function and myogenic potential of myofibers [131]. NF-κB inducing kinase (NIK) and IKK-α were shown to play a role in myogenin expression and multi-nucleated myotube formation [132]. This study also showed that IKK-α, but not IKK-β, was required for differentiation. Both NIK and IKK-α play a role in the activation of the alternate pathway of NF-κB [23]. Thus, the alternate pathway of NF-

κB activation is important for induction and maintenance of muscle fiber differentiation. Moreover, it is known that the alternate pathway of NF-κB activation is triggered by inhibition of the classical pathway [127, 133]. Our findings of increased expression of RelB and decreased expression of p65 in regenerating muscle fibers is consistent with activation of the alternate pathway and inhibition of the classical pathway of NF-κB activation as a consequence of over-expression of A20. Taking the results of these prior studies into consideration suggests that down-regulation of p65 in regenerating myofibers signals RelB activation and up-regulation in these fibers. This implies that the direct role of A20 is to regulate the classical pathway but not the alternate pathway of NF-κB activation. This finding is important since it could be postulated that A20 delivered therapeutically would inhibit only the classical NF-κB activation pathway responsible for inhibition of myogenesis, and not the alternate pathway required for its maintenance. However, it is important to note that in humans, development of DMD pathology is chronically progressive. The patient declines due to myriad complications related to dystrophin deficiency, including muscle atrophy and cardiac and respiratory failure and exhaustion of progenitor cells. Here I have shown that A20 inhibits NF-κB activation and promotes muscle regeneration in *mdx* mice. However, due to chronic NF-κB activation, dystrophin-deficient muscle fibers ultimately degenerate and fail to regenerate due to exhaustion of muscle satellite cells that are required for muscle regeneration [134]. I would speculate that intervention with A20 as a therapeutic would be most effective at a time when enough muscle fibers remain, such that A20 could protect them from degeneration. A20 would help restore the muscle and prevent chronic activation of the NF-κB pathway, thus improving muscle strength and stability, but would most likely need to be instituted early in the disease process.

In summary, I have shown a novel mechanism in muscular dystrophy of NF-κB inactivation by A20 and characterized this mechanism in skeletal muscle of *mdx* mice. These observations contribute to the understanding of how inhibition of NF-κB activation has the potential to play an important role in the reduction of dystrophic pathology and the preservation of muscle strength and health. These results provide evidence that A20 plays a pivotal role in muscle differentiation and regeneration with the potential to inhibit NF-κB activation in DMD and ameliorate dystrophic pathology. Furthermore, A20 may have potential as a therapeutic target in DMD.

3.0 OVEREXPRESSION OF A20 USING AN AAV8 VIRUS IN *MDX* MICE

3.1 RATIONALE

A20 is known as a critical negative regulator of the NF-κB pathway in several cell types, including macrophages, and organs such as the lymph nodes and spleen. In the previous chapter, I established that A20 plays a role in regulating the NF-κB pathway in skeletal muscle, and knockdown of A20 led to impaired differentiation capacity in myoblasts. I also observed that A20 localizes almost exclusively in regenerating fibers. Taken together, I can conclude that A20 plays a role in muscle regeneration, and does this through the inhibition of the classical NF-κB pathway. Hence, I wanted to test the therapeutic potential of A20 in *mdx* mice. I hypothesized that, if over-expressed in *mdx* mice, A20 would cause reduction in the chronic activation of the NF-κB pathway in muscle and subsequently improve muscle health. I used adeno-associated virus serotype 8 (AAV8) to overexpress A20 driven by a truncated muscle creatine kinase promoter, whose expression is limited to skeletal muscle.

3.2 INTRODUCTION

Several previous studies have focused on inhibition of the NF-κB pathway activation in *mdx* mice as a therapeutic target to ameliorate the severity of DMD symptoms. Inhibition of NF-κB in *mdx* mice led to improved membrane stability, enhanced regeneration, and reduced inflammation, improving overall health of muscle. In my previous study, A20 has been shown to play a critical role in the inhibition of the classical NF-κB pathway in skeletal muscle.

rAAV vectors are being studied as promising candidates for gene therapy for a wide range of human diseases. Different serotypes of AAV have been shown to display distinct tissue tropism and transduction efficiencies. AAV serotype 8 was shown to have high transduction efficiency of skeletal muscle and heart [135-137]. AAV8 was also able to equally efficiently transduce both fast and slow fibers [138]. Studies have also shown that AAV8 was able to maintain expression of a transgene at therapeutic levels in rats [139]. Thus, AAV8 is an ideal viral vector for gene therapy in skeletal muscle.

In this chapter, I explore the potential of A20 as a therapeutic agent to ameliorate DMD symptoms in *mdx* mice. To this end, I used AAV8 to over-express murine A20 in skeletal muscle of *mdx* mice. In order to specifically express A20 in skeletal muscle, I used the muscle-specific truncated muscle creatine kinase (tMCK) promoter to restrict the over-expression to skeletal muscle. The tMCK promoter, about 720bp in length, was generated by ligating three tandem copies of the MCK enhancer to its basal promoter [140]. The tMCK promoter was the strongest promoter among the other muscle-specific promoters tested by Wang et al [140]. The promoter was also shown to preferentially transduce fast-twitch fibers. This was particularly of interest, since fast fibers are the first to be affected by undergoing degeneration in DMD patients. The promoter, however, was shown to have weak expression in heart, diaphragm and liver [140].

I assessed the effect of over-expression of A20 on the NF-κB pathway activation compared to mice treated with saline. I assessed the protein levels of the transcription factors required for muscle differentiation. I also studied the effect of A20 over-expression on muscle regeneration and overall muscle pathology. I assessed levels of necrosis in the muscles, and evaluated the degree and type of inflammatory cell infiltration in skeletal muscle. The lack of significant levels of direct expression from the tMCK promoter in the diaphragm provided the opportunity to assess whether overexpression of A20 in other skeletal muscles would have a remote effect on the diaphragm.

3.3 MATERIALS AND METHODS

Mice and Reagents: C57BL/10ScSn-*Dmd*^{mdx}/J (*mdx*) mice were purchased from The Jackson Laboratory (Bar Harbor, ME) and were housed at the University of Pittsburgh Animal Housing Facility and used under approval by the University of Pittsburgh Institutional Animal Care and Use Committee (IACUC).

Antibodies used for western blotting and immunohistochemical analyses were A20 (sc-22834), RelB (sc-28689), GAPDH (sc-25778), MyoD (sc-760), Myf-5 (sc-302), secondary antibody for Western blotting goat anti-rabbit HRP (sc-2030) (Santa Cruz Biotechnology, Inc, Santa Cruz, CA). Antibody for CD4 T-cells (16-0041-81) was obtained from ebiosciences, San Diego, CA, for CD8 T-cells and secondary antibody biotinylated goat anti-rat IgG were obtained from Pharmingen; San Jose, CA. Monoclonal antibodies were used to detect myosin heavy chain (MHC, Fast and Slow) (Vector Laboratories, Burlingame, CA). Monoclonal antibodies to embryonic MHC (eMyHC) (F1.652), used to detect regenerating fibers, obtained from the

Developmental Studies Hybridoma Bank, developed by Helen Blau (University of Iowa, Department of Biological Sciences, Iowa City, IA).

Virus preparation and injections: The recombinant AAV8-tMCK-A20 vector used in this study was constructed using a murine A20 plasmid that was obtained from BCCM/LMBP Plasmid collection, Belgium (LMBP 4801). The tMCK promoter used for the study was obtained from Dr. Bing Wang (University of Pittsburgh, PA). The AAV vector contains inverted terminal repeats of the viral genome and packaging signal, but does not contain any other viral coding sequences. AAV-293 cells were used for large-scale virus production. The viral titer was quantified using quantitative dot blot assays.

Neonatal *mdx* pups (2-3 days old) were injected intraperitoneally using a sterile needle with 6.25×10^{10} vector genomes in a volume of about 30µl. The mice were sacrificed at 8 weeks to collect muscles. Saline injected, age-matched mice were used as a control.

Electrophoretic mobility shift assay (EMSA): Nuclear extracts were obtained using NE-PER nuclear and cytoplasmic extraction reagent (ThermoFisher Scientific, Rockford, IL) from quadriceps and diaphragms of A20- or saline-injected *mdx* mice. Protein concentrations of the extracts were measured using the BCA assay (ThermoFisher Scientific, Rockford, IL). In order to study NF-κB activity the nuclear extracts was pre-incubated with 5X gel shift binding buffer (Promega, Madison, WI) and nuclease-free dH_2O. This was followed by incubation with an γ-^{32}P-deooxycytidine triphosphate (CTP)-labeled, double-stranded DNA probe containing the NF-κB binding domain (Perkin Elmer, Waltham, MA). The probe was added at a count per minute (cpm) of ~100,000µl to bring the final volume to 10µl. The NF-κB probe was designed as described previously (18). Briefly, 15bp annealing nucleotides were annealed to a 31bp oligonucleotide template at the 3' end of the template strand. The overhang was filled in with

dNTPs in conjunction with ^{32}P dCTP using Polymerase I, Large (Klenow) fragment (Invitrogen, Carlsbad, CA). Labeled reactions were purified using MicroSpin G50 columns (GE Healthcare, Piscataway, NJ). Oligonucleotide sequences were as follows – NF-κB template: 5' – cagggctggggattccccatctccacagtttcacttc – 3'; NF-κB annealing: 5' – gaagtgaaactgtgg – 3' (Integrated DNA Technologies, Inc, Coralville, IA). DNA-protein complexes were separated on 6% polyacrylamide gels and resolved by electrophoresis in 1X TBE buffer at 100V for 1 hr. The gel was then dried at 80°C for 1 hr and autoradiographed at -80°C for 24-48 hrs.

Western blot analysis: Total lysates from quadriceps ad diaphragm tissues were obtained using T-PER Tissue Extraction Reagent (ThermoFisher Scientific, Rockford, IL). Lysates were run on 10% SDS-PAGE gel for 1 hr and transferred onto a Hybond nitrocellulose membrane at 100V for 90 min. Membranes were blocked using blocking buffer (1X PBS with 10% goat serum) for 1 hr, followed by incubation with specific primary antibodies and HRP-conjugated secondary antibodies. The blot was then incubated with electrochemiluminescence reagents (GE Healthcare, Piscataway, NJ) and autoradiographed to visualize protein bands. Standard protein markers were run with proteins to determine protein size. All quantifications were performed using MCID software (InterFocus Imaging Ltd, Cambridge, England).

Muscle tissue processing: Hind limb muscles and diaphragms obtained from *mdx* mice were snap-frozen using 2-methylbutane pre-cooled on dry ice and stored at -80°C. For immunohistochemical analysis, tissue samples were sectioned at a thickness of 10μm and transferred onto slides.

Immunohistochemical analysis: Quadriceps and diaphragm sections of 10μm in thickness were thawed at room temperature for 5 min and hydrated using 1X PBS. The sections were then blocked using blocking buffer (10% goat serum in 1X PBS) for 1 hr and probed with

specific primary and secondary antibodies diluted in DAKO antibody diluent (Invitrogen, Carlsbad, CA). Sections were then washed and mounted using Dapi FluoromountG mounting medium in the dark. Sections that were incubated with anti-mouse antibodies were treated with an additional blocking step using MOM Mouse IgG blocking reagent (Vector Laboratories, Burlingame, CA) in 1X PBS for 1 hr.

For CD4 and CD8 staining, I used a DAB staining protocol as described previously [141]. Briefly, rehydrated sections were blocked in peroxidase blocking reagent (Invitrogen, Carlsbad, CA) for 5 minutes, and then incubated in blocking buffer (10% goat serum in PBS) for 1 hr. The sections were then incubated with specific primary antibodies diluted in blocking buffer for 1.5 hrs. Sections were incubated for 1 hour with secondary antibody, biotinylated goat anti-rat, diluted in DAKO antibody diluent (Invitrogen, Carlsbad, CA). Sections were incubated in ABC Vectastain avidin-HRP detection solution (Vector Laboratories; Burlingame, CA) for 30 minutes at room temperature and DAB peroxidase substrate solution (Vector Laboratories; Burlingame, CA) for 4 minutes. Sections were counterstained with eosin to visualize muscle fibers. The number of infiltrating cells in each group was quantified by counting the total number of cells per field in a section of vector-injected quadriceps and about 8 fields per section of 2 sections were counted for each mouse.

Statistical Analysis: All values are presented as mean ± standard error of mean (SEM) from independent animals in each group. Significance was determined using the 2-tailed and unpaired Student's t test. p-values < 0.05 were considered significant.

3.4 RESULTS

3.4.1 Over-expression of A20 driven by a muscle-specific promoter using an AAV8 virus vector

Knock down of A20 was shown to cause chronic activation of NF-κB, indicating its role in regulation of the pathway [142]. I hypothesized that overexpression of A20 in skeletal muscle would have a therapeutic benefit on muscle improving muscle health. To test this hypothesis, I used an AAV serotype 8 to overexpress A20 driven by the tMCK promoter that limits transgene expression to skeletal muscle. The schematic of the viral plasmid is shown in Figure 17. Neonatal *mdx* pups were given an intraperitoneal injection of 6.25 x 10^{10} vg of AAV8-tMCK-A20. Treated mice were sacrificed and muscles collected at 8 weeks of age. Pups injected with saline were used as a control. I chose 8 weeks as the time-point, because the degree of pathological dystrophic changes in muscle in *mdx* mice reaches a peak around the 8-12 wks of age, with a subsequent decrease in the degree of pathological change.

Figure 18: Schematic of the AAV-tMCK-A20 plasmid.

ITR – Inverted terminal repeats, tMCK – truncated muscle creatin kinase.

I first assessed A20 protein levels in skeletal muscles of the injected mice. I observed a 1.4 fold increase in A20 protein levels in quadriceps of *mdx* mice injected with AAV8-tMCK-A20 as compared to saline-treated mice (Figure 18A). However, I did not observe any significant difference in A20 expression in diaphragms of *mdx* mice treated with A20 as compared to saline

(Figure 18B), as expected because the tMCK promoter is known to have weak expression in the diaphragm. Analysis of pathological change in the diaphragm allowed me to explore whether A20 over-expression in other skeletal muscle could have a remote effect on diaphragm.

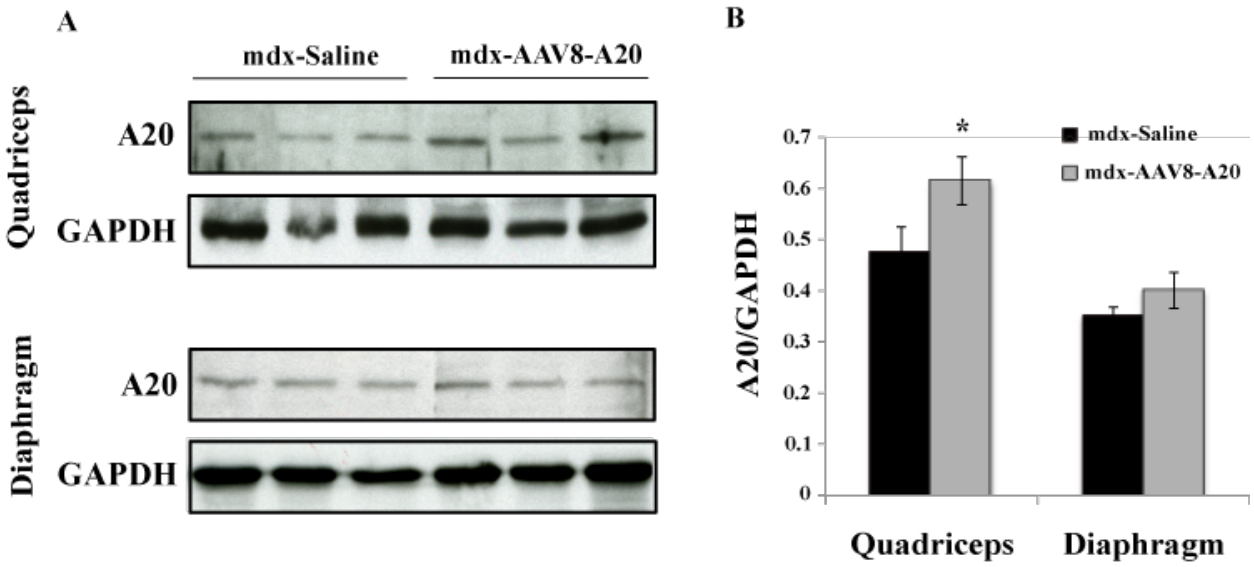

Figure 19: A20 protein levels in muscles of AAV8-A20-treated *mdx* mice as compared with saline-treated *mdx* mice.

A) Total lysates from quadriceps and diaphragm from 8wk old *mdx* mice treated with AAV8-A20 or saline were analyzed for A20 protein levels by Western blotting. Results from three representative mice are shown. B) Quantification of A20 protein levels normalized to GAPDH levels are shown. Asterisk indicates significance; $p<0.05$. n=8 for quadriceps and n=5 for diaphragm.

3.4.2 Protein levels of the alternate pathway subunit RelB, and differentiation factor, Myf-5 increased upon A20 treatment

I had previously shown that A20 is upregulated in regenerating fibers in skeletal muscle of *mdx* mice. RelB, a subunit of the alternate pathway, but not p65, a member of the classical pathway, was also upregulated in these fibers. Hence, I wanted to assess the effect of A20 overexpression on the RelB protein levels. I observed an increase in RelB protein levels in quadriceps muscle of

mdx mice treated with AAV8-A20 (average RelB/GAPDH ratio=0.9) as compared to mice treated with saline (average RelB/GAPDH ratio=0.5) (Figure 19). I also analyzed protein levels of MyoD, and Myf-5, transcription factors required for differentiation of muscle. I observed an increase in Myf-5, but not MyoD levels in quadriceps muscle of AAV8-A20 treated *mdx* mice compared to saline. These levels remained unaffected in the diaphragm of the AAV8-A20 treated mice compared to saline (Figure 19).

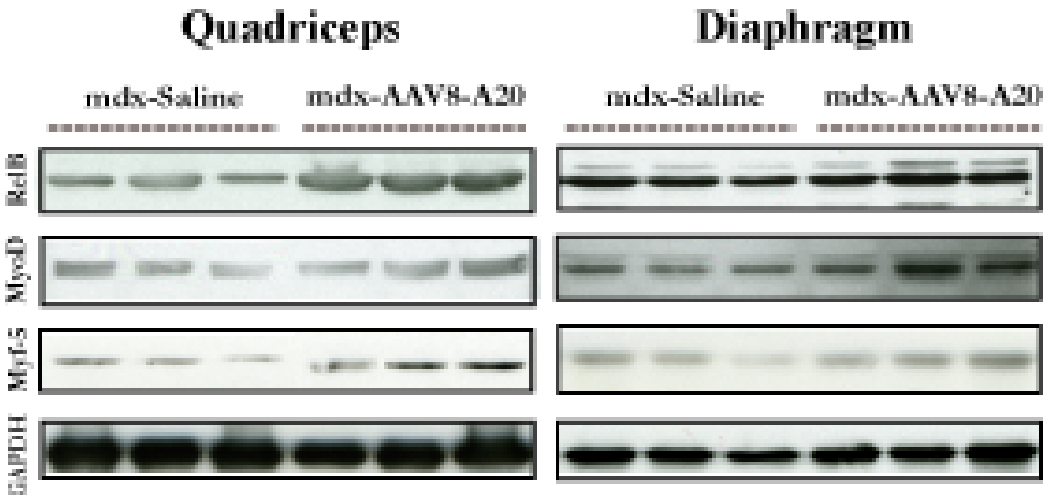

Figure 20: Protein levels of RelB, and differentiation factors MyoD and Myf-5.

A) Total lysates from quadriceps and diaphragm from 8wk old *mdx* mice treated with AAV8-A20 or saline were analyzed for RelB, MyoD and Myf-5 protein levels by Western blotting. Results from three representative mice are shown. n=8 for quadriceps and n=5 for diaphragm.

3.4.3 A20 overexpression decreases activation of the NF-κB pathway

A20 plays a critical role in negatively regulating the TNF-α-induced NF-κB pathway activation in skeletal muscle-derived cells. Knockdown of A20 in *mdx* myotubes caused chronic activation of the NF-κB pathway. I assessed NF-κB pathway activity in quadriceps and diaphragm of control C57 mice and *mdx* mice treated with either AAV8-A20 or saline. I observed a significant

reduction in NF-κB pathway activation when treated with AAV8-A20 as compared to saline in quadriceps by electrophoretic mobility shift assay (EMSA) (Figure 20A). In the diaphragm, however, I did not see any significant reduction in NF-κB activity (Figure 20B).

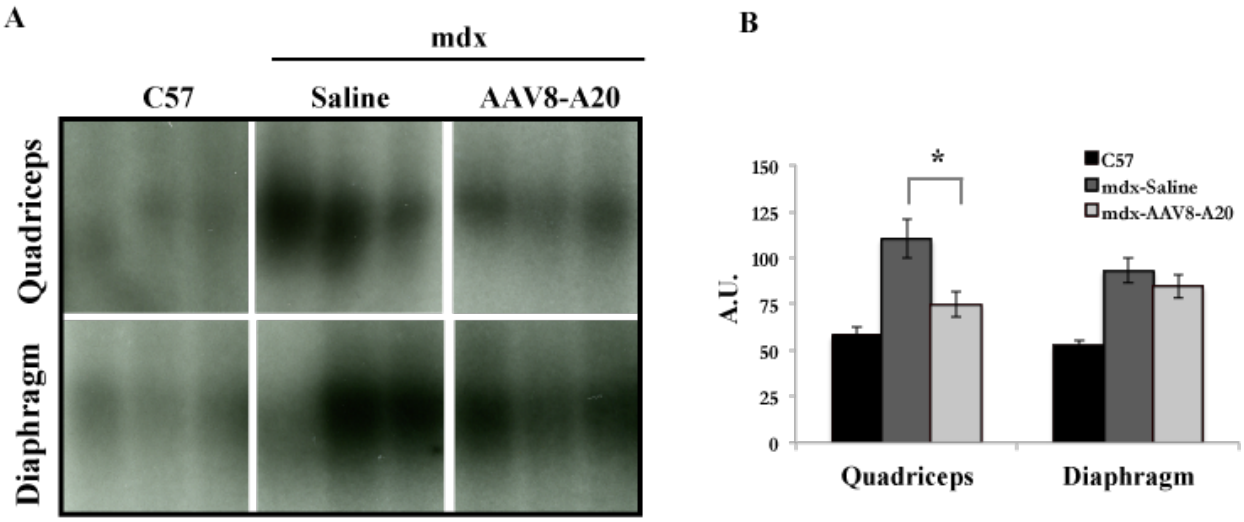

Figure 21: EMSA to analyze NF-κB activation in *mdx* quadriceps and diaphragm.

A) Nuclear extracts from quadriceps and diaphragm of C57 and *mdx* mice treated with AAV8-A20 or saline were assessed for NF-κB activity using the EMSA assay. Results from three representative mice from each group are shown. B) Quantification of the NF-κB activation. Band intensities from each blot were measured and averaged for each group. The asterisk indicates significance; $p<0.05$. n=3 for C57 mice, n=9 for saline-treated *mdx* mice, n=12 for A20-treated *mdx* mice.

3.4.4 Overexpression of A20 causes a decrease in muscle fibers harboring centrally-placed nuclei in quadriceps

Due to the lack of dystrophin and chronic activation of the NF-κB pathway, *mdx* skeletal muscle fiber sarcolemma lose integrity, thus subjecting muscle tissue to protein degradation and atrophy; this triggers satellite cell activation which leads to muscle fiber repair and regeneration. Thus, myofibers undergo repeated cycles of degeneration and regeneration. Because of this chronic

cycle of damage and repair, myofibers do not fully mature, and thus, nuclei in regenerating myofibers remain centrally located. Thus, presence of centrally nucleated muscle fibers is a marker for this continuous cycle of degeneration and regeneration of muscle fibers. I assessed the effect of A20 overexpression on this process in quadriceps of mice treated with AAV8-A20 compared to saline. I observed a significant decrease in the percentage of fibers with centrally-placed nuclei in quadriceps, but not in the diaphragm (Figure 21A, B).

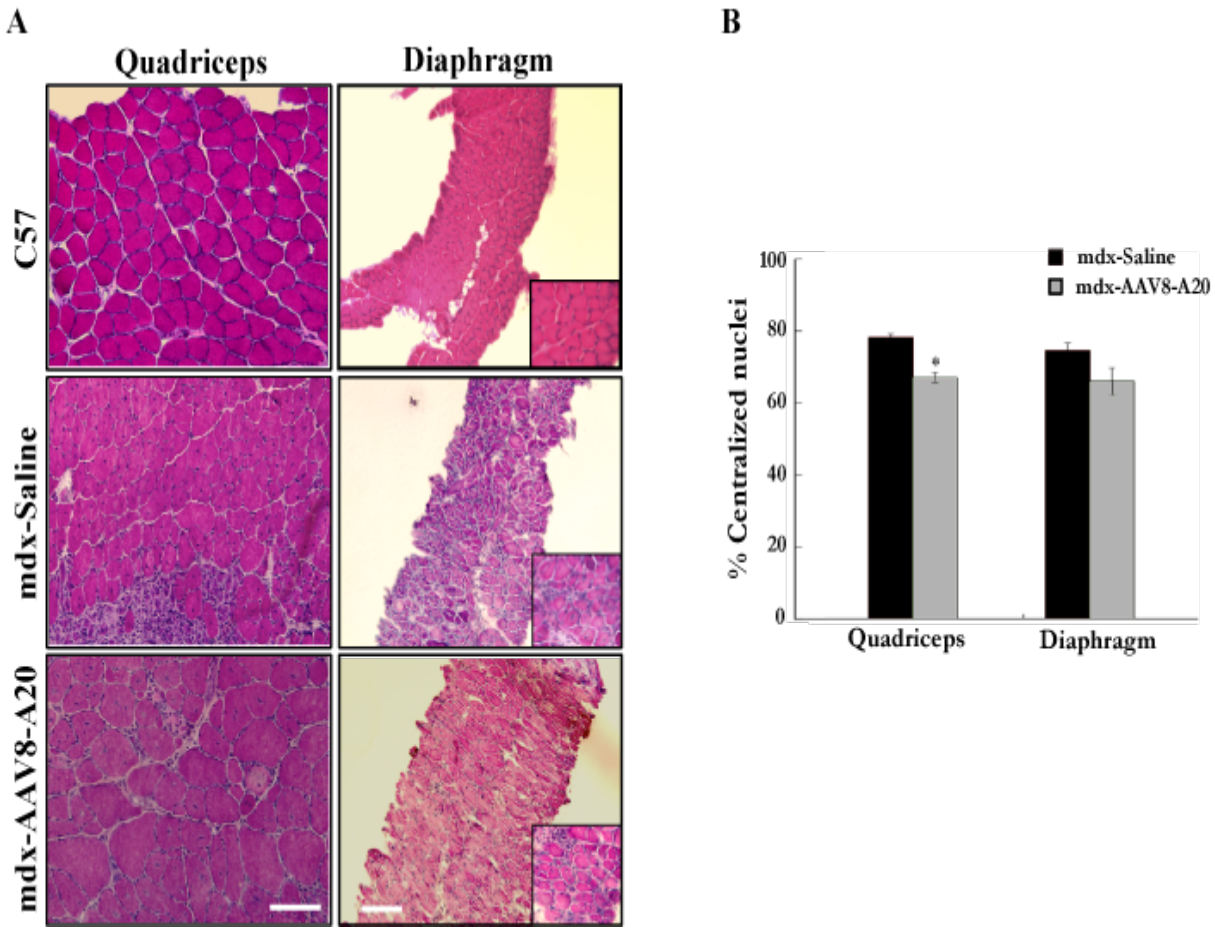

Figure 22: Histological analysis of AAV8-A20 and saline injected muscles.

A) Quadriceps and diaphragm from C57 mice and *mdx* mice treated with AAV8-A20 or saline were stained with hematoxylin and eosin. B) Quantification of number of centralized nuclei in quadriceps and diaphragm of saline- or AAV8-A20-treated *mdx* mice. The number of myofibers harboring centralized nuclei were counted from three fields per section of two sections per mouse and then averaged for each group. The asterisk indicates significance; $p<0.05$.

n=9 for saline treated *mdx* mice, n=12 for AAV8-A20 treated *mdx* mice. Scale bar-Quadriceps-150μm; Diaphragm-100μm.

3.4.5 A20 overexpression decreases regeneration, but has no effect on necrosis in skeletal muscle

Since I observed a decrease in the number of fibers harboring centrally-placed nuclei and the decrease in this pathological finding is indicative of a reduction in the degeneration and regeneration in *mdx* muscle, I speculated that this finding was indicative of improved muscle health. I confirmed this by analyzing the number of regenerating fibers in quadriceps and diaphragm. I observed a decrease in the percentage of regenerating fibers in quadriceps (Figure 22A, B). Interestingly, I also observed a decrease in the percentage of regenerating fibers in the diaphragm of treated mice (Figure 22B).

A decreased number of fibers with centrally-placed nuclei and percent regeneration indicate that the muscle is undergoing fewer cycles of degeneration and regeneration. To confirm a decrease in degeneration and atrophy in muscle, I assessed the amount of necrotic fibers in the muscles. I observed no significant decrease in the percentage of necrotic fibers in quadriceps and the diaphragm (Figure 22C). I also observed a lot of variability for the percentage of necrotic fibers between mice, as illustrated in the graph (Figure 22D).

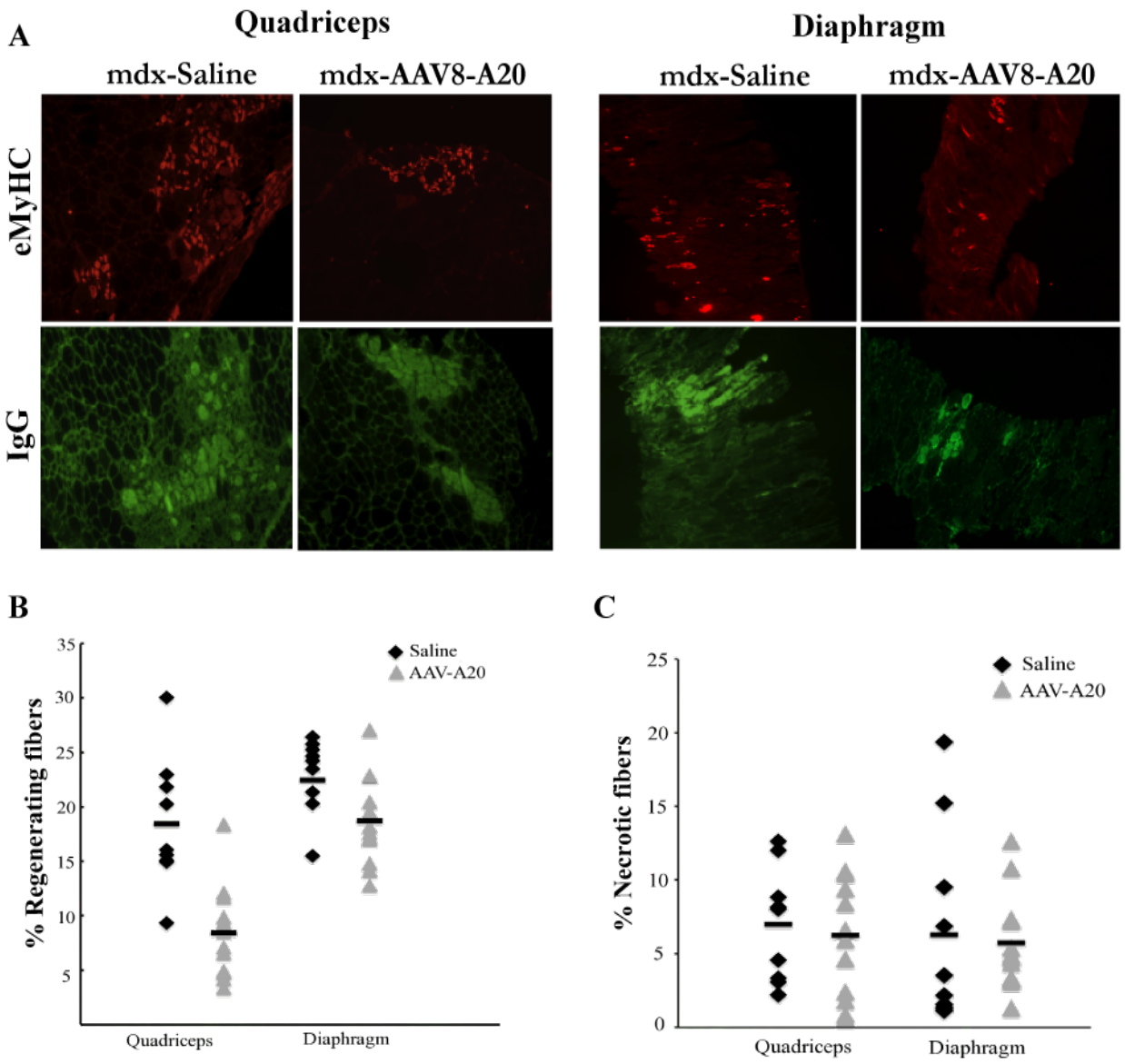

Figure 23: Analysis of regeneration and necrosis in quadriceps and diaphragm of *mdx* mice.

A) Quadriceps and diaphragm treated with AAV8-A20 or saline were immunolabeled with either embryonic myosin heavy chain (eMyHC) antibody (red) or IgG (green) to assess the number of regenerating fibers and necrotic fibers, respectively. B) and C) Quantification of the percentage of regenerating (B) and necrotic (C) fibers. Number of regenerating and necrotic fibers per section were counted and plotted as a percentage of the total number of fibers. Two sections per mouse were counted and averaged for each group. n=9 for saline treated *mdx* mice, n=12 for AAV8-A20 treated *mdx* mice.

3.4.6 Decrease in infiltrating inflammatory T-cells in skeletal muscle of *mdx* mice treated with AAV8-A20

Chronic inflammation in muscle is one of the causes of protein degradation and subsequent muscle atrophy. Chronic NF-κB activation in muscle leads to infiltration of macrophages, T-cells and cytokines such as TNF-α. Because overexpression of A20 caused a reduction in NF-κB activation in *mdx* mouse muscle, I analyzed quadriceps and diaphragm for the presence of CD4 and CD8 inflammatory T-cells. In quadriceps, I observed a significant decrease in the number of CD4 T-cells in AAV8-A20-treated *mdx* mice (Figure 23A). The number of CD8 T-cells were however unaffected in quadriceps of AAV8-A20-treated *mdx* mice (Figure 23A, B).

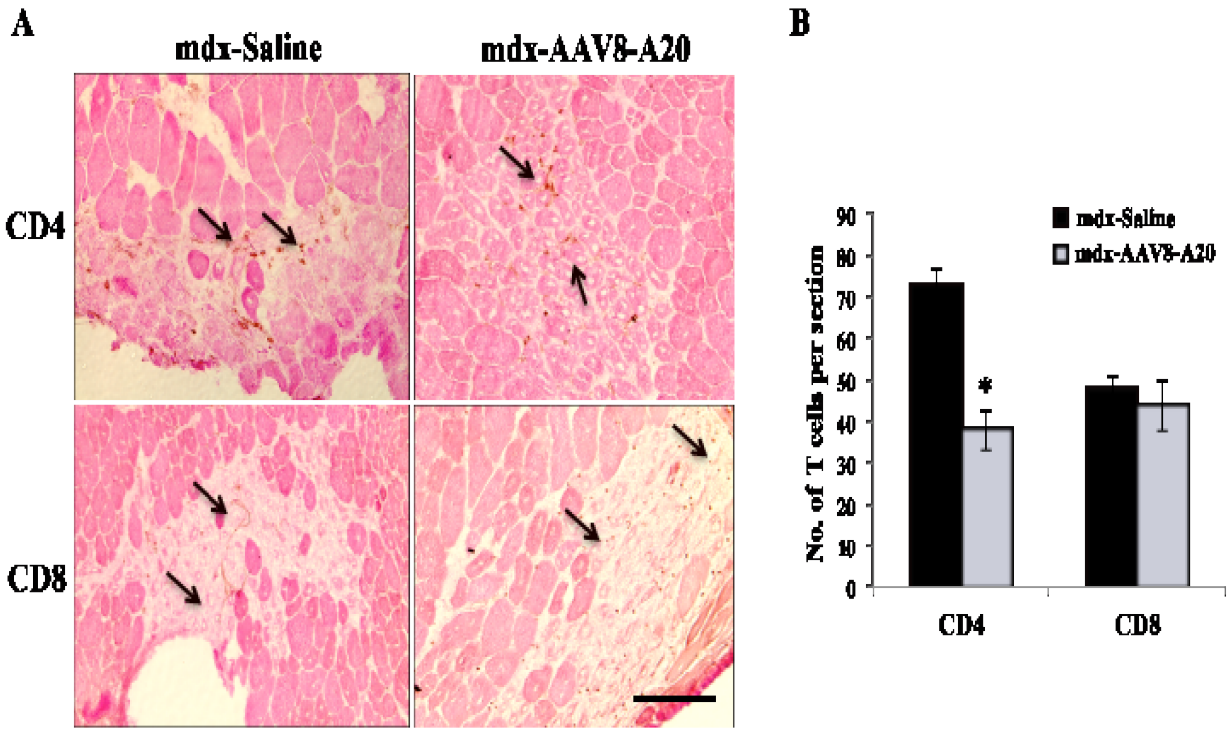

Figure 24: Analysis of infiltrating CD4 and CD8 T-cells in quadriceps.

A) Quadriceps muscles from AAV8-A20-treated or saline-treated *mdx* mice were immunostained for infiltrating CD4 and CD8 T-cells. B) For quantification, the total number of infiltrating T-cells was counted per section, and two sections were counted per mouse, and were averaged for each group. The asterisk indicates significance; $p<0.05$. n=9 for *mdx* mice treated with saline and n=12 for *mdx* mice treated with AAV8-A20. Scale bar – 150μm.

3.5 DISCUSSION

Chronic activation of the NF-κB pathway in DMD leads to many of the pathological findings in DMD [19, 52, 58, 143, 144] and inhibition of the pathway ameliorates many of those findings [145, 146]. I show the role of A20 as a potential therapeutic molecule for DMD in *mdx* mice. I assessed the pathological changes in *mdx* mice upon over-expression of A20 in skeletal muscle achieved by systemic AAV8-A20 gene delivery. I found that increased protein expression of

A20 led to a significant decrease in NF-κB pathway activation in quadriceps of *mdx* mice. I also observed an increase in protein levels of RelB, a subunit of the alternate pathway and Myf-5, a muscle transcription factor required for differentiation. Moreover, I observed a decrease in the number of fibers with centrally placed nuclei and a decreased percent regeneration in the quadriceps of *mdx* mice. Lastly, I detected a reduction in the number of infiltrating inflammatory CD4 T-cells in the quadriceps of AAV8-A20-treated *mdx* mice. Taken together, I conclude that A20 effectively reduces the activation of the classical NF-κB pathway and leads to histological findings of improved muscle health. These findings suggest that A20 should be explored further as a therapeutic molecule for treatment of DMD.

Expression of A20 following systemic delivery with an AAV8 vector carrying the murine A20 cDNA driven by the muscle-specific tMCK promoter was increased almost 1.5 fold in quadriceps. This seemed to be a modest increase in the A20 protein levels in the quadriceps. One possible reason for this could be delivery of insufficient number of viral genomes. I was able to inject 6.25×10^{10} vg/mouse, as the total volume that could be injected into neonatal mice was a limiting factor. Nonetheless, even with a 1.5 fold increase of A20 expression, I could achieve a significant reduction in the activation of the NF-κB pathway in skeletal muscle. This confirmed my hypothesis that overexpression of A20 would be able to regulate the NF-κB pathway in muscle. Interestingly, I also observed an increase in the expression levels of RelB, a subunit of the NF-κB alternate pathway. This was a very interesting observation, since I have previously shown that RelB is overexpressed in regenerating fibers and that A20 plays a role in muscle regeneration by inhibiting the classical but not the alternate pathway. In studies by others, the alternate pathway was shown to be required for myogenesis and maintenance of the myofibers [127]. Thus, I can speculate that overexpression of A20 inhibits the classical pathway and

promotes the up-regulation of the alternate pathway thus enhancing muscle regeneration. I also assessed the effect of A20 overexpression on the diaphragm, since many of the complications in DMD patients arise due to weakness in the diaphragm ultimately leading to respiratory failure. Since the tMCK promoter is known to have weak expression in the diaphragm [140], I did not see any increase in A20 protein levels in the diaphragm.

Absence of dystrophin in the muscle impairs the integrity of the muscle membrane, causing the muscle fibers to undergo cycles of degeneration and regeneration [147, 148]. Due to this constant damage to muscle, myofibers become unstable ultimately leading to protein degradation and muscle atrophy [147]. I analyzed the effect of overexpression of A20 on this cycle of damage and repair. I observed a significant decrease in the number of fibers with centrally placed nuclei, a well-studied marker of continuous regeneration-degeneration, in the quadriceps of AAV8-A20-treated *mdx* mice. Earlier studies have also shown that reduced activation of the NF-κB pathway causes decreased regeneration and increased stability of muscle [84, 145]. Consistent with these studies, I also observed a decrease in the number of regenerating fibers in quadriceps of AAV8-A20 treated *mdx* mice. This suggests a decrease in the damaging cycles of myofiber degeneration that leads to regeneration and an overall improvement in muscle health. Interestingly, albeit modest, this decrease in the number of regenerating fibers was also observed in the diaphragm. This was a very surprising observation, since I did not see any significant increase in A20 protein expression in the diaphragm. One possible explanation for this decrease could be that the weak increase in expression levels of A20 in the diaphragm was sufficient to dampen NF-κB activation enough to promote muscle health. I did observe decreased NF-κB activation in the diaphragm of AAV8-A20-treated as compared to saline-treated *mdx* mice (Figure 21), however this did not reach statistical significance ($p=0.19$). A detailed study

focusing on the expression levels of A20, perhaps driven by a ubiquitous promoter such as the cytomegalovirus (CMV) promoter in the diaphragm would further help elucidate this observation.

The muscle pathology in DMD is thought to be caused by an imbalance between the amount of regeneration and the amount of necrosis in muscle tissue [147]. One of the reasons muscle fibers degenerate is due to NF-κB induced activation of transcription targets such as MuRF1 and atrogin-1 that mediate upregulation of the ubiquitin-proteosome pathway causing necrosis of the muscle fibers [149-151]. I analyzed the effect of A20 overexpression on the number of necrotic fibers in skeletal muscle of treated *mdx* mice. To my surprise, overexpression of A20 did not have any effect on necrosis in quadriceps and the diaphragm. I observed no change in the number of necrotic fibers in AAV8-A20-treated as compared to saline-treated *mdx* mice. Although there was a reduction in regeneration, AAV8-A20 treatment did not confer an effect an effect on the level of necrosis in the muscles of the treated *mdx* mice. One explanation for this could relate to the dose of A20 transgene that could be delivered to each mouse. Since, the A20 transgene was delivered to neonates, its early expression during development may have helped maintain the health and stability of muscle fibers by inhibiting activation of the NF-κB pathway. This could explain the reduction in the number of regenerating fibers at 8wk of age in the *mdx* mice. However, the lower transgene expression may not have been sufficient to sustain its function to completely inhibit NF-κB activation leading to the transcription of its downstream targets causing muscle fiber necrosis. Future studies analyzing the effect of the dose of the delivered transgene with relation to mouse age at the time of delivery would increase understanding of the lack of inhibition of necrosis in A20-treated skeletal muscle.

Chronic activation of the NF-κB pathway leads to the infiltration of inflammatory cells, such as macrophages, and cytokines and chemokines in skeletal muscle [152]. Specifically, CD4-positive and CD8-positive T-cells were shown to play a role in dystrophic pathology and depletion of these cells in prior studies by others led to improvement of histopathology in *mdx* mice [153]. Since A20 causes reduction of NF-κB pathway activation, I speculated that this reduction would decrease the amount of inflammation in muscle. I observed a reduction in the number of infiltrating CD4 positive T-cells in the quadriceps of AAV8-A20-treated *mdx* mice. I did not, however, observe any decrease in the number of CD8 positive T-cells in these mice. Although, both CD4 and CD8 T-cells are known to play a role in inflammation in *mdx* mice, biopsies from DMD patients showed a predominance of CD4-positive T-cells as compared to CD8-positive T-cells [147, 154]. Also, CD4-positive cells were found to be localized around macrophages and individual muscle fibers, whereas, CD8-positive cells were scattered throughout muscle tissue [154]. Hence, others speculated that CD4-positive cells, and not CD8-positive cells, played a major role in causing muscle damage via cytotoxicity [154, 155]. A better understanding of the specific role of A20 in the immune response is needed to further understand this observation. A recent study showed that AAV vectors alone were capable of activating the alternate pathway in HeLa cells [156]. This was a very interesting observation from a therapeutic point of view, since AAV-mediated transfer would be able to not only inhibit the classical pathway, reducing inflammation, but also promote activation of the alternate pathway, promoting muscle regeneration. However, control experiments using the introduction of the AAV vector alone in mice would shed light on its function in skeletal muscle in mice.

In conclusion, I have shown that A20 is a potent negative regulator of the classical NF-κB pathway and plays a role in muscle regeneration by inhibition of the pathway in *mdx* mice.

A20 mediated inhibition of the NF-κB pathway led to decreased dystrophic pathology and improved muscle health. Thus, AAV-mediated delivery of A20 has potential to be explored further as a promising therapeutic target for DMD and future studies need to be carried out to elucidate the exact mechanism and function of A20 over-expression in skeletal muscle.

4.0 CHARACTERIZATION OF A20 IN *mdx*;p65$^{+/-}$ MICE

4.1 RATIONALE

Mdx mice with a heterozygous deficiency of the p65 subunit also show improved muscle health and increased levels of muscle fiber regeneration [20]. Since A20 plays a role in muscle regeneration by reducing NF-κB pathway activation [142], I wanted to characterize the expression and localization of A20 in the absence of one copy of the p65 subunit. I obtained p65 heterozygous mice, and generated *mdx*;p65$^{+/-}$ mice to assess the protein levels of A20 in these mice. The aim was to study A20 expression in skeletal muscle of mdx mice that also have a heterozygous p65 subunit deletion and is compared to *mdx* mice with normal p65 expression, over a range of ages. Since A20 was shown to inhibit the classical, but not the alternate pathway, characterization of A20 in the *mdx* mice lacking one copy of p65 would help shed light on the molecular function of A20 in *mdx* mice and help dissect the role of A20 in the dystrophic phenotype.

4.2 INTRODUCTION

The five members of the NF-κB family are capable of forming homodimers and heterodimers, and each type of dimerization has a specific function in different cell types. The p65 subunit forms a heterodimer with the p50 subunit, and this p50-p65 heterodimer is the most commonly occurring and well-studied heterodimer. Upon phosphorylation and subsequent ubiquitination of the cytoplasmic inhibitor, IκB, the p65 subunit is phosphorylated leading to activation and translocation into the nucleus.

A20 has been shown to play a role in regulating NF-κB activation in skeletal muscle [142]. In Chapter 2, I noted that A20 inhibited only the classical, but not the alternate pathway of NF-κB activation. The classical pathway consists of the heterodimer comprising NF-κB subunits p50 and p65 translocating into the nucleus initiating the activation of downstream NF-κB targets [23, 157, 158]. Chronic activation of the pathway in muscle in DMD has been shown to increase activity of downstream targets such as the ubiquitin-proteasome pathway [54] and increase cytokine expression that ultimately causes protein degradation and muscle atrophy. Negative regulators of the NF-κB pathway have been shown to reduce activation of the pathway and improve muscle stability and health [127, 144-146, 159]. Genetic perturbations such as homozygous deletion of the p65 subunit in mice caused embryonic lethality and liver degeneration [160]. Knockout of p50 in mice, the other subunit of the heterodimer and member of the NF-κB family, led to defects in the immune response, but displayed normal development [161]. Thus, it was speculated that p65 might play a unique role in early development and survival [160]. These mice could be rescued by a double knockout of TNF-α, due to the absence of TNF-α induced cytotoxicity [162]. These TNF-$\alpha^{-/-}$;$p65^{-/-}$ double knockout mice showed a significant increase in myogenesis, and decrease in muscle inflammation and thus displayed an

improved muscle phenotype [127, 131]. *Mdx* mice that had a heterozygous deficiency of p65 also showed an improved dystrophic phenotype by displaying an increase in regeneration and decrease in necrosis and inflammation [20].

I sought to characterize the protein expression profile of A20 in *mdx* mice with a heterozygous deletion of the p65 subunit at different ages. I also characterized the number of fibers with centrally placed nuclei and levels of regeneration and necrosis in these mice as a function of age.

4.3 MATERIALS AND METHODS

Animals and reagents: C57BL/10/J (C57) and C57BL/10ScSn-*Dmd*^{mdx}/J (*mdx*) mice were purchased from The Jackson Laboratory (Bar Harbor, ME) and were housed at the University of Pittsburgh Animal Housing Facility and used under approval by the University of Pittsburgh Institutional Animal Care and Use Committee (IACUC). In order to generate the *mdx*;p65+/- mice, I crossed *mdx* mice with the p65+/- mice twice to get the mutation completely onto the *mdx* background. The mice were ear-tagged and genotyped and the heterozygous mice were chosen for the study.

Antibodies used for western blotting and immunohistochemical analyses were A20 (sc-22834), GAPDH (sc-25778), secondary antibody for Western blotting goat anti-rabbit HRP (sc-2030) (Santa Cruz Biotechnology, Inc, Santa Cruz, CA). Monoclonal antibodies to embryonic MHC (eMyHC) (F1.652), used to detect regenerating fibers, obtained from the Developmental Studies Hybridoma Bank, developed by Helen Blau (University of Iowa, Department of Biological Sciences, Iowa City, IA).

Genotyping of mice: *mdx* mice were crossed with $p65^{+/-}$ mice in order to obtain *mdx*;$p65^{+/-}$ mice. Mice were ear-tagged for identification and their tails were clipped for genotyping. DNA from the tail clippings was isolated using the DNeasy Blood and Tissue kit (Qiagen Sciences, Maryland, USA). Briefly, clipped tails from mice were incubated in proteinase K overnight at 56°C. DNA was eluted using a spin-column and stored at -20°C for further use.

I used PCR technique to genotype the mice. Primers used for the PCR were as follows: p65 5' WT: cctatagaggagcagcgcggg, p65 3' REC: aaatgtgtcagtttcatagcctgaagaacg, p65 3' WT: aatcggatgtgagaggacagg. Amplification was carried out by preheating at 95°C for 10mins, followed by 30 cycles of 95°C for 15s, 60°C for 60s followed by final extension at 72°C for 7mins. The PCR products were run in a 1% agarose gel for 1hr at 100V and the bands were visualized.

Western blot analysis: Total lysates from muscle tissues were obtained using T-PER Tissue Extraction Reagent (ThermoFisher Scientific, Rockford, IL). Nuclear and cytoplasmic extracts were obtained using NE-PER nuclear and cytoplasmic extraction reagent (ThermoFisher Scientific, Rockford, IL). Lysates were run on 10% SDS-PAGE gel for 1 hr and transferred onto a Hybond nitrocellulose membrane at 100V for 90 min. Membranes were blocked using blocking buffer (1X PBS with 10% goat serum) for 1 hr, followed by incubation with specific primary antibodies and HRP-conjugated secondary antibodies. The blot was then incubated with electrochemiluminescence reagents (GE Healthcare, Piscataway, NJ) and autoradiographed to visualize protein bands. Standard protein markers were run with proteins to determine protein size. All quantifications were performed using MCID software (InterFocus Imaging Ltd, Cambridge, England).

Muscle tissue processing: Hind limb muscles and diaphragms obtained from *mdx* mice were snap-frozen using 2-methylbutane pre-cooled on dry ice and stored at -80°C. For immunohistochemical analysis, tissue samples were sectioned at a thickness of 10μm and transferred onto slides. For biochemical and genetic analysis, tissues samples were extracted as described in each relevant section.

Immunohistochemical analysis: Muscle sections were thawed at room temperature for 5 min and hydrated using 1X PBS. The sections were then blocked using blocking buffer (10% goat serum in 1X PBS) for 1 hr and probed with specific primary and secondary antibodies diluted in DAKO antibody diluent (Invitrogen, Carlsbad, CA). Sections were then washed and mounted using Dapi FluoromountG mounting medium in the dark. Sections that were incubated with anti-mouse antibodies were treated with an additional blocking step using MOM Mouse IgG blocking reagent (Vector Laboratories, Burlingame, CA) in 1X PBS for 1 hr.

Statistical Analysis: All values are presented as mean ± standard error of mean (SEM) from independent animals. Significance was determined using the 2-tailed and unpaired Student's t test. p-values < 0.05 were considered significant.

4.4 RESULTS

4.4.1 A20 expression levels in different ages of the *mdx*;p65$^{+/-}$ mice

A time profile of the expression pattern of A20 in the quadriceps of *mdx* mice showed an increase in A20 expression around 10wks of age and gradually decreased around 14wks and 20 wks coming back to lower levels when compared to normal C57 mice. I analyzed whether

decreased expression of p65 affected expression levels of A20 in *mdx* mice at different ages. In contrast to *mdx*;p65$^{+/+}$, heterozygous deletion of p65 in *mdx* mice showed a decrease in A20 expression at 7wks of age; however I observed an increase in A20 protein expression in the p65 deficient mice at 14wk and 20 wk of age (Figure 24). This pattern of A20 expression in p65-deleted *mdx* mice was similar to patterns of A20 expression at different ages in C57 mice (Figure 24).

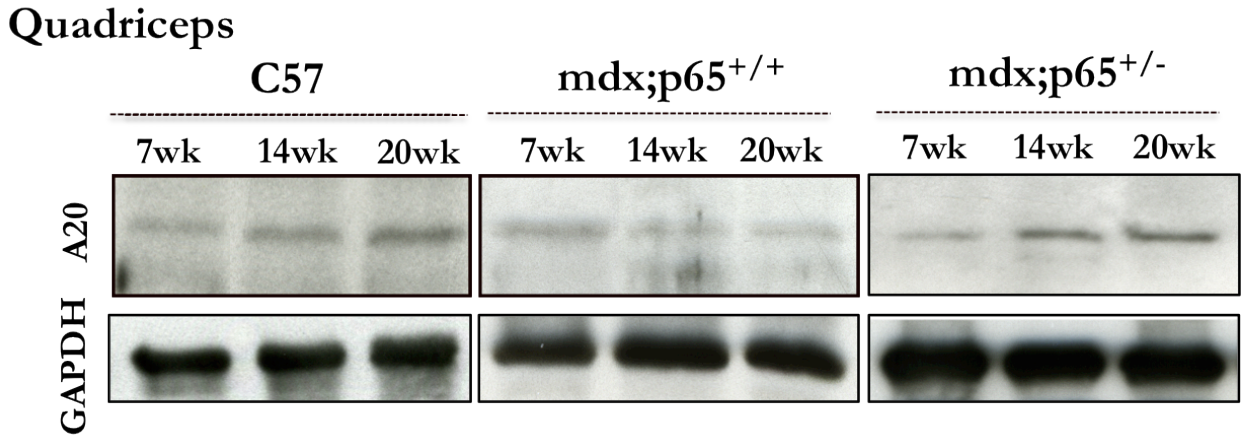

Figure 25: A20 protein levels as a function of p65 dosage in *mdx* mice.

Total lysates from quadriceps of C57, *mdx*;p65$^{+/+}$ and *mdx*;p65$^{+/-}$ mice, aged 7, 14 and 20wks were analyzed for A20 protein levels using Western blotting. GAPDH was used as a loading control. Representative results are shown.

4.4.2 NF-κB activation in p65 deficient mice

The NF-κB pathway is chronically activated in *mdx* mice. To assess the affect of heterozygous deletion of p65 on the activation of the NF-κB pathway, I performed an EMSA on nuclear extracts obtained from quadriceps and diaphragm of *mdx*;p65$^{+/-}$ mice. I analyzed NF-κB activation at different ages of these mice. As expected, I observed a decrease in NF-κB activation

in both the quadriceps and diaphragm of *mdx* mice with a heterozygous deletion of p65 (Figure 25). This reduction of NF-κB pathway activation persisted through 20wks of age (Figure 25).

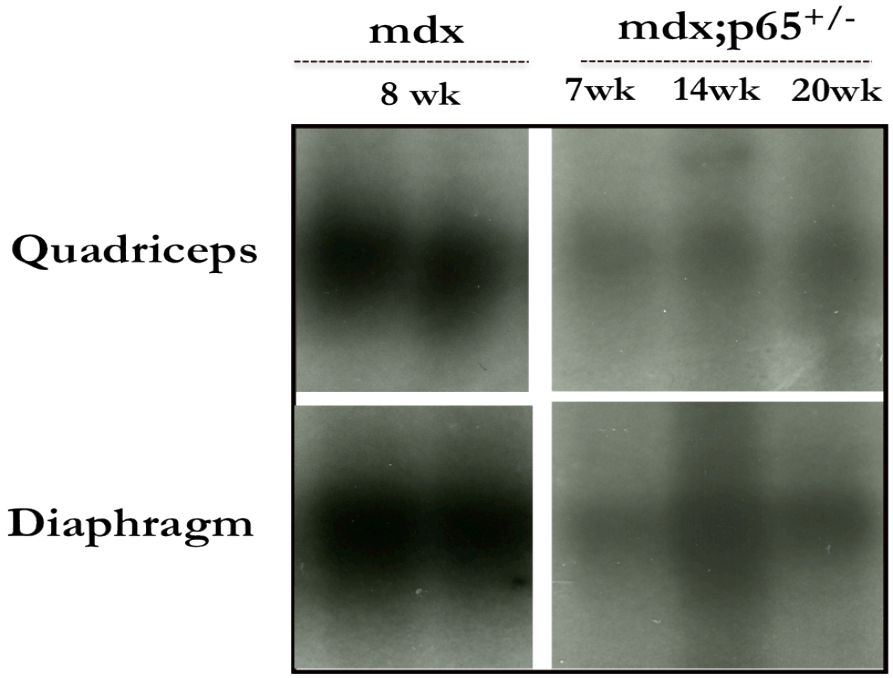

Figure 26: EMSA to analyze activation of the NF-κB pathway in *mdx*;p65$^{+/-}$ mice at different ages. Nuclear extracts obtained from quadriceps and diaphragm of 8 wk old *mdx*;p65$^{+/+}$ mice and 7, 14 and 20wk old *mdx*;p65$^{+/-}$ mice were analyzed for NF-κB pathway activation using the EMSA.

4.4.3 Histological analysis of p65 deficient mice

In past studies, heterozygous deletion of p65 in *mdx* mice demonstrated increases in regeneration and decreases in necrosis and inflammation in skeletal muscle [20]. Acharyya and colleagues analyzed the gastrocnemius muscle of 7wk old *mdx*;p65$^{+/-}$ mice and observed a decrease in the proportion of fibers with centrally placed nuclei, an increase in the number of regenerating fibers

and fiber size, and a decrease in the amount of infiltrating inflammatory cells and necrosis [20]. I decided to analyze the effect of heterozygous deletion of p65 in *mdx* mice in a time-profile manner to assess the long-term effects of the deficiency of p65 in skeletal muscle of *mdx* mice. I analyzed the percentage of fibers with centrally placed nuclei in the quadriceps muscles of *mdx*;p65$^{+/-}$ mice compared to *mdx*;p65$^{+/+}$ mice at ages 7, 10, 14 and 20wks (Figure 26A). I observed no difference in the percentage of fibers with centrally placed nuclei in *mdx*;p65$^{+/-}$ mice at 7 wks of age (Figure 26B). However, I observe an increase in the number of fibers at around 10wks of age followed by a decrease in the percentage of fibers with centrally placed nuclei at 14wk and 20wks of age (Figure 26B).

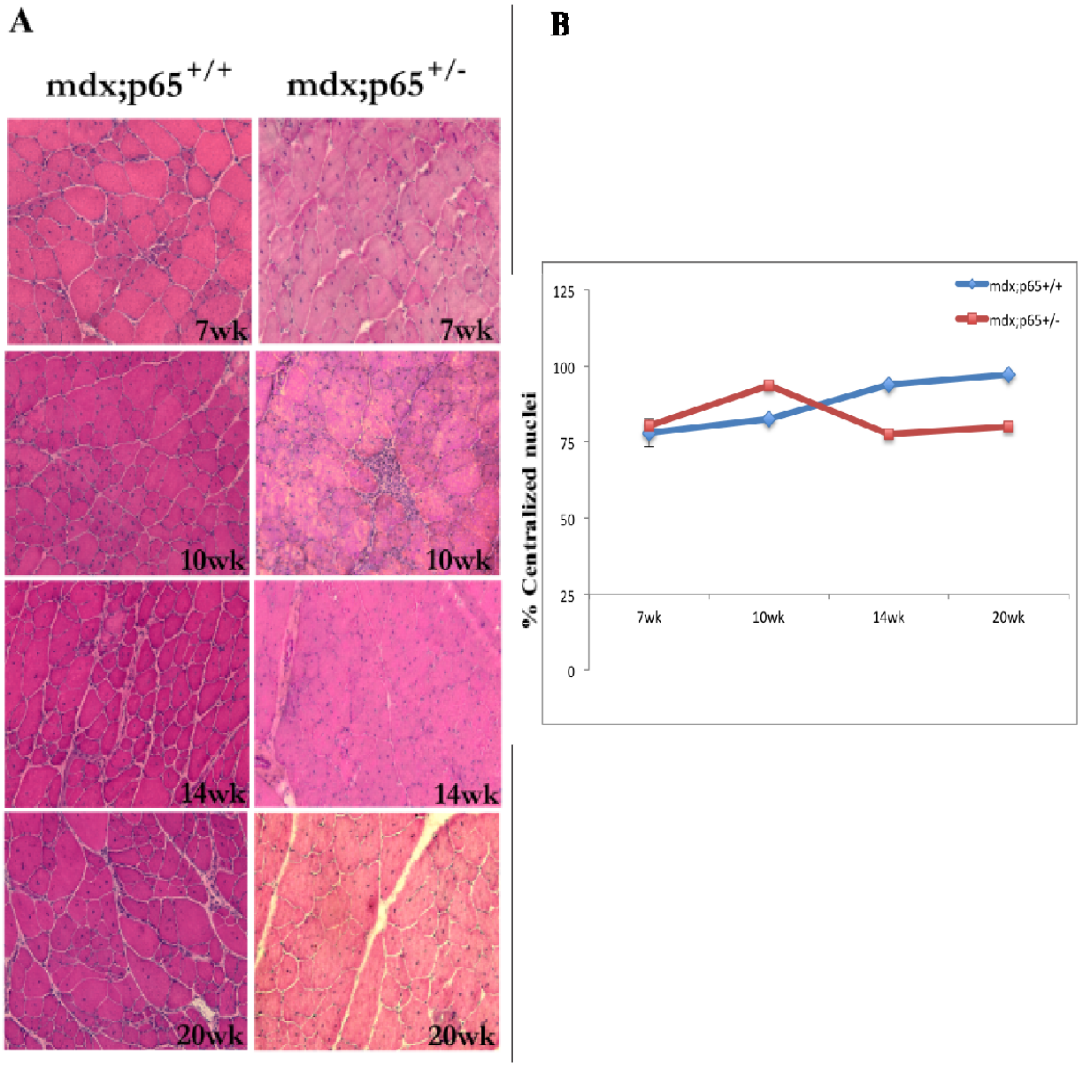

Figure 27: Analysis of number of fibers with centrally placed nuclei in *mdx*;p65$^{+/-}$ mice.

A) Sections of quadriceps from *mdx*;p65$^{+/+}$ and *mdx*;p65$^{+/-}$ mice, aged 7, 10, 14 and 20 wks were stained with H&E for histological analysis. B) Quantification of the percentage of fibers with centrally placed nuclei in the muscle. Number of regenerating fibers were counted and plotted as a percentage of the total number of all fibers counted. Two sections per mouse was counted and averaged for each group. n=2-3 per age group.

4.4.4 Number of regenerating fibers in *mdx*;p65$^{+/-}$ mice.

Since the percentage of fibers with centrally placed nuclei differed with age in *mdx*;p65$^{+/-}$ mice, I assessed the amount of regenerating fibers in these mice at different ages. Cycles of degeneration and regeneration in *mdx* mice are observed around the 7wks of age, peak at around 10 wks of age and gradually decline around 14wks of age. I observed a decrease in the number of regenerating fibers at 10wks of age in *mdx*;p65$^{+/-}$ mice as compared to *mdx*;p65$^{+/+}$ mice (Figure 27A, B). I did not observe any change in the percentage of regenerating fibers at 7, 14 or 20wks of age in these mice (Figure 27B).

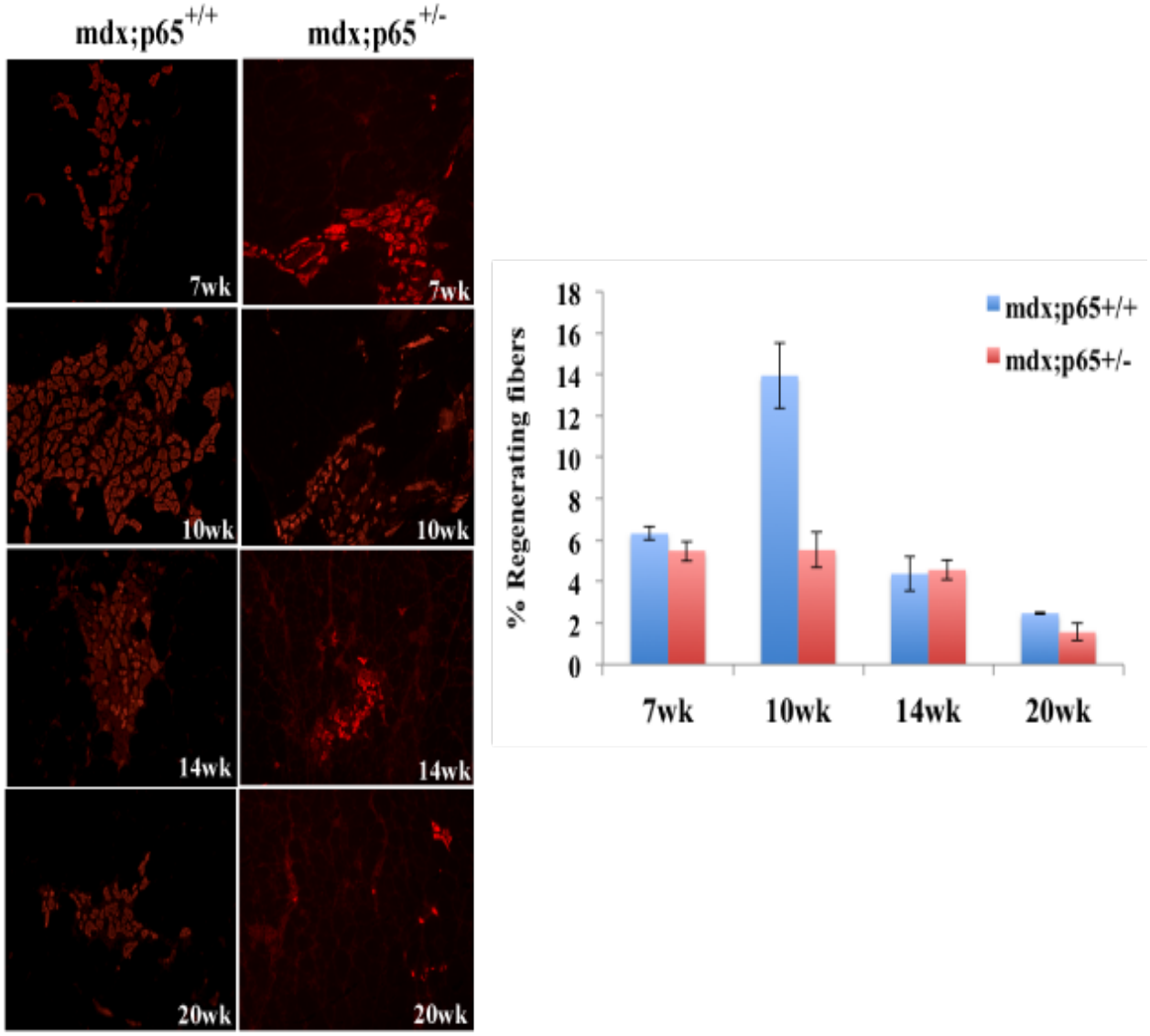

Figure 28: Analysis of amount of regeneration at different ages in *mdx*;p65$^{+/-}$ mice.

A) Sections of quadriceps from *mdx*;p65$^{+/+}$ and *mdx*;p65$^{+/-}$ mice, aged 7, 10, 14, 20 wks were immunostained with embryonic myosin heavy chain (eMyHC), a marker for regenerating fibers. B) Quantification of the percentage of regenerating fibers in the muscle. Number of regenerating fibers were counted and plotted as a percentage of the total number of all fibers counted. Two sections per mouse were counted and averaged for each group. n=2-3 per age group.

4.4.5 Analysis of necrosis in 10wk old p65 deficient mice

Since I observed a sharp decrease in the percentage of regenerating fibers at 10wks of age in *mdx*;p65$^{+/-}$ mice, I speculated that this decrease could either be due to improved muscle health, or due to increased necrosis. To confirm this, I analyzed the number of necrotic fibers at this time-point in these p65 deficient *mdx* mice. I observed a decrease in the number of necrotic fibers in *mdx*;p65$^{+/-}$ mice as compared to *mdx*;p65$^{+/+}$ mice (Figure 28).

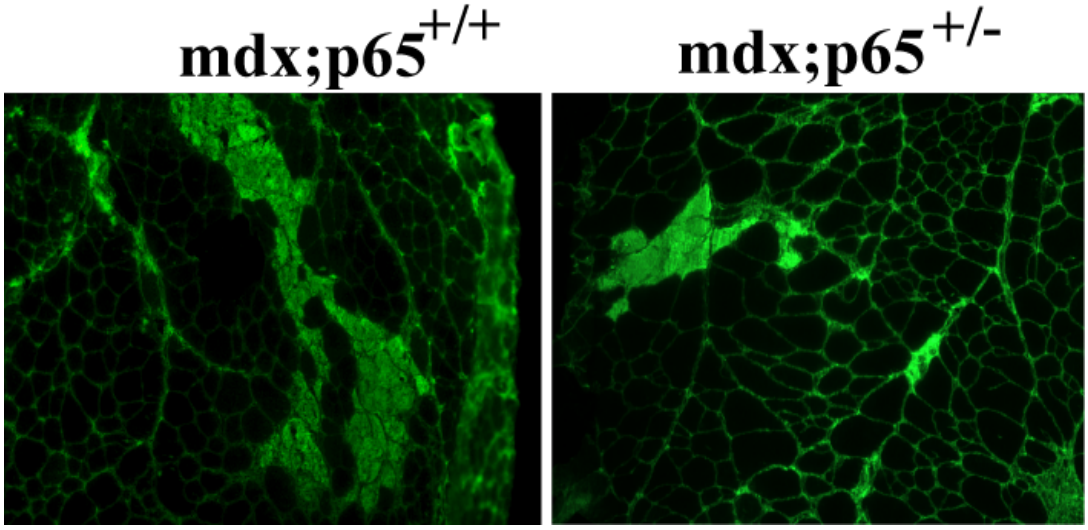

Figure 29: Analysis of necrosis in 10wk old *mdx*;p65$^{+/-}$ mice.

Sections of quadriceps from *mdx*;p65$^{+/+}$ and *mdx*;p65$^{+/-}$ mice, aged 10 wks were immunostained with mouse IgG for detection of necrotic fibers (green).

4.5 DISCUSSION

This is the first observation of the effect of heterozygous deleted p65 subunit in relation to age in *mdx* mice. I assessed the degree of dystrophic phenotype in relation to age in these mice and observed that *mdx* mice with a heterozygous p65 deletion displayed distinct histopathological changes in skeletal muscle depending on the age of the mice. I observed a decrease in the number of fibers with centrally placed nuclei in *mdx*;p65$^{+/-}$ mice later in age at 14 and 20wks, but not earlier, at the peak of cycles of degeneration and regeneration, at 7 and 10wks. Interestingly, I observed a sharp decrease in the number of regenerating fibers during this peak at 10wks of age of *mdx*;p65$^{+/-}$ mice, but the percentage was unaffected before or after this peak of damage and repair. Analysis of the amount of necrotic fibers in 10wk old *mdx*;p65$^{+/-}$ mice revealed a reduction in necrosis as compared to *mdx*;p65$^{+/+}$ mice. These data suggest that heterozygous deletion of p65 in *mdx* mice leads to amelioration of the dystrophic phenotype specific to the age of the mice.

Heterozygous deletion of the p65 subunit was shown to improve the dystrophic phenotype in *mdx* mice and enhance myogenesis in C2C12 myoblasts and muscle stem cells [20, 127, 134]. Heterozygous deletion of the p50 subunit in *mdx* mice, however, failed to rescue dystrophic pathology [20]. The authors studied the effect of heterozygous deletion of p65 in *mdx* mice at a specific time-point at 7wks and observed an increase in the number of fibers with centrally placed nuclei and regenerating fibers. I decided to do a time-profile analysis of the change in dystrophic phenotype in the heterozygous p65-deleted *mdx* mice. I had observed earlier that A20 protein levels were increased at 10wks of age in *mdx* mice, the age when there are cycles of degeneration and regeneration taking place in skeletal muscle. These levels gradually decrease at 14 wks and 20 wks of age. I also observed a peak in p65 expression at

10wks of age in *mdx* mice. Thus, a time profile analysis of A20 protein expression and the pathology of the *mdx*;p65$^{+/-}$ mice would give a better understanding of the effect of p65 deficiency in *mdx* mice.

I observed a reduction in NF-κB activation with heterozygous deletion of the p65 subunit in *mdx* mice. This reduction of activation was observed at all ages analyzed: from 7wk to 20 wks of age. Thus inhibition of the NF-κB pathway in *mdx* mice would be able to improve the regeneration capacity of skeletal muscle and reduce necrosis and muscle atrophy. Analysis of fibers with centrally placed nuclei in the *mdx*;p65$^{+/-}$ mice revealed a distinct pattern of the number of fibers with centrally placed nuclei in relation to the age of the mice. In *mdx* mice with normal p65 expression, the number of fibers with centralized nuclei gradually increases with age, and at 20 wks, about 90% of the total fibers have centrally placed nuclei. In *mdx*;p65$^{+/-}$ mice, at 7wks, I observed no change in the percentage of fibers with centralized nuclei as compared to *mdx* mice. However, at 10wks, there is an increase in the centrally nucleated fibers, which then gradually decreases at 14wk and 20wks of age. A pattern emerges when we correlate this data with the A20 expression profile at these ages. Analysis of A20 expression in a time-profile manner in *mdx*;p65$^{+/-}$ mice revealed a decrease in protein levels at 7wks of age, which then increases at 14wk and 20wks of age. This expression profile observed was in contrast to the *mdx*;p65$^{+/+}$ mice, which showed an increase in A20 protein expression at 7wks, which gradually decreases by 14wk and 20wks. This is an interesting observation since it suggests that there is a burst of regeneration taking place at 10wks in *mdx*;p65$^{+/-}$ mice, however, instead of undergoing degeneration and subsequent regeneration as observed in *mdx* mice, these regenerating fibers undergo maturation and become mature myofibers by 14wks of age. This is also corroborated by the decrease in necrosis observed in the skeletal muscle of *mdx*;p65$^{+/-}$ mice. Increased expression

of A20 at 14wk and 20wks indicates that A20 is also playing a role in promoting muscle regeneration at these ages. Thus, one can speculate that heterozygous deletion of the p65 subunit in *mdx* mice promotes myogenesis via the inhibition of the NF-κB pathway activation and increased expression of A20.

In conclusion, I have shown a correlation between the p65 subunit of the NF-κB pathway, expression of A20 and myogenesis in the skeletal muscle of *mdx* mice. Deletion of the p65 subunit in *mdx* mice causes upregulation of A20 expression at later stages in life of the *mdx* mice, and helps promote and maintain myogenesis improving dystrophic pathology.

5.0 CONCLUSIONS AND DISCUSSION

Despite the clinical description of DMD over a century ago, no cure for the disorder is yet in sight. Patients suffering from DMD lose ambulation by their teens, and succumb to respiratory and cardiac failure by their late twenties. Although the lack of a functional dystrophin causes DMD, a milieu of other secondary factors, including increased oxidative and mechanical stress, increased contraction-induced muscle damage leading to muscle atrophy and chronic inflammation in muscles, all contributes to dystrophic pathology. Several studies have evaluated each aspect of these secondary factors, and have elucidated various therapeutic approaches that could be beneficial from a clinical point of view, but few have proven successful or shown to have long-term benefits.

NF-κB was discovered by Sen and Baltimore, about 25 years ago as a transcription factor that could be activated by several external stimuli [163, 164]. In 25 years, discoveries about the cellular mechanisms, molecular function and role of the NF-κB pathway have grown exponentially. The NF-κB pathway was shown to play a role in many physiological processes, and activation of the pathway has been implicated in several disorders, such as cancers, arthritis and muscular dystrophy. In DMD, chronic activation of the NF-κB pathway contributes to several pathological symptoms including chronic inflammation in muscle, up-regulation of the ubiquitin-proteosome pathway causing protein degradation and subsequent muscle atrophy. Understanding the molecular properties of the pathway would help develop therapeutic

approaches to inhibit the activation of the NF-κB pathway. Over the years, there have been many molecules of interest that showed promise as NF-κB inhibitors. One review has estimated that almost 800 inhibitors of the NF-κB pathway have been studied so far [48]. Each of the inhibitors targets a particular stage of activation of the NF-κB pathway, including upstream molecules of the pathway and downstream effector targets. However, a lot remains to be understood about the pathway and its mechanism of action, and more discoveries would lead to more efficient inhibitors of the pathway.

In this thesis, I characterized the role of A20, a naturally occurring critical regulator of the NF-κB pathway, in skeletal muscle of dystrophic mice. The role of A20 in skeletal muscle was previously unknown and my findings showed that A20 played a role in the inhibition of the NF-κB pathway in muscle and also played a role in muscle regeneration. This was a novel observation and associated A20 function with muscle regeneration in dystrophic mice. Since A20 was shown to play a role in muscle regeneration by inhibition of the NF-κB pathway, I studied the potential of A20 as a therapeutic target for amelioration of dystrophic symptoms. Over-expression of A20 caused reduction of chronic NF-κB activation, and also by reduction of number of fibers with centrally placed nuclei and regeneration, indicating improved muscle health. These results confirmed the role of A20 as a negative regulator of the NF-κB pathway, and established its role as a novel therapeutic for treatment of DMD.

My studies demonstrating the role of A20 in dystrophic pathology have shown a clear link between A20 and muscle regeneration. However, to establish the therapeutic ability of A20, future studies further characterizing the properties of A20 as a NF-κB pathway inhibitor would help the effort to take A20 ‘from bench to bedside’. Future studies would include assessing the long-term effects of A20 over-expression in *mdx* mice. This would help establish the long-term

therapeutic benefits of A20 in the muscle and confirm its ability to improve muscle health throughout the life of the *mdx* mice. This would also rule out any detrimental effects to the muscle due to A20 or vector related toxicity or non-specific effects on other pathways in the muscle. Analyzing the effect of A20 treatment on properties of muscle behavior, such as membrane stability, muscle force and fatigue would help quantify the improvement in muscle health. Studying the efficacy of A20 treatment on larger animal models such as the dog model for DMD would help identify the problems associated with gene therapy, such as activation of the immune response and bio-distribution.

A20 is known to be a negative regulator of inflammation, and this negative regulation is mainly through the inhibition of the NF-κB pathway. However, studies indicate that A20 might play a role in other pathways such as skin differentiation [97], anti-apoptosis [165], angiogenesis [122] and the negative regulation of the JNK pathway [97]. However, it is unclear if A20 plays a functional role in these pathways via the regulation of the NF-κB pathway or independent of it. Thus, understanding the function of A20 in the immune response, other than regulating the NF-κB pathway would provide more insight to the therapeutic role of A20 in muscle. Although A20 was shown not to be required for embryonic survival, mice deficient in A20 were reported to die within a short period after birth, due to severe inflammation and tissue damage in multiple organs [97]. However, in these studies, the effect of A20 deficiency was not analyzed in skeletal muscle. A detailed study of the pathways perturbed in the muscles of A20 deficient mice would help provide insight to the molecular mechanisms of action of A20 in skeletal muscle. For instance, analyzing the effect of lack of A20 genetically introduced in *mdx* mice would confirm the role of A20 on muscle development, regeneration and health.

In conclusion, the findings presented in this thesis provide a novel insight to the mechanism of the NF-κB pathway in muscular dystrophy, and the effects of inhibition of the pathway by A20 on the pathology in skeletal muscle. I have also shown the role of A20 as a potential therapeutic target in the muscles of dystrophic mice. Since A20 is a critical negative regulator of the NF-κB pathway, I would expect these findings would also initiate the study of A20 as a therapeutic target in other disease models, such as in lymphomas and glioblastomas, and in autoimmune disorders such as lupus and arthritis.

APPENDIX A

CONTROL EXPERIMENTS PERFORMED

A.1 SPECIFICITY OF PROBE BINDING IN EMSA ASSAY

One of the mechanisms to analyze specificity of the NF-κB probe binding in the Electrophoretic mobility shift assay (EMSA) is to introduce competitive non-radioactive (cold) specific probe and cold mutated probe. The consensus cold probe would bind to the NF-κB protein competing with the radioactive probe and displacing it. As an additional control, a mutated probe would be unable to bind to the protein, thus unable to displace the radioactive probe. As a control, samples were co-incubated with either cold consensus (wild-type) probe or cold mutated probe. The NF-κB consensus oligonucleotide (sc-2505) and NF-κB mutated oligonucleotide (sc-2511) were purchased from SantaCruz Biotechnologies.

The cold wild-type probe, but not the mutated probe was able to compete out the radioactive probe, indicating the NF- κB probe used was specific (Figure 29).

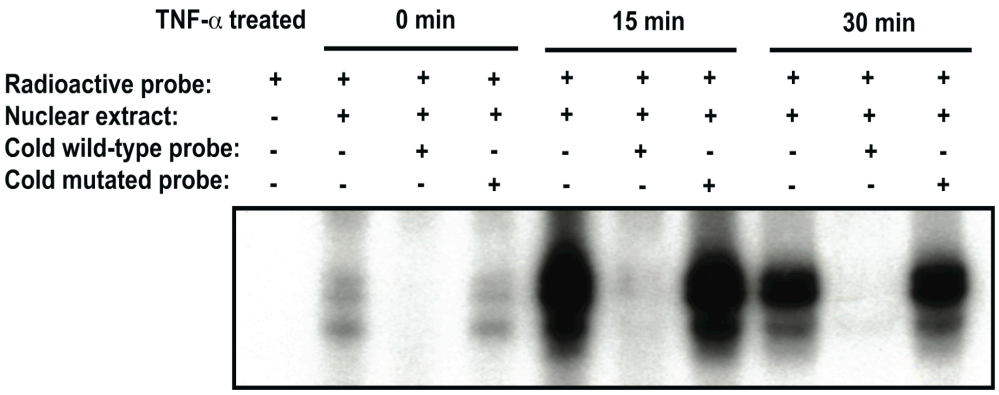

Figure 30: Binding of NF-κB probe in nuclear extracts is specific.

Specificity of NF-κB activation was confirmed using electrophoretic mobility shift assay. C2C12 cells were treated with TNF-α (10ng/ml) for 15 and 30 mins and nuclear extracts were obtained. Extracts were incubated with wild-type probe or mutated probe to assess specificity of radioactive probe binding.

A.2 COMPARISON OF IN VITRO EXPRESSION OF AAV2-GFP AND AAV8-GFP

AAV serotypes have differential transduction efficiencies and expression levels in different tissue types. The transduction also varies whether the introduction of the transgene was in vivo or in vitro. I assessed in vitro GFP expression in C2C12 cells using AAV serotype 2 and 8, driven by a cytomegalovirus (CMV) promoter. I assessed expression at different multiplicity of infections (MOI) of 1, 10 and 100. At MOI of 10, AAV2 displayed better transduction efficiency as compared to AAV8 (Figure 30). This observation corroborates with the earlier published data that showed ability of AAV2 to transduce efficiently in vitro compared to weak AAV8 transduction efficiency [166].

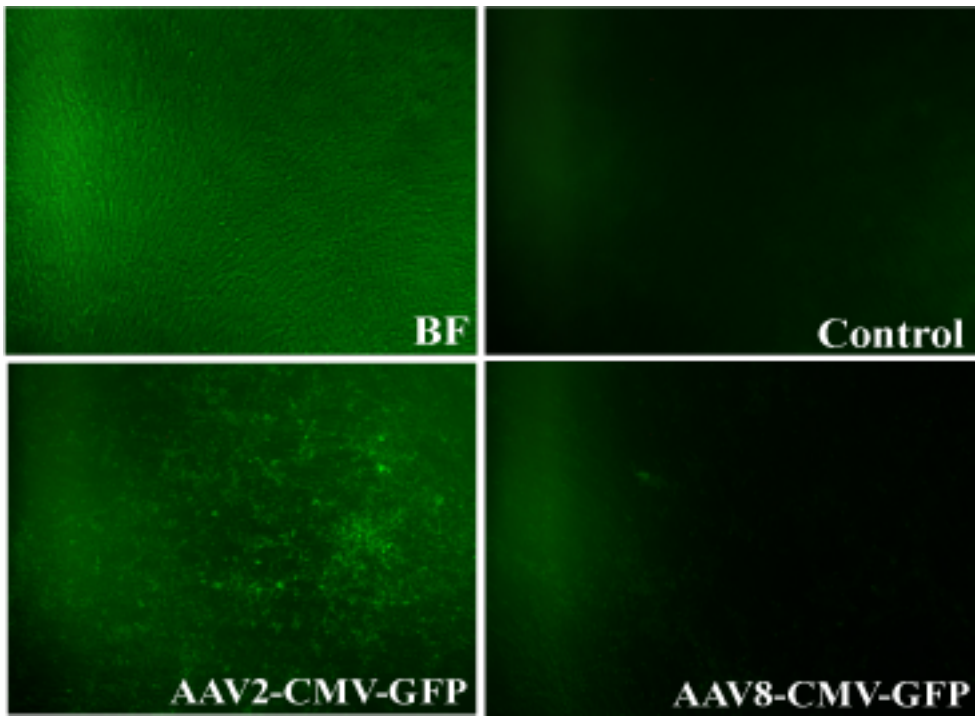

Figure 31: GFP expression in C2C12 myotubes.

C2C12 myoblasts were transduced with either AAV2-CMV-GFP or AAV8-CMV-GFP virus at a MOI of 10 and induced to differentiate to form myotubes. BF- Brightfield image.

A.3 A20 PLASMID EXPRESSION IN C2C12 CELLS

Upon generation of the AAV-tMCK-A20 plasmid, I looked for in vitro expression of the plasmid in C2C12 cells to confirm the expression of A20 protein. C2C12 myoblasts were transfected with saline or AAV-tMCK-A20 plasmid and induced to undergo differentiation by serum starvation. I observed an increase in the expression levels of A20 protein in the AAV-tMCK-A20 plasmid transfected cells as compared to mock-transfected cells (Figure 31A, B). This confirmed the accuracy of the cloning and efficacy of the plasmid for over-expression of A20 in muscle cells.

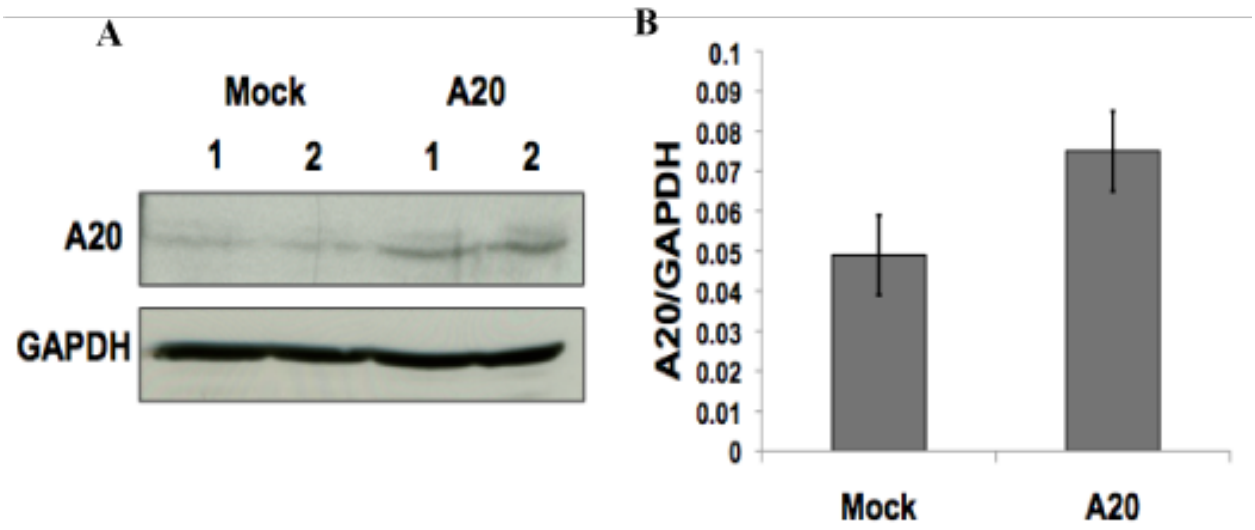

Figure 32: Analysis of A20 plasmid expression in vitro in C2C12 cells.

C2C12 myoblasts were transfected with AAV-tMCK-A20 plasmid and induced to differentiate to myotubes. A) Analysis of A20 protein levels in mock or A20 plasmid transfected cells using Western Blotting. B) Quantification of A20 protein levels normalized to GAPDH. Experiments were performed in duplicates.

BIBLIOGRAPHY

1. Harrison, V. F., *A review of skeletal muscle.* Phys Ther Rev, 1961. **41**: p. 17-24.

2. *Myology, 3rd edition*, ed. Franzini-Armstrong, Andrew G Engel and Clara2004: McGraw-Hill.

3. *Structure of skeletal muscle*. [cited 2011 Nov. 1]; Available from: http://training.seer.cancer.gov/module_anatomy/unit4_2_muscle_structure.html.

4. Grounds, M. D., *Towards understanding skeletal muscle regeneration.* Pathol Res Pract, 1991. **187**(1): p. 1-22.

5. *Muscle Regeneration*, ed. A, Mauro1979, New York: Raven Press.

6. *DeLee: DeLee and Drez's Orthopaedic Sports Medicine, 3rd ed.* , ed. Jesse C. Delee, David Drez, Jr and Mark Miller2009: Saunders, An imprint of Elsevier.

7. ValéRia Augusto, Carlos Roberto Padovani and Gerson Eduardo Rocha Campos, *Skeletal muscle fiber types in C57BL6J mice.* Braz. J. morphol. Sci., 2004. **21**(2): p. 89-94.

8. Emery, A E, *Population frequencies of inherited neuromuscular diseases--a world survey.* Neuromuscul Disord, 1991. **1**(1): p. 19-29.

9. Chargé, Sophie B P and Rudnicki, Michael A, *Cellular and molecular regulation of muscle regeneration.* Physiol Rev, 2004. **84**(1): p. 209-38.

10. Hoffman, E, Brown, R, and Kunkel…, L, *Dystrophin: the protein product of the Duchenne muscular dystrophy locus.* Cell, 1987.

11. Zubrzycka-Gaarn, E E, Hutter, O F, Karpati, G, Klamut, H J, Bulman, D E, Hodges, R S, Worton, R G, and Ray, P N, *Dystrophin is tightly associated with the sarcolemma of mammalian skeletal muscle fibers.* Exp Cell Res, 1991. **192**(1): p. 278-88.

12. Matsumura, K, Ervasti, J M, Ohlendieck, K, Kahl, S D, and Campbell, K P, *Association of dystrophin-related protein with dystrophin-associated proteins in mdx mouse muscle.* Nature, 1992. **360**(6404): p. 588-91.

13. Batchelor, Clare L and Winder, Steve J, *Sparks, signals and shock absorbers: how dystrophin loss causes muscular dystrophy.* Trends in Cell Biology, 2006. **16**(4): p. 198-205.

14. Shaikhly, K. I., Hamdan, F. B., and Al-Ani, F. S., *Power spectrum analysis and conventional electromyogram in Duchenne muscular dystrophy.* Saudi Med J, 2000. **21**(11): p. 1038-42.

15. Webster, C, Silberstein, L, Hays, A P, and Blau, H M, *Fast muscle fibers are preferentially affected in Duchenne muscular dystrophy.* Cell, 1988. **52**(4): p. 503-13.

16. Fenichel, G M, Florence, J M, Pestronk, A, Mendell, J R, Moxley, R T, Griggs, R C, Brooke, M H, Miller, J P, Robison, J, and King, W, *Long-term benefit from prednisone therapy in Duchenne muscular dystrophy.* Neurology, 1991. **41**(12): p. 1874-7.

17. Manzur, A Y, Kuntzer, T, Pike, M, and Swan, A, *Glucocorticoid corticosteroids for Duchenne muscular dystrophy.* Cochrane database of systematic reviews (Online), 2004(2): p. CD003725.

18. Bulfield, G., Siller, W. G., Wight, P. A., and Moore, K. J., *X chromosome-linked muscular dystrophy (mdx) in the mouse.* Proc Natl Acad Sci U S A, 1984. **81**(4): p. 1189-92.

19. Kumar, Ashok and Boriek, Aladin M, *Mechanical stress activates the nuclear factor-kappaB pathway in skeletal muscle fibers: a possible role in Duchenne muscular dystrophy.* FASEB J, 2003. **17**(3): p. 386-96.

20. Acharyya, Swarnali, Villalta, S Armando, Bakkar, Nadine, Bupha-Intr, Tepmanas, Janssen, Paul M L, Carathers, Micheal, Li, Zhi-Wei, Beg, Amer A, Ghosh, Sankar, Sahenk, Zarife, Weinstein, Michael, Gardner, Katherine L, Rafael-Fortney, Jill A, Karin, Michael, Tidball, James G, Baldwin, Albert S, and Guttridge, Denis C, *Interplay of IKK/NF-kappaB signaling in macrophages and myofibers promotes muscle degeneration in Duchenne muscular dystrophy.* J Clin Invest, 2007. **117**(4): p. 889-901.

21. Sen, R and Baltimore, D, *Multiple nuclear factors interact with the immunoglobulin enhancer sequences.* Cell, 1986. **46**(5): p. 705-16.

22. Ghosh, Sankar and Karin, Michael, *Missing pieces in the NF-kappaB puzzle.* Cell, 2002. **109 Suppl**: p. S81-96.

23. Hayden, M S, West, A P, and Ghosh, S, *NF-kappaB and the immune response.* Oncogene, 2006. **25**(51): p. 6758-80.

24. Baeuerle, P A and Baltimore, D, *A 65-kappaD subunit of active NF-kappaB is required for inhibition of NF-kappaB by I kappaB.* Genes Dev, 1989. **3**(11): p. 1689-98.

25. Bonizzi, Giuseppina and Karin, Michael, *The two NF-kappaB activation pathways and their role in innate and adaptive immunity.* Trends in Immunology, 2004. **25**(6): p. 280-8.

26. Yaron, A, Gonen, H, Alkalay, I, Hatzubai, A, Jung, S, Beyth, S, Mercurio, F, Manning, A M, Ciechanover, A, and Ben-Neriah, Y, *Inhibition of NF-kappa-B cellular function via specific targeting of the I-kappa-B-ubiquitin ligase.* EMBO J, 1997. **16**(21): p. 6486-94.

27. Huxford, Tom, Huang, De-Bin, Malek, Shiva, and Ghosh, Gourisankar, *The Crystal Structure of the IkappaBalpha/NF-kappaB Complex*

Reveals Mechanisms of NF-kappaB Inactivation. Cell, 1998. **95**: p. 759-770.

28. Jacobs, M D and Harrison, S C, *Structure of an IkappaBalpha/NF-kappaB complex.* Cell, 1998. **95**(6): p. 749-58.

29. Alkalay, I, Yaron, A, Hatzubai, A, Orian, A, Ciechanover, A, and Ben-Neriah, Y, *Stimulation-dependent I kappa B alpha phosphorylation marks the NF-kappa B inhibitor for degradation via the ubiquitin-proteasome pathway.* Proc Natl Acad Sci USA, 1995. **92**(23): p. 10599-603.

30. Johnson, C, Van Antwerp, D, and Hope, T J, *An N-terminal nuclear export signal is required for the nucleocytoplasmic shuttling of IkappaBalpha.* EMBO J, 1999. **18**(23): p. 6682-93.

31. Senftleben, U., Cao, Y., Xiao, G., Greten, F. R., Krahn, G., Bonizzi, G., Chen, Y., Hu, Y., Fong, A., Sun, S. C., and Karin, M., *Activation by IKKalpha of a second, evolutionary conserved, NF-kappa B signaling pathway.* Science, 2001. **293**(5534): p. 1495-9.

32. Xiao, G., Fong, A., and Sun, S. C., *Induction of p100 processing by NF-kappaB-inducing kinase involves docking IkappaB kinase alpha (IKKalpha) to p100 and IKKalpha-mediated phosphorylation.* J Biol Chem, 2004. **279**(29): p. 30099-105.

33. Heusch, M., Lin, L., Geleziunas, R., and Greene, W. C., *The generation of nfkb2 p52: mechanism and efficiency.* Oncogene, 1999. **18**(46): p. 6201-8.

34. Ruland, J., *Return to homeostasis: downregulation of NF-kappaB responses.* Nat Immunol, 2011. **12**(8): p. 709-14.

35. Nishikori, Momoko, *Classical and alternative NF-κB activation pathways and their roles in lymphoid malignancies.* Journal of Clinical and Experimental Hematopathology, 2005. **45**(1): p. 15-24.

36. Dejardin, E., *The alternative NF-kappaB pathway from biochemistry to biology: pitfalls and promises for future drug development.* Biochem Pharmacol, 2006. **72**(9): p. 1161-79.

37. Luftig, M., Yasui, T., Soni, V., Kang, M. S., Jacobson, N., Cahir-Mcfarland, E., Seed, B., and Kieff, E., *Epstein-Barr virus latent infection membrane protein 1 TRAF-binding site induces NIK/IKK alpha-dependent noncanonical NF-kappaB activation.* Proc Natl Acad Sci U S A, 2004. **101**(1): p. 141-6.

38. Hayden, Matthew S and Ghosh, Sankar, *Signaling to NF-kappaB.* Genes Dev, 2004. **18**(18): p. 2195-224.

39. Sato, Shintaro, Sanjo, Hideki, Takeda, Kiyoshi, Ninomiya-Tsuji, Jun, Yamamoto, Masahiro, Kawai, Taro, Matsumoto, Kunihiro, Takeuchi, Osamu, and Akira, Shizuo, *Essential function for the kinase TAK1 in innate and adaptive immune responses.* Nat Immunol, 2005. **6**(11): p. 1087-95.

40. Hsu, H, Huang, J, Shu, H B, Baichwal, V, and Goeddel, D V, *TNF-dependent recruitment of the protein kinase RIP to the TNF receptor-1 signaling complex.* Immunity, 1996. **4**(4): p. 387-96.

41. Morlon, A, *TAB2, TRAF6 and TAK1 are involved in NF- B activation induced by the TNF-receptor, Edar and its adaptator Edaradd.* Human Molecular Genetics, 2005. **14**(23): p. 3751-3757.

42. Wertz, Ingrid E, O'rourke, Karen M, Zhou, Honglin, Eby, Michael, Aravind, L, Seshagiri, Somasekar, Wu, Ping, Wiesmann, Christian, Baker, Rohan, Boone, David L, Ma, Averil, Koonin, Eugene V, and Dixit, Vishva M, *De-ubiquitination and ubiquitin ligase domains of A20 downregulate NF-kappaB signalling.* Nature, 2004. **430**(7000): p. 694-9.

43. Abbott, Derek W, Yang, Yibin, Hutti, Jessica E, Madhavarapu, Swetha, Kelliher, Michelle A, and Cantley, Lewis C, *Coordinated regulation of Toll-like receptor and NOD2 signaling by K63-linked polyubiquitin chains.* Molecular and Cellular Biology, 2007. **27**(17): p. 6012-25.

44. Naumann, M and Scheidereit, C, *Activation of NF-kappa B in vivo is regulated by multiple phosphorylations.* EMBO J, 1994. **13**(19): p. 4597-607.

45. Zhong, Haihong, Voll, Reinhard E, and Ghosh, Sankar, *Phosphorylation of NF-kappa B p65 by PKA stimulates transcriptional activity by promoting a novel bivalent interaction with the coactivator CBP/p300.* Mol Cell, 1998. **1**(April): p. 661-671.

46. Arenzana-Seisdedos, F, Turpin, P, Rodriguez, M, Thomas, D, Hay, R T, Virelizier, J L, and Dargemont, C, *Nuclear localization of I kappa B alpha promotes active transport of NF-kappa B from the nucleus to the cytoplasm.* Journal of Cell Science, 1997. **110 (Pt 3)**: p. 369-78.

47. Sethi, Gautam, Sung, Bokyung, and Aggarwal, Bharat B, *Nuclear factor-kappaB activation: from bench to bedside.* Exp Biol Med (Maywood), 2008. **233**(1): p. 21-31.

48. Gilmore, T D and Herscovitch, M, *Inhibitors of NF-kappaB signaling: 785 and counting.* Oncogene, 2006. **25**(51): p. 6887-99.

49. Ishii, Yuki, Waxman, Samuel, and Germain, Doris, *Targeting the ubiquitin-proteasome pathway in cancer therapy.* Anti-cancer agents in medicinal chemistry, 2007. **7**(3): p. 359-65.

50. Ji, C, Kozak, K R, and Marnett, L J, *IkappaB kinase, a molecular target for inhibition by 4-hydroxy-2-nonenal.* J Biol Chem, 2001. **276**(21): p. 18223-8.

51. Wullaert, Andy, Heyninck, Karen, Janssens, Sophie, and Beyaert, Rudi, *Ubiquitin: tool and target for intracellular NF-kappaB inhibitors.* Trends in Immunology, 2006. **27**(11): p. 533-40.

52. Monici, M C, Aguennouz, M, Mazzeo, A, Messina, C, and Vita, G, *Activation of nuclear factor-kappaB in inflammatory myopathies and Duchenne muscular dystrophy.* Neurology, 2003. **60**(6): p. 993-7.

53. Cai, D., Frantz, J. D., Tawa, N. E., Jr., Melendez, P. A., Oh, B. C., Lidov, H. G., Hasselgren, P. O., Frontera, W. R., Lee, J., Glass, D. J., and Shoelson, S. E., *IKKbeta/NF-kappaB activation causes severe muscle wasting in mice.* Cell, 2004. **119**(2): p. 285-98.

54. Kumamoto, T, Fujimoto, S, Ito, T, Horinouchi, H, Ueyama, H, and Tsuda, T, *Proteasome expression in the skeletal muscles of patients with muscular dystrophy.* Acta Neuropathol, 2000. **100**(6): p. 595-602.

55. Magnani, M, Crinelli, R, Bianchi, M, and Antonelli, A, *The ubiquitin-dependent proteolytic system and other potential targets for the modulation of nuclear factor-kB (NF-kB).* Current drug targets, 2000. **1**(4): p. 387-99.

56. Guttridge, D C, Mayo, M W, Madrid, L V, Wang, C Y, and Baldwin, A S, *NF-kappaB-induced loss of MyoD messenger RNA: possible role in muscle decay and cachexia.* Science, 2000. **289**(5488): p. 2363-6.

57. Hnia, K, Gayraud, J, Hugon, G, Ramonatxo, M, De La Porte, S, Matecki, S, and Mornet, D, *L-Arginine Decreases Inflammation and Modulates the Nuclear Factor-{kappa}B/Matrix Metalloproteinase Cascade in Mdx Muscle Fibers.* Am J Pathol, 2008.

58. Bhatnagar, Shephali and Kumar, Ashok, *Therapeutic targeting of signaling pathways in muscular dystrophy.* J Mol Med, 2010. **88**(2): p. 155-66.

59. Rando, Thomas A, *Get personal with gene therapy for muscular dystrophy.* Lancet neurology, 2008. **7**(3): p. 196-8.

60. Grounds, M, *Two-tiered hypotheses for Duchenne muscular dystrophy.* Cell Mol Life Sci, 2008.

61. Scimè, Anthony and Rudnicki, Michael A, *Molecular-targeted therapy for duchenne muscular dystrophy: progress and potential.* Molecular diagnosis & therapy, 2008. **12**(2): p. 99-108.

62. Wehling-Henricks, M, Oltmann, M, Rinaldi, C, Myung, K, and Tidball, J, *Loss of positive allosteric interactions between neuronal nitric oxide synthase and phosphofructokinase contribute to defects in glycolysis and increased fatigability in muscular dystrophy.* Human Molecular Genetics, 2009.

63. Lai, Yi, Thomas, Gail D, Yue, Yongping, Yang, Hsiao T, Li, Dejia, Long, Chun, Judge, Luke, Bostick, Brian, Chamberlain, Jeffrey S, Terjung, Ronald L, and Duan, Dongsheng, *Dystrophins carrying spectrin-like repeats 16 and 17 anchor nNOS to the sarcolemma and enhance exercise performance in a mouse model of muscular dystrophy.* J Clin Invest, 2009. **119**(3): p. 624-35.

64. Van Deutekom, J. C., Janson, A. A., Ginjaar, I. B., Frankhuizen, W. S., Aartsma-Rus, A., Bremmer-Bout, M., Den Dunnen, J. T., Koop, K., Van Der Kooi, A. J., Goemans, N. M., De Kimpe, S. J., Ekhart, P. F., Venneker, E. H., Platenburg, G. J., Verschuuren, J. J., and Van Ommen, G. J., *Local dystrophin restoration with antisense oligonucleotide PRO051.* N Engl J Med, 2007. **357**(26): p. 2677-86.

65. Kawano, Ryoko, Ishizaki, Masatoshi, Maeda, Yasushi, Uchida, Yuji, Kimura, En, and Uchino, Makoto, *Transduction of full-length dystrophin to multiple skeletal muscles improves motor performance and life span in utrophin/dystrophin double knockout mice.* Mol Ther, 2008. **16**(5): p. 825-31.

66. Reay, D P, Bilbao, R, Koppanati, B M, Cai, L, O'day, T L, Jiang, Z, Zheng, H, Watchko, J F, and Clemens, P R, *Full-length dystrophin gene transfer to the mdx mouse in utero.* Gene Ther, 2008. **15**(7): p. 531-6.

67. Merlini, L., Cicognani, A., Malaspina, E., Gennari, M., Gnudi, S., Talim, B., and Franzoni, E., *Early prednisone treatment in Duchenne muscular dystrophy.* Muscle Nerve, 2003. **27**(2): p. 222-7.

68. Hussein, M. R., Hamed, S. A., Mostafa, M. G., Abu-Dief, E. E., Kamel, N. F., and Kandil, M. R., *The effects of glucocorticoid therapy on the inflammatory and dendritic cells in muscular dystrophies.* Int J Exp Pathol, 2006. **87**(6): p. 451-61.

69. Gosselin, L. E., Williams, J. E., Personius, K., and Farkas, G. A., *A comparison of factors associated with collagen metabolism in different skeletal muscles from dystrophic (mdx) mice: impact of pirfenidone.* Muscle Nerve, 2007. **35**(2): p. 208-16.

70. Spurney, C. F., Sali, A., Guerron, A. D., Iantorno, M., Yu, Q., Gordish-Dressman, H., Rayavarapu, S., Van Der Meulen, J., Hoffman, E. P., and Nagaraju, K., *Losartan decreases cardiac muscle fibrosis and improves cardiac function in dystrophin-deficient mdx mice.* J Cardiovasc Pharmacol Ther, 2011. **16**(1): p. 87-95.

71. Pan, Y., Chen, C., Shen, Y., Zhu, C. H., Wang, G., Wang, X. C., Chen, H. Q., and Zhu, M. S., *Curcumin alleviates dystrophic muscle pathology in mdx mice.* Mol Cells, 2008. **25**(4): p. 531-7.

72. May, M. J., D'acquisto, F., Madge, L. A., Glockner, J., Pober, J. S., and Ghosh, S., *Selective inhibition of NF-kappaB activation by a peptide that blocks the interaction of NEMO with the IkappaB kinase complex.* Science, 2000. **289**(5484): p. 1550-4.

73. Peterson, J. M., Kline, W., Canan, B. D., Ricca, D. J., Kaspar, B., Delfin, D. A., Dirienzo, K., Clemens, P. R., Robbins, P. D., Baldwin, A. S., Flood, P., Kaumaya, P., Freitas, M., Kornegay, J. N., Mendell, J. R., Rafael-Fortney, J. A., Guttridge, D. C., and Janssen, P. M., *Peptide-based inhibition of NF-kappaB rescues diaphragm muscle contractile dysfunction in a murine model of Duchenne muscular dystrophy.* Mol Med, 2011. **17**(5-6): p. 508-15.

74. Reay, D. P., Yang, M., Watchko, J. F., Daood, M., O'day, T. L., Rehman, K. K., Guttridge, D. C., Robbins, P. D., and Clemens, P. R., *Systemic delivery of NEMO binding domain/IKKgamma inhibitory peptide to young mdx mice improves dystrophic skeletal muscle histopathology.* Neurobiol Dis, 2011. **43**(3): p. 598-608.

75. Delfin, D. A., Xu, Y., Peterson, J. M., Guttridge, D. C., Rafael-Fortney, J. A., and Janssen, P. M., *Improvement of cardiac contractile function by peptide-based inhibition of NF-kappaB in the utrophin/dystrophin-deficient murine model of muscular dystrophy.* J Transl Med, 2011. **9**: p. 68.

76. Bonuccelli, Gloria, Sotgia, Federica, Schubert, William, Park, David S, Frank, Philippe G, Woodman, Scott E, Insabato, Luigi, Cammer, Michael, Minetti, Carlo, and Lisanti, Michael P, *Proteasome inhibitor (MG-132) treatment of mdx mice rescues the expression and membrane localization of dystrophin and dystrophin-associated proteins.* Am J Pathol, 2003. **163**(4): p. 1663-75.

77. Bonuccelli, Gloria, Sotgia, Federica, Capozza, Franco, Gazzerro, Elisabetta, Minetti, Carlo, and Lisanti, Michael P, *Localized treatment with a novel FDA-approved proteasome inhibitor blocks the degradation of dystrophin and dystrophin-associated proteins in mdx mice.* Cell Cycle, 2007. **6**(10): p. 1242-8.

78. Lawler, J. M., *Exacerbation of pathology by oxidative stress in respiratory and locomotor muscles with Duchenne muscular dystrophy.* J Physiol, 2011. **589**(Pt 9): p. 2161-70.

79. Spurney, C. F., Rocha, C. T., Henricson, E., Florence, J., Mayhew, J., Gorni, K., Pasquali, L., Pestronk, A., Martin, G. R., Hu, F., Nie, L., Connolly, A. M., and Escolar, D. M., *CINRG pilot trial of coenzyme Q10 in steroid-treated Duchenne muscular dystrophy.* Muscle Nerve, 2011. **44**(2): p. 174-8.

80. Messina, S., Bitto, A., Aguennouz, M., Vita, G. L., Polito, F., Irrera, N., Altavilla, D., Marini, H., Migliorato, A., Squadrito, F., and Vita, G., *The soy isoflavone genistein blunts nuclear factor kappa-B, MAPKs and TNF-alpha activation and ameliorates muscle function and morphology in mdx mice.* Neuromuscul Disord, 2011. **21**(8): p. 579-89.

81. Hibaoui, Y., Reutenauer-Patte, J., Patthey-Vuadens, O., Ruegg, U. T., and Dorchies, O. M., *Melatonin improves muscle function of the dystrophic mdx5Cv mouse, a model for Duchenne muscular dystrophy.* J Pineal Res, 2011. **51**(2): p. 163-71.

82. Chahbouni, M., Escames, G., Lopez, L. C., Sevilla, B., Doerrier, C., Munoz-Hoyos, A., Molina-Carballo, A., and Acuna-Castroviejo, D., *Melatonin treatment counteracts the hyperoxidative status in erythrocytes of patients suffering from Duchenne muscular dystrophy.* Clin Biochem, 2011. **44**(10-11): p. 853-8.

83. Qureshi, M. M., Mcclure, W. C., Arevalo, N. L., Rabon, R. E., Mohr, B., Bose, S. K., Mccord, J. M., and Tseng, B. S., *The Dietary Supplement Protandim Decreases Plasma Osteopontin and Improves Markers of Oxidative Stress in Muscular Dystrophy Mdx Mice.* J Diet Suppl, 2010. **7**(2): p. 159-178.

84. Tang, Y., Reay, D. P., Salay, M. N., Mi, M. Y., Clemens, P. R., Guttridge, D. C., Robbins, P. D., Huard, J., and Wang, B., *Inhibition of the IKK/NF-kappaB pathway by AAV gene transfer improves muscle regeneration in older mdx mice.* Gene Ther, 2010. **17**(12): p. 1476-83.

85. Chen, Zhijian J, *Ubiquitin signalling in the NF-kappaB pathway.* Nat Cell Biol, 2005. **7**(8): p. 758-65.

86. Hasselgren, Per-Olof, *Ubiquitination, phosphorylation, and acetylation--triple threat in muscle wasting.* J. Cell. Physiol., 2007. **213**(3): p. 679-89.

87. Harhaj, E. W. and Dixit, V. M., *Deubiquitinases in the regulation of NF-kappaB signaling.* Cell Res, 2011. **21**(1): p. 22-39.

88. Opipari, A. W., Jr., Hu, H. M., Yabkowitz, R., and Dixit, V. M., *The A20 zinc finger protein protects cells from tumor necrosis factor cytotoxicity.* J Biol Chem, 1992. **267**(18): p. 12424-7.

89. He, Kai-Li and Ting, Adrian T, *A20 inhibits tumor necrosis factor (TNF) alpha-induced apoptosis by disrupting recruitment of TRADD and RIP to the TNF receptor 1 complex in Jurkat T cells.* Mol Cell Biol, 2002. **22**(17): p. 6034-45.

90. Komander, D. and Barford, D., *Structure of the A20 OTU domain and mechanistic insights into deubiquitination.* Biochem J, 2008. **409**(1): p. 77-85.

91. Lin, S. C., Chung, J. Y., Lamothe, B., Rajashankar, K., Lu, M., Lo, Y. C., Lam, A. Y., Darnay, B. G., and Wu, H., *Molecular basis for the unique deubiquitinating activity of the NF-kappaB inhibitor A20.* J Mol Biol, 2008. **376**(2): p. 526-40.

92. Song, H Y, Rothe, M, and Goeddel, D V, *The tumor necrosis factor-inducible zinc finger protein A20 interacts with TRAF1/TRAF2 and inhibits NF-kappaB activation.* Proc Natl Acad Sci USA, 1996. **93**(13): p. 6721-5.

93. Boone, D. L., Turer, E. E., Lee, E. G., Ahmad, R. C., Wheeler, M. T., Tsui, C., Hurley, P., Chien, M., Chai, S., Hitotsumatsu, O., Mcnally, E., Pickart, C., and Ma, A., *The ubiquitin-modifying enzyme A20 is required for termination of Toll-like receptor responses.* Nat Immunol, 2004. **5**(10): p. 1052-60.

94. Evans, P. C., *Regulation of pro-inflammatory signalling networks by ubiquitin: identification of novel targets for anti-inflammatory drugs.* Expert Rev Mol Med, 2005. **7**(12): p. 1-19.

95. Parvatiyar, K. and Harhaj, E. W., *Regulation of inflammatory and antiviral signaling by A20.* Microbes Infect, 2011. **13**(3): p. 209-15.

96. Verstrepen, Lynn, Verhelst, Kelly, Van Loo, Geert, Carpentier, Isabelle, Ley, Steven C, and Beyaert, Rudi, *Expression, biological activities and mechanisms of action of A20 (TNFAIP3).* Biochemical Pharmacology, 2010. **80**(12): p. 2009-20.

97. Lee, E G, Boone, D L, Chai, S, Libby, S L, Chien, M, Lodolce, J P, and Ma, A, *Failure to regulate TNF-induced NF-kappaB and cell death responses in A20-deficient mice.* Science, 2000. **289**(5488): p. 2350-4.

98. Schmitz, Roland, Hansmann, Martin-Leo, Bohle, Verena, Martin-Subero, Jose Ignacio, Hartmann, Sylvia, Mechtersheimer, Gunhild, Klapper, Wolfram, Vater, Inga, Giefing, Maciej, Gesk, Stefan, Stanelle, Jens, Siebert, Reiner, and Küppers, Ralf, *TNFAIP3 (A20) is a tumor suppressor gene in Hodgkin lymphoma and primary mediastinal B cell lymphoma.* Journal of Experimental Medicine, 2009. **206**(5): p. 981-9.

99. Malynn, Barbara A and Ma, Averil, *A20 takes on tumors: tumor suppression by an ubiquitin-editing enzyme.* Journal of Experimental Medicine, 2009. **206**(5): p. 977-80.

100. Bueler, H., *Adeno-associated viral vectors for gene transfer and gene therapy.* Biol Chem, 1999. **380**(6): p. 613-22.

101. Zhang, X. and Godbey, W. T., *Viral vectors for gene delivery in tissue engineering.* Adv Drug Deliv Rev, 2006. **58**(4): p. 515-34.

102. Srivastava, A., Lusby, E. W., and Berns, K. I., *Nucleotide sequence and organization of the adeno-associated virus 2 genome.* J Virol, 1983. **45**(2): p. 555-64.

103. Buning, H., Ried, M. U., Perabo, L., Gerner, F. M., Huttner, N. A., Enssle, J., and Hallek, M., *Receptor targeting of adeno-associated virus vectors.* Gene Ther, 2003. **10**(14): p. 1142-51.

104. Lusby, E., Fife, K. H., and Berns, K. I., *Nucleotide sequence of the inverted terminal repetition in adeno-associated virus DNA.* J Virol, 1980. **34**(2): p. 402-9.

105. Carter, P. J. and Samulski, R. J., *Adeno-associated viral vectors as gene delivery vehicles.* Int J Mol Med, 2000. **6**(1): p. 17-27.

106. Schlehofer, J. R., Ehrbar, M., and Zur Hausen, H., *Vaccinia virus, herpes simplex virus, and carcinogens induce DNA amplification in a human cell line and support replication of a helpervirus dependent parvovirus.* Virology, 1986. **152**(1): p. 110-7.

107. Buller, R. M., Janik, J. E., Sebring, E. D., and Rose, J. A., *Herpes simplex virus types 1 and 2 completely help adenovirus-associated virus replication.* J Virol, 1981. **40**(1): p. 241-7.

108. Owens, R. A., *Second generation adeno-associated virus type 2-based gene therapy systems with the potential for preferential integration into AAVS1.* Curr Gene Ther, 2002. **2**(2): p. 145-59.

109. Kotin, R. M., Siniscalco, M., Samulski, R. J., Zhu, X. D., Hunter, L., Laughlin, C. A., Mclaughlin, S., Muzyczka, N., Rocchi, M., and Berns, K. I., *Site-specific integration by adeno-associated virus.* Proc Natl Acad Sci U S A, 1990. **87**(6): p. 2211-5.

110. Grimm, D. and Kay, M. A., *From virus evolution to vector revolution: use of naturally occurring serotypes of adeno-associated virus (AAV) as novel vectors for human gene therapy.* Curr Gene Ther, 2003. **3**(4): p. 281-304.

111. Summerford, C. and Samulski, R. J., *Membrane-associated heparan sulfate proteoglycan is a receptor for adeno-associated virus type 2 virions.* J Virol, 1998. **72**(2): p. 1438-45.

112. Akache, B., Grimm, D., Pandey, K., Yant, S. R., Xu, H., and Kay, M. A., *The 37/67-kilodalton laminin receptor is a receptor for adeno-associated virus serotypes 8, 2, 3, and 9.* J Virol, 2006. **80**(19): p. 9831-6.

113. Mayor, H. D., Drake, S., Stahmann, J., and Mumford, D. M., *Antibodies to adeno-associated satellite virus and herpes simplex in sera from cancer patients and normal adults.* Am J Obstet Gynecol, 1976. **126**(1): p. 100-4.

114. Jiang, Zhilong and Clemens, Paula R, *Cellular caspase-8-like inhibitory protein (cFLIP) prevents inhibition of muscle cell differentiation induced by cancer cells.* FASEB J, 2006. **20**(14): p. 2570-2.

115. Messina, S., Vita, G. L., Aguennouz, M., Sframeli, M., Romeo, S., Rodolico, C., and Vita, G., *Activation of NF-kappaB pathway in Duchenne muscular dystrophy: relation to age.* Acta Myol, 2011. **30**(1): p. 16-23.

116. Shembade, Noula, Ma, Averil, and Harhaj, Edward W, *Inhibition of NF-kappaB signaling by A20 through disruption of ubiquitin enzyme complexes.* Science, 2010. **327**(5969): p. 1135-9.

117. Ladner, Katherine J, Caligiuri, Michael A, and Guttridge, Denis C, *Tumor necrosis factor-regulated biphasic activation of NF-kappa B is required for cytokine-induced loss of skeletal muscle gene products.* J Biol Chem, 2003. **278**(4): p. 2294-303.

118. Guttridge, D C, Albanese, C, Reuther, J Y, Pestell, R G, and Baldwin, A S, *NF-kappaB controls cell growth and differentiation through transcriptional regulation of cyclin D1.* Molecular and Cellular Biology, 1999. **19**(8): p. 5785-99.

119. Kunter, Uta, Daniel, Soizic, Arvelo, Maria B, Choi, Jean, Shukri, Tala, Patel, Virendra I, Longo, Christopher R, Scali, Salvatore T, Shrikhande, Gautam, Rocha, Eduardo, Czismadia, Eva, Mottley, Christina, Grey, Shane T, Floege, Jürgen, and Ferran, Christiane, *Combined expression of A1 and A20 achieves optimal protection of renal proximal tubular epithelial cells.* Kidney Int, 2005. **68**(4): p. 1520-32.

120. Tran, T, Temkin, V, Shi, B, Pagliari, L, Daniel, S, Ferran, C, and Pope, R, *TNFalpha-induced macrophage death via caspase-dependent and independent pathways.* Apoptosis, 2009.

121. Bockhold, K J, Rosenblatt, J D, and Partridge, T A, *Aging normal and dystrophic mouse muscle: analysis of myogenicity in cultures of living single fibers.* Muscle Nerve, 1998. **21**(2): p. 173-83.

122. Chng, H. W., Camplejohn, R. S., Stone, M. G., Hart, I. R., and Nicholson, L. J., *A new role for the anti-apoptotic gene A20 in angiogenesis.* Exp Cell Res, 2006. **312**(15): p. 2897-907.

123. Grounds, Miranda D and Torrisi, Jo, *Anti-TNFalpha (Remicade) therapy protects dystrophic skeletal muscle from necrosis.* FASEB J, 2004. **18**(6): p. 676-82.

124. Krikos, A, Laherty, C D, and Dixit, V M, *Transcriptional activation of the tumor necrosis factor alpha-inducible zinc finger protein, A20, is mediated by kappa B elements.* J Biol Chem, 1992. **267**(25): p. 17971-6.

125. Dixit, V M, Green, S, Sarma, V, Holzman, L B, Wolf, F W, O'rourke, K, Ward, P A, Prochownik, E V, and Marks, R M, *Tumor necrosis factor-alpha induction of novel gene products in human endothelial cells including a macrophage-specific chemotaxin.* J Biol Chem, 1990. **265**(5): p. 2973-8.

126. Opipari, A W, Boguski, M S, and Dixit, V M, *The A20 cDNA induced by tumor necrosis factor alpha encodes a novel type of zinc finger protein.* J Biol Chem, 1990. **265**(25): p. 14705-8.

127. Bakkar, Nadine, Wang, Jingxin, Ladner, Katherine J, Wang, Huating, Dahlman, Jason M, Carathers, Micheal, Acharyya, Swarnali, Rudnicki, Michael A, Hollenbach, Andrew D, and Guttridge, Denis C, *IKK/NF-kappaB regulates skeletal myogenesis via a signaling switch to inhibit differentiation and promote mitochondrial biogenesis.* J Cell Biol, 2008. **180**(4): p. 787-802.

128. Lassar, A B, Skapek, S X, and Novitch, B, *Regulatory mechanisms that coordinate skeletal muscle differentiation and cell cycle withdrawal.* Curr Opin Cell Biol, 1994. **6**(6): p. 788-94.

129. Nordquist, Jenny, Höglund, Anna-Stina, Norman, Holly, Tang, Xiaorui, Dworkin, Barry, and Larsson, Lars, *Transcription factors in muscle atrophy caused by blocked neuromuscular transmission and muscle unloading in rats.* Mol Med, 2007. **13**(9-10): p. 461-70.

130. Weih, F, Carrasco, D, Durham, S K, Barton, D S, Rizzo, C A, Ryseck, R P, Lira, S A, and Bravo, R, *Multiorgan inflammation and hematopoietic abnormalities in mice with a targeted disruption of RelB, a member of the NF-kappa B/Rel family.* Cell, 1995. **80**(2): p. 331-40.

131. Bakkar, Nadine and Guttridge, Denis C, *NF-kappaB signaling: a tale of two pathways in skeletal myogenesis.* Physiological Reviews, 2010. **90**(2): p. 495-511.

132. Canicio, J, Ruiz-Lozano, P, Carrasco, M, Palacin, M, Chien, K, Zorzano, A, and Kaliman, P, *Nuclear factor kappa B-inducing kinase and Ikappa B kinase-alpha signal skeletal muscle cell differentiation.* J Biol Chem, 2001. **276**(23): p. 20228-33.

133. Dahlman, Jason M, Bakkar, Nadine, He, Wei, and Guttridge, Denis C, *NF-kappaB functions in stromal fibroblasts to regulate early postnatal muscle development.* Journal of Biological Chemistry, 2010. **285**(8): p. 5479-87.

134. Lu, A., Proto, J. D., Guo, L., Tang, Y., Lavasani, M., Tilstra, J. S., Niedernhofer, L. J., Wang, B., Guttridge, D. C., Robbins, P. D., and Huard, J., *NF-kappaB Negatively Impacts the Myogenic Potential of Muscle-derived Stem Cells.* Mol Ther, 2011.

135. Inagaki, K., Fuess, S., Storm, T. A., Gibson, G. A., Mctiernan, C. F., Kay, M. A., and Nakai, H., *Robust systemic transduction with AAV9 vectors in mice: efficient global cardiac gene transfer superior to that of AAV8.* Mol Ther, 2006. **14**(1): p. 45-53.

136. Wang, Z., Zhu, T., Qiao, C., Zhou, L., Wang, B., Zhang, J., Chen, C., Li, J., and Xiao, X., *Adeno-associated virus serotype 8 efficiently delivers genes to muscle and heart.* Nat Biotechnol, 2005. **23**(3): p. 321-8.

137. Vandendriessche, T, Thorrez, L, Acosta-Sanchez, A, Petrus, I, Wang, L, Ma, L, De Waele, L, Iwasaki, Y, Gillijns, V, Wilson, J M, Collen, D, and Chuah, M K L, *Efficacy and safety of adeno-associated viral vectors based on serotype 8 and 9 vs. lentiviral vectors for hemophilia B gene therapy.* J Thromb Haemost, 2007. **5**(1): p. 16-24.

138. Louboutin, J. P., Wang, L., and Wilson, J. M., *Gene transfer into skeletal muscle using novel AAV serotypes.* J Gene Med, 2005. **7**(4): p. 442-51.

139. Graham, T., Mcintosh, J., Work, L. M., Nathwani, A., and Baker, A. H., *Performance of AAV8 vectors expressing human factor IX from a hepatic-selective promoter following intravenous injection into rats.* Genet Vaccines Ther, 2008. **6**: p. 9.

140. Wang, B, Li, J, Fu, F H, Chen, C, Zhu, X, Zhou, L, Jiang, X, and Xiao, X, *Construction and analysis of compact muscle-specific promoters for AAV vectors.* Gene Ther, 2008. **15**(22): p. 1489-99.

141. Eghtesad, Saman, Jhunjhunwala, Siddharth, Little, Steven R, and Clemens, Paula R, *Rapamycin ameliorates dystrophic phenotype in mdx mouse skeletal muscle.* Molecular medicine (Cambridge, Mass), 2011.

142. Charan, Rakshita A, Hanson, Ryan, and Clemens, Paula R, *Deubiquitinating enzyme A20 negatively regulates NF-{kappa}B signaling in skeletal muscle in mdx mice.* FASEB J, 2011.

143. Cossu, Giulio and Sampaolesi, Maurilio, *New therapies for Duchenne muscular dystrophy: challenges, prospects and clinical trials.* Trends in molecular medicine, 2007. **13**(12): p. 520-6.

144. Mourkioti, Foteini and Rosenthal, Nadia, *NF-kappaB signaling in skeletal muscle: prospects for intervention in muscle diseases.* J Mol Med, 2008. **86**(7): p. 747-59.

145. Pan, Y, Chen, C, Shen, Y, Zhu, C, Wang, G, Wang, X, Chen, H, and Zhu, M, *Curcumin Alleviates Dystrophic Muscle Pathology in mdx Mice.* Mol Cells, 2008. **25**(4).

146. Messina, Sonia, Bitto, Alessandra, Aguennouz, M'hammed, Minutoli, Letteria, Monici, Maria C, Altavilla, Domenica, Squadrito, Francesco, and Vita, Giuseppe, *Nuclear factor kappa-B blockade reduces skeletal muscle degeneration and enhances muscle function in Mdx mice.* Experimental Neurology, 2006. **198**(1): p. 234-41.

147. Deconinck, Nicolas and Dan, Bernard, *Pathophysiology of duchenne muscular dystrophy: current hypotheses.* Pediatric Neurology, 2007. **36**(1): p. 1-7.

148. Ervasti, James M, *Dystrophin, its interactions with other proteins, and implications for muscular dystrophy.* Biochim Biophys Acta, 2007. **1772**(2): p. 108-17.

149. Tisdale, Michael J, *The ubiquitin-proteasome pathway as a therapeutic target for muscle wasting.* The journal of supportive oncology, 2005. **3**(3): p. 209-17.

150. Glass, David J, *Skeletal muscle hypertrophy and atrophy signaling pathways.* Int J Biochem Cell Biol, 2005. **37**(10): p. 1974-84.

151. Kandarian, Susan C and Jackman, Robert W, *Intracellular signaling during skeletal muscle atrophy.* Muscle Nerve, 2006. **33**(2): p. 155-65.

152. Spencer, M. J. and Tidball, J. G., *Do immune cells promote the pathology of dystrophin-deficient myopathies?* Neuromuscul Disord, 2001. **11**(6-7): p. 556-64.

153. Spencer, M. J., Montecino-Rodriguez, E., Dorshkind, K., and Tidball, J. G., *Helper (CD4(+)) and cytotoxic (CD8(+)) T cells promote the pathology of dystrophin-deficient muscle.* Clin Immunol, 2001. **98**(2): p. 235-43.

154. Mcdouall, R. M., Dunn, M. J., and Dubowitz, V., *Nature of the mononuclear infiltrate and the mechanism of muscle damage in juvenile dermatomyositis and Duchenne muscular dystrophy.* J Neurol Sci, 1990. **99**(2-3): p. 199-217.

155. Rosenschein, U., Radnay, J., Shoham, D., Shainberg, A., Klajman, A., and Rozenszajn, L. A., *Human muscle-derived, tissue specific, myocytotoxic T cell lines in dermatomyositis.* Clin Exp Immunol, 1987. **67**(2): p. 309-18.

156. Jayandharan, G. R., Aslanidi, G., Martino, A. T., Jahn, S. C., Perrin, G. Q., Herzog, R. W., and Srivastava, A., *Activation of the NF-kappaB pathway by adeno-associated virus (AAV) vectors and its implications in immune response and gene therapy.* Proc Natl Acad Sci U S A, 2011. **108**(9): p. 3743-8.

157. Pomerantz, Joel L and Baltimore, David, *Two pathways to NF-kappaB.* Mol Cell, 2002. **10**(4): p. 693-5.

158. Oeckinghaus, Andrea, Hayden, Matthew S, and Ghosh, Sankar, *Crosstalk in NF-κB signaling pathways.* Nat Immunol, 2011. **12**(8): p. 695-708.

159. Senf, S, Dodd, S, Mcclung, J, and Judge, A, *Hsp70 overexpression inhibits NF-{kappa} B and Foxo3a transcriptional activities and prevents skeletal muscle atrophy.* The FASEB Journal, 2008.

160. Beg, A. A., Sha, W. C., Bronson, R. T., Ghosh, S., and Baltimore, D., *Embryonic lethality and liver degeneration in mice lacking the RelA component of NF-kappa B.* Nature, 1995. **376**(6536): p. 167-70.

161. Sha, W. C., Liou, H. C., Tuomanen, E. I., and Baltimore, D., *Targeted disruption of the p50 subunit of NF-kappa B leads to multifocal defects in immune responses.* Cell, 1995. **80**(2): p. 321-30.

162. Doi, T S, Marino, M W, Takahashi, T, Yoshida, T, Sakakura, T, Old, L J, and Obata, Y, *Absence of tumor necrosis factor rescues RelA-deficient mice from embryonic lethality.* Proc Natl Acad Sci USA, 1999. **96**(6): p. 2994-9.

163. Sen, R and Baltimore, D, *Inducibility of kappa immunoglobulin enhancer-binding protein Nf-kappa B by a posttranslational mechanism.* Cell, 1986. **47**(6): p. 921-8.

164. Baltimore, David, *NF-κB is 25.* Nat Immunol, 2011. **12**(8): p. 683-5.

165. Lademann, U., Kallunki, T., and Jaattela, M., *A20 zinc finger protein inhibits TNF-induced apoptosis and stress response early in the signaling cascades and independently of binding to TRAF2 or 14-3-3 proteins.* Cell Death Differ, 2001. **8**(3): p. 265-72.

166. Wang, X. T., Liu, P. Y., Tang, J. B., Mizukami, H., Xin, K. Q., Ozawa, K., and Ushijima, H., *Tendon healing in vitro: adeno-associated virus-2 effectively transduces intrasynovial tenocytes with persistent expression of the transgene, but other serotypes do not.* Plast Reconstr Surg, 2007. **119**(1): p. 227-34.